2007

Structural Manipulation of Pyrrole-Terminated Dendrimers to Create a More Efficient Encapsulation/Release System

Henry Wiggins
Louisiana State University and Agricultural and Mechanical College

STRUCTURAL MANIPULATION OF PYRROLE-TERMINATED DENDRIMERS TO CREATE A MORE EFFICIENT ENCAPSULATION/RELEASE SYSTEM

A Dissertation

Submitted to the Graduate Faculty of the
Louisiana State University and
Agricultural and Mechanical College
in partial fulfillment of the
requirements for the degree of
Doctor of Philosophy

In

The Department of Chemistry

by
Henry Wiggins
B.S., Nicholls State University, 2001
May, 2007

Dedication

This dissertation is dedicated to:

My wife, Sarah Wiggins

My son, Lance Wiggins

My parents, Donald and Carol Wiggins.

Acknowledgements

I would first and foremost like to thank my wife, Sarah, for her endless love and support throughout my graduate career. Your ears were always open, and your compassion and understanding were always present. Thanks for all of the encouragement along the way. I could not have asked for a better person to share in this journey.

I would like to acknowledge my parents for their devotion in my upbringing. You've both instilled in me tremendous family values and taught me that hard work and determination are the only ways to success. Mom, thank you for your unwavering love and never ending support. Dad, thanks for constantly reminding me of how long I've been in school.

I'd like to thank Dr. McCarley for his direction through my graduate career and the opportunity to work in his research group. Thanks for teaching me what it means to be a scientist. My work under you has led me to numerous places and exposed me to numerous aspects of chemistry. I appreciate you giving me the ability to be a part of a challenging educational experience and helping prepare me for what lies ahead.

I have to acknowledge the great deal of time awarded to me by Dr. Cook and Dr. Treleaven. No matter how busy you were, you always found time to sit down and discuss NMR results with me. I appreciate the tremendous amounts of time you gave me. Your discussions gave me a much better understanding of the work I was doing, far better than any book I've read.

I would like to thank the McCarley group for all of your help. Though the makeup of the group has changed a great deal over the years, the friendly environment never has. Everyone was always more than willing, when asked, to provide any assistance. One of the best experiences of my life was experiencing and learning about the different cultural backgrounds that made up the group. I hope you enjoyed the wild game as much as I enjoyed the excellent

variety of food that you provided for the rest of us. Becky, thanks for providing, and occasionally being the subject, of the endless entertainment that made school more bearable. I really appreciate all the free lunches; you were truly a great sport through it all. Winston thanks for your versatility in being able to aid in research one second and analyzing last night's game the next. You were a tremendous asset to this group. I can honestly say I enjoyed working with everyone that was ever a member of this group.

Table of Contents

List of Tables

List of Figures

List of Abbreviations

1D	one dimensional
2D	two dimensional
AA	ascorbic acid
Ag	silver
Ar	argon
Au	gold
BOC	butoxycarbonyl
C343	Coumarin 343
CAMELSPIN	cross-relaxation appropriate for minimolecules emulated by locked spins
CD_2Cl_2	deuterated methylene chloride
cm	centimeters
CO_2	carbon dioxide
Con A	concanavalin A
CPMG	Carr-Purcell-Meiboom-Gill
Cr	chromium
D_1	relaxation delay in nuclear magnetic resonance
D_2O	deuterium oxide
DCl	deuterium chloride
DCM	methylene chloride
DCU	dicyclohexylurea
DHB	2,5-dihydroxybenzoic acid
DOSY	diffusion-ordered spectroscopy

DOX	doxorubicin
Et_3N	triethylamine
Fc	ferrocene
FcCOOH	ferrocene carboxylic acid
FcCOCl	ferrocenoyl chloride
Fe	iron
$Fe(NO_3)_3$	iron(III) nitrate
$Fe(NO_3)_3 \cdot 9H_2O$	iron(III) nitrate nonahydrate
FID	free induction decay
FT-IR	Fourier-transform infrared spectroscopy
GC-MS	gas chromatograph-mass spectrometer
HCl	hydrochloric acid
HF	hydrofluoric acid
ICT	internal charge transfer
ip	in-plane (ring deformation in infrared spectroscopy)
IPA	isopropanol
K	Kelvin
KBr	potassium bromide
LCST	lower critical solution temperature
M	molar
MALDI-MS	matrix-assisted laser desorption/ionization mass spectrometry
MCT	mercury-cadmium-telluride
mg	milligrams

min	minutes
mL	milliliters
m/z	mass per charge
NaCl	sodium chloride
$NaHCO_3$	sodium bicarbonate
Na_2SO_4	sodium sulfate
NaOH	sodium hydroxide
nm	nanometers
N	nitrogen
NMR	nuclear magnetic resonance
NOE	nuclear Overhauser Effect
NOESY	nuclear Overhauser Effect Spectroscopy
$O(BOC)_2$	di-*tert*-butyl dicarbonante
oligo	oligomerized
oop	out-of-plane (ring reformation in infrared spectroscopy)
PAMAM	poly(amido amine)
pNIPAAm	poly(*N*-isopropylacrylamide
PPI	poly(propylene imine)
ppm	chemical shift in nuclear magnetic resonance
Py	polypyrrole
Py_3	oligomer made of 3 pyrrole monomers
Py_5	oligomer made of 5 pyrrole monomers
Py_7	oligomer made of 7 pyrrole monomers

PPy	polypyrrole with more than 20 unit lengths
RAIRS	reflection-absorption infrared spectroscopy
RF	radiofrequency (pulse in nuclear magnetic resonance)
ROESY	Rotational nuclear Overhauser Effect Spectroscopy
s	seconds
SANS	small-angle neutron scattering
t_1	evolution time in nuclear magnetic resonance
T_1	spin-lattice relaxation time constant
T_2	spin-spin relaxation time constant
T5	pentathiophene
TGS	triglycine sulfate
TICT	twisted-internal charge transfer
t_m	mixing time in nuclear magnetic resonance
t_{max}	relaxation period in nuclear magnetic resonance
TOCSY	total correlated spectroscopy
UV-vis	ultraviolet-visible spectroscopy
V	volts
VRA-RMA	versatile reflection accessory-retro mirror attachment
μL	microliters
μm	micrometers
μs	microseconds
τ	relaxation delay in nuclear magnetic resonance

DAB-Am_4	poly(propylene imine) tetramine dendrimer, generation 1.0, (4-1° amine termini)
DAB-Am_8	poly(propylene imine) octamine dendrimer, generation 2.0, (8-1° amine termini)
DAB-Am_{16}	poly(propylene imine) hexadecamine dendrimer, generation 3.0, (16-1° amine termini)
DAB-Am_{32}	poly(propylene imine) dotriacontaamine dendrimer, generation 4.0, (32-1° amine termini)
DAB-Am_{64}	poly(propylene imine) tetrahexacontamine dendrimer, generation 5.0, (64-1° amine termini)
DAB-BOC_4	poly(propylene imine) tetramine dendrimer, generation 1.0, (4-butoxycarbonyl termini)
DAB-BOC_8	poly(propylene imine) octamine dendrimer, generation 2.0, (8-butoxycarbonyl termini)
DAB-BOC_{16}	poly(propylene imine) hexadecamine dendrimer, generation 3.0, (16-butoxycarbonyl termini)
DAB-BOC_{32}	poly(propylene imine) dotriacontaamine dendrimer, generation 4.0, (32-butoxycarbonyl termini)
DAB-BOC_{64}	poly(propylene imine) tetrahexacontamine dendrimer, generation 5.0, (64-butoxycarbonyl termini)
DAB-Fc_4	poly(propylene imine) tetramine dendrimer, generation 1.0, (4-ferrocenoyl termini)
DAB-Fc_8	poly(propylene imine) octamine dendrimer, generation 2.0, (8-ferrocenoyl termini)
DAB-Fc_{16}	poly(propylene imine) hexadecamine dendrimer, generation 3.0, (16-ferrocenoyl termini)
DAB-Fc_{32}	poly(propylene imine) dotriacontaamine dendrimer, generation 4.0, (32-ferrocenoyl termini)
DAB-Fc_{64}	poly(propylene imine) tetrahexacontamine dendrimer, generation 5.0, (64-ferrocenoyl termini)

DAB-Py_4	poly(propylene imine) tetramine dendrimer, generation 1.0, (4-(*ω*-(*N*-pyrrolylhexanoyl) termini))
DAB-Py_8	poly(propylene imine) octamine dendrimer, generation 2.0, (8-(*ω*-(*N*-pyrrolylhexanoyl) termini))
DAB-Py_{16}	poly(propylene imine) hexadecamine dendrimer, generation 3.0, (16-(*ω*-(*N*-pyrrolylhexanoyl) termini))
DAB-Py_{32}	poly(propylene imine) dotriacontaamine dendrimer, generation 4.0, (32-(*ω*-(*N*-pyrrolylhexanoyl) termini))
DAB-Py_{64}	poly(propylene imine) tetrahexacontamine dendrimer, generation 5.0, (64-(*ω*-(*N*-pyrrolylhexanoyl) termini))

Abstract

This work demonstrates the ability to manipulate the structure of pyrrole-terminated dendrimers by modifying solution conditions which directly affects their encapsulation properties. Investigations were conducted using FTIR and 2D NMR to determine the location of end groups. NMR relaxation studies were conducted at various temperatures and different solution pH to gain an understanding of the relative mobility and rigidity of different areas of the dendrimer. It was found that that the release properties were affected by the solution pH and the presence of salt. Further the effectiveness of retaining molecular guests by oligo-pyrrole terminated dendrimers with a range of oligomer lengths was investigated.

Hydrogen-Bonding studies, conducted on an FTIR, and 2D NMR data suggest the end groups of similarly structured PPI dendrimers are not backfolded into the interior of the dendrimer. Results from H-Bonding studies, as well as NMR relaxation studies, demonstrate an increase in steric crowding at the periphery of dendrimers as the dendrimer generation is increased. NMR relaxation measurements revealed that the mobility along the periphery of the dendrimer was dependant upon the solution pH. Longer oligomers were formed upon chemical oxidation of the pyrrole termini at higher pH, when the dendrimer possessed a more rigid structure.

Nile Red was encapsulated by the dendrimer host and its release was measured by visible spectroscopy. It was found that increasing the solution pH caused the dendrimer to retain encapsulated guests at a higher efficiency than when the pH was decreased. It is also shown that the addition of salt causes the dendrimer to quickly expel any encapsulated guests. Further, the effectiveness of the oligo-pyrroles in retaining encapsulated guests was investigated. As it turns out, longer oligomers about the periphery of the dendrimer were less successful in retaining

incarcerated guests. Shorter oligomers obtained from oligomerization at pH 2 proved to be more efficient in retaining encapsulated guests than longer oligomers formed at pH 7. This work demonstrates that the encapsulation and release properties can be controlled by altering simple solution parameters.

Chapter 1

Introduction

1.1 Research Goals

The research at hand is directed towards optimizing solution conditions so that the encapsulation and release efficiency of small molecular guests can be increased for a stimuli-responsive host previously reported by this group.[1] This dendrimer system has proven to be effective as a host and may lead to its use as a drug delivery vehicle. The dendrimer periphery was functionalized with pyrrole end groups which can undergo oxidative coupling to form oligo(pyrroles). It is my goal to determine the optimum solution conditions such that the dendritic structure will possess more efficient encapsulation and release properties.

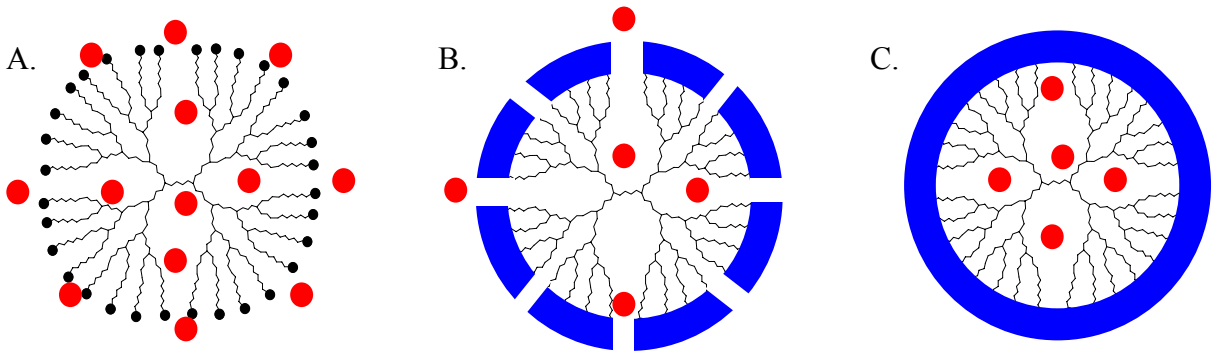

Figure 1.1 A scheme depicting the dynamic trapping of guests in a pyrrole-terminated dendrimer in which guests are free to diffuse in and out of the dendrimer core (A), oligo-pyrrole periphery in which release of guests is restricted but some guests can still diffuse out of the core (B), and after optimization of solution conditions static trapping is observed (C).

Conflicting reports are found in the literature regarding the location of the end groups of dendrimers, as this topic is still debated throughout the scientific community. Some believe the end groups are located along the periphery of the dendrimer,[2] and others believe the majority of the end groups are backfolded into the dendrimer core.[3] If the end groups are located along the periphery, the resulting structure is a macromolecule with a dense outer shell and an interior composed of cavities. The cavities make it possible for the dendrimer to harbor prospective

guests, while the crowded periphery of the dendrimer may help retain those guests by sterically trapping them inside the internal cavities. If the internal cavities are filled with the peripheral functional groups, encapsulation may not occur. If encapsulation does occur, the periphery may not be dense enough to prevent leakage of entrapped guests. It is necessary to determine the location of the functional groups to increase the efficiency of the system.

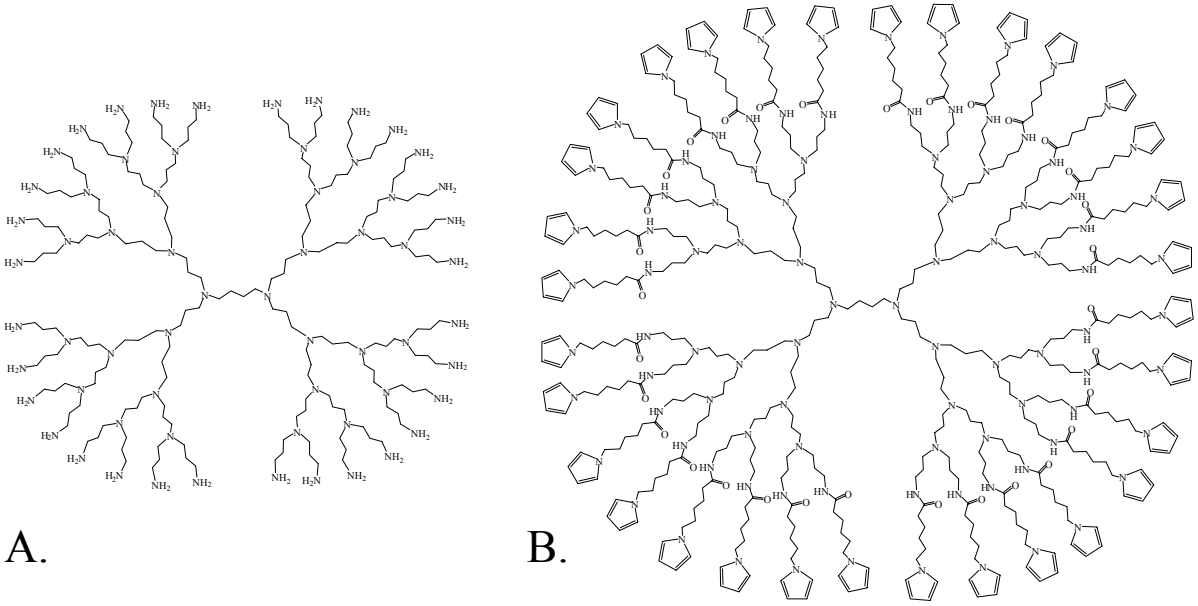

Figure 1.2 The fourth-generation, commercially available poly(propylene imine) dendrimer (A) and the redox-active, pyrrole-terminated dendrimer that is the focus of these studies (B).

This research involves modification of commercially available poly(propylene imine) dendrimers with pyrrole end groups. The pyrrole functional group was chosen because it can be chemically oxidized to yield oligomers.[4-8] It is believed these oligomers will aid in trapping any guest molecules inside the core of the dendrimer and reduce leakage of guests until release is desired (triggered), as demonstrated in Figure 1.1 The oligo(pyrrole) moieties along the periphery of the dendrimer can be reversibly oxidized and reduced affecting the structure of the dendrimer. Molecular modeling predicts that these dendrimers possess larger cavities when the oligo(pyrrole) moieties are in the oxidized state and smaller cavities in the reduced state.[1]

Therefore oxidation of the oligomers may enhance guest retention, while reduction may aid in release. The hypothesis is that by varying the length of the pyrrole oligomers, the impact of oxidation and reduction of pyrrole oligomers on the dendrimer structure can be increased.

1.2 Research Synopsis

1.2.1 Location of End Groups

Defining dendrimers as macromolecules with a dense outer shell and hollow interior is based on the assumption that the end groups are located along the periphery of the dendrimer when the material is dissolved in a given solvent. It has been shown that in some dendrimer systems the majority of the end groups are backfolded into the interior of the dendrimer.[3] If the pyrrole monomers in our system are located inside the dendrimer, then uptake of guests may not be possible if sufficient space for guests does not exist. Even if guest uptake is possible, it may not be posssible to form the oligo(pyrrole) periphery to efficiently retain any guests that may be inside the dendrimer.

The location of various functional groups attached to poly(propylene imine), PPI, dendrimers was studied using indirect and direct methods. The intra-dendrimer hydrogen bonding of ferrocene- and butoxycarbonyl-terminated PPI dendrimers will be monitored with infrared spectroscopy (IR) by observing shifts in key absorption bands as a function of dendrimer size (generation). The extent of the hydrogen-bonding is directly related to the distance between end groups along the periphery. If the end groups are located along the periphery, one would expect the functional groups to become closer together as generation increases. Two dimensional nuclear magnetic resonance (2D NMR) techniques, such as nuclear Overhauser effect spectroscopy (NOESY) and rotational nuclear Overhauser effect spectroscopy (ROESY), will be utilized to corroborate the IR studies. The presence of any cross peaks between pyrrole

protons and protons in the interior of the dendrimer would provide direct evidence that back folding is occurring.

1.2.2 Environmental Effects on Dendritic Structure

A nuclear magnetic resonance (NMR) spin-lattice relaxation method was used to monitor the local molecular mobility of monomeric pyrrole-terminated dendrimers under various solution conditions. The pH and ionic strength of the dendrimer solutions were altered to manipulate the dendrimer structure, and the T_1 relaxation values were determined. The relaxation values allowed the determination of whether the pyrroles along the dendrimer periphery had high or low mobility. A system in which the pyrrole groups have low mobility (rigid periphery) may not allow the pyrrole monomers to approach each other to couple together and form oligomers. If the pyrrole groups are too mobile, possibly indicating that they are located far from each other, these monomers may not be close enough for a sufficient time interval for coupling to occur. The results of these studies lead us to the solution conditions that resulted in the longest pyrrole oligomers (and the shortest) and may also prove useful in determining alternative methods in encapsulating and releasing guest molecules. Perhaps the initial dendrimer structure (before oligomerization) can be changed sufficiently so that the structure of the oligomeric dendrimer is such that incarceration of guests is preferred at one end of the pH scale and release is preferred at the opposite end of the pH scale.

It has been shown that the location of end groups is dependent upon solution conditions such as pH and ionic strength.[9-11] Studies have shown that dendrimer conformations possessing a dense shell (end groups located near the periphery) are predominant in solutions with low pH and in the absence of salt. However, adding salt[11] or increasing the pH[9,10] results in a dense core conformation where the endgroups are backfolded into the interior of the dendrimer. Welch

suggested that one may use these results to encapsulate guests at low pH or ionic strength and then release the entrapped guests upon addition of salt or increasing the pH.[11] It is believed that the backfolded branches at higher pH and ionic strength will displace any guests located in the internal cavities of the dendrimers.

1.3 Dendrimer Background

The host used for these studies is a dendrimer, which is a highly branched symmetrical macromolecule. There are currently two routes for synthesis of dendrimers: divergent[12] and convergent.[13] Dendrimers are synthesized in the divergent manner by constructing dendrimer branches from a multifunctional core through the addition of individual monomers in a stepwise fashion. Hence, the dendrimer is built from the inside out.[12] It is also possible to construct a dendrimer by synthesizing the outer branch components first and then attaching them to the multifunctional core; this is the convergent method.[13] There are several advantages and disadvantages for each synthesis route.

Synthesis of dendrimers using the divergent method[12] may result in products containing some impurities. When using this method, one starts with the central core and builds up the "layers" of dendritic branches through a series of monomer addition reaction steps. The result of this approach is a product containing the fully functionalized material (monodisperse) but also a small percentage of flawed dendrimer possessing molecular weights very close to that of the fully functionalized dendrimer; separation of the monodisperse material from the others is often difficult. However, this route allows one to readily produce a series of different generation dendrimers. Fréchet proposed a convergent synthetic approach in which the dendritic arms are synthesized first and then attached to a desired core.[13] Any dendrimer not completely functionalized will have a structure significantly different from the completely functionalized

product. However, these impurities are easier to remove from the product mixture; therefore, dendrimers produced from the convergent route will be highly uniform (monodisperse). However, this method makes it necessary to conduct multiple reactions if several generations are desired.

The structure of dendrimers can be affected by environmental conditions, such as pH, temperature, and concentration. However, changes in these conditions will not result in dismemberment of the dendritic arms, with the exception of specially designed dendrimers in which cleavage is desired.[14-16] Other hosts currently used to harbor prospective guests such as micelles, vesicles, and capsules may completely dissociate upon slight changes in solution conditions. Dendrimers also offer the advantage of being relatively monodisperse.

1.4 Encapsulation Systems

Host-guest systems have been the subject of many studies over the last several years due to their potential use in drug delivery and catalysis. Some systems that have been used to incarcerate molecular guests include capsules,[17-20] micelles,[21-25] vesicles,[26-28] and dendrimers.[16,29-34] Also, prodrug and prodrug-like systems have been achieved with dendrimers.[16] These systems may lead to many different uses such as in catalysis and drug delivery. The goal of many researchers is to create a system in which catalysts, drugs, environmentally important compounds, or any other desired guest can be incarcerated by hosts, thereby isolating them from the bulk environment. It is hoped that site isolation is achieved, and the functionality of the guests is preserved. In some cases it may be desired to encapsulate the guest permanently, while in other cases release of the guests may be necessary to fulfill its purpose.

1.4.1 Various Non-Dendrimer Host Systems

Okahata introduced nylon capsule membranes that could have their permeability controlled by the addition of concanavalin A (Con A). Con A was found to increase the permeability of NaCl from capsules corked with bilayers having the α-D-glucopyranosyl head group. Con A was also shown to decrease the permeability of water-soluble dyes for capsules grafted with polymers possessing α-D-glucopyranosyl functional groups. The permeability could then be increased to the original rate upon addition of excess monosaccharides. The permeability of polymers grafted with β-D-glucopyranosyl was unaffected by addition of Con A and therefore these systems could be used as "smart permeation valves".[17] Okahata has also shown that the permeability of capsules grafted with viologen-containing polymers can be reversibly changed upon oxidation with cerium(IV) salt and reduction with sodium dithionite. The viologen polymeric chains repel one another due to charge repulsion when in the oxidized form increasing permeability and become entangled when reduced covering the pores of the capsule decreasing permeability.[18] One can change the encapsulation/release properties of capsules by regulating the permeability.

The encapsulation of pyrene microcrystals in microcapsules composed of alternating charged layers of polyelectrolytes has been demonstrated by Caruso.[19] The microcapsules are dissolved in water and pyrene is released upon addition of ethanol. These systems result in long release times, which are directly related to the number of polyelectrolyte layers comprising the capsule. Sukhorukov produced polyelectrolyte capsules which decompose at low pH by assembling dextran sulfate and protamine (both biodegradable polyelectrolytes) on melamine formaldehyde microcores. The capsules swell at high pH, enabling them to encapsulate

peroxidase maintaining 57% of its activity. Upon lowering the pH, the enzyme was released and exhibited 90-95% of its activity prior to encapsulation.[20]

Vesicles are another option for researchers interested in encapsulation/release chemistry. Chattaraj and Das were able to incorporate viral influenza vaccine antigen in neutral vesicles.[26] It was shown that the encapsulation process had very little effect on the structure and activity of the antigen which may lead to its use as a possible treatment for influenza by means of nasal delivery. Chung and co-workers encapsulated pyranine inside a vesicle with a polymerized outer shell.[27] This system was specifically designed such that the vesicles would break apart in basic solutions. These pH responsive hosts may also be used as a drug delivery vehicle. Qin and co-workers developed a thermo-responsive vesicle to be used in cancer treatment.[28] Polymers were used that self-assemble into vesicles at temperatures equal to or above the normal body temperature (37°C). Disassembly occurs at temperatures below 37°C, thereby releasing any encapsulated drugs.

A great deal of research has been conducted on the encapsulation ability of liposomes as well, that is vesicles composed of a lipid and cholesterol bilayer. Liposomes facilitate gene[35-37] and drug[38-41] delivery to cells that alone will not penetrate a cell's membrane under most normal conditions. However, the liposome's bilayer can fuse with the similar cell membrane and deposit its contents into the cell. The host/delivery properties of liposomes have lead to their use in numerous applications ranging from the treatment of acne[42-44] to cancer.[45-47]

Micelles have also been the focus of many researchers for encapsulation/release systems. Rotello demonstrated that ferrocenyl guests can be incarcerated by micelles formed from diaminotriazine-functionalized polymers in nonpolar solvents. Site isolation was achieved, thereby preventing aggregation of the oxidized ferrocenyl species in aqueous media.[21] Sakurai

has synthesized hollow spheres from shell cross-linked micelles. The dye 5,6-carboxyfluorescein was encapsulated in these cross-linked micelles in water and then released slowly after dialysis against water for several days.[22,23] Eisenburg has shown that poly(caprolactone)-block-poly(ethylene oxide) micelles were able to encapsulate the hydrophobic probes benzo[a]pyrene and Cell-Tracker DM-DiI. These probes were released upon dialysis using the "kitchen sink method" and it was shown that the release is diffusion controlled.[24] In this process the dialysate is constantly added and removed from the system. Therefore the diffusion of the released guests out of the dialysis membrane is not subject to concentration equilibrium effects. Billingham used triblock copolymers that formed micelles at pH 8 to encapsulate pyrene and dipyridamole. The release of guests in this system at pH 7.4 is also diffusion controlled; however, lowering the pH to 3 results in the dissociation of the micelles yielding a rapid-triggered release.[25]

Capsules, vesicles, and micelles offer the advantage that complete release is achieved upon dissociation, however this characteristic may also lead to complications. Specific conditions must be present for the systems described above to self-organize into micelles and vesicles. The pH, temperature, and concentration of the starting products are often highly important, and a slight change in any of these conditions may prevent the micelles or capsules from forming. If any of the conditions are altered slightly, dissociation of the host may occur, resulting in premature release. For drug delivery purposes and catalytic purposes, it is imperative that the guests remain incarcerated until release is desired. Dendrimers offer an alternative route for encapsulation and release of guests, a route that may help prevent premature leakage of the internalized guests.

1.4.2 Dendrimers as Hosts

Although Vögtle first introduced dendrimers in 1978,[48] their ability to host molecules was not demonstrated until the mid 1980s by Newkome[49] and Tomalia.[50] Currently the use of dendrimers as hosts is the focus of a large number of researchers.[51-53] Many dendrimers are commercially available which allows researchers more time to focus on the many possible uses of dendrimers, rather than their synthesis. Due to the fact that many of the available dendrimers are functionalized with a variety of reactive groups along the periphery, it is possible to add almost any desired moiety as an end group to achieve the desired function of the dendrimer. Dendrimer hosts can be used for separation techniques,[29] catalysis,[31] light emitting diodes,[54] or drug delivery systems,[16,34] depending on the peripheral functionality chosen.

Meijer was able to encapsulate Rose Bengal in his "dendritic box."[55] However, the bulky amino acids at the periphery of the dendrimer prevented the guests from being released. Ideally one would like to control the incarceration of guests and be able to release the guests upon command. Vögtle's azobenzene-terminated dendrimer was the first stimuli-responsive dendrimer in which the release of guests could be controlled.[56] The photoisomerization properties of azobenzene were used to control the release of eosin from the dendrimer core. Prior to being irradiated by a light source, the azobenzene end groups exist in the *trans* form, and guests are able to diffuse from the dendrimer. Retainment of guests was increased when the azobenzene end groups were irradiated with 545 nm light causing the azobenzene structure to "switch" to the *cis* form. Vögtle's work demonstrated that the encapsulation and release properties of dendrimers can be controlled by manipulating the dendrimer structure.

Crooks showed the versatility of dendrimers by demonstrating the ability to alter the permeability of amine-terminated dendrimer thin films supported on gold electrodes. Cations

were able to penetrate the dendrimer at high pH and anions were able to penetrate at low pH.[29] These ion selective materials may prove useful for separation techniques. The ability of dendrimers to remove polycyclic aromatic hydrocarbons from water has also been investigated.[30] Paleos and coworkers have shown that poly(propylene imine) dendrimers equipped with terminal aliphatic chains absorb pyrene, phenanthrene, and fluoranthene from water. The guests are subsequently released from the dendrimers upon addition of hyrdrochloric acid or sodium chloride. These systems may also be useful for separation techniques such as in water purification.

Kimura developed a temperature-sensitive dendrimer that is capable of encapsulating and releasing guests.[31] Poly(propylene imine) dendrimers were functionalized with the temperature-responsive polymer poly(*N*-isopropylacrylamide), pNIPAAm. The catalytic activity of encapsulated cobalt(II) phthalocyanine complexes toward thiol oxidation was significantly decreased when the temperature was below the lower critical solution temperature (LCST) of the pNIPAAm. The catalytic activity (turnover frequency) was then 3 times greater when the temperature was increased to or above the LCST. When the temperature is below the LCST the polymer arms are soluble in water and extended creating a sterically crowded periphery preventing subtrate access to the incarcerated catalyst. The polymer arms shrink when the temperature is increased above the LCST, allowing the substrate to penetrate the periphery of the dendrimer.[31] This system has proven to be useful as a temperature-sensitive host for catalysts. Paleos and coworkers have attached poly(ethylene glycol) chains to poly(propylene imine) dendrimers to serve as a drug delivery system. Encapsulation of pyrene and the anti-inflammatory corticosteroid betamethasone valerate was demonstrated, as well as its release from the dendrimer upon titration with hydrochloric acid and sodium chloride.[34]

In order to create a system that emits multiple colors for use in color tunable display systems, the use of multiple dyes in such systems is required. However, if site isolation is not achieved in these tunable display systems, dye-dye energy transfer will often occur, resulting in single color emission (as opposed to multiple color) from the dye with the lowest HOMO-LUMO band gap.[54] Fréchet has shown that site isolation can be achieved when dyes are encapuslated in high-generation dendrimers.[32,33] In their studies, Coumarin 343 (C343) and pentathiophene (T5) dicarboxylic ester were used as the cores of the dendrimer, while the periphery of the dendrimer was functionalized with triarylamine. Thin films of these dendrimers were spun onto glass substrates, yielding a film thickness between 110 and 130 nm. The triarylamine functional groups were excited at 350 nm and energy transfer to the core is achieved. Emission was then observed at both 470 nm and 525 nm values which correlate well with the emissions of C343 and T5 respectivelly.[32,33] Therefore Fréchet has shown the capability of dendrimers to achieve site isolation for molecules located in the core of higher generation dendrimers.

Most studies to date involve manipulating the structure of dendrimers to promote incarceration or release of guest molecules. McGrath entertained the idea of disassembling dendrimers by means of a depolymerization reaction.[14,15] It was shown that dendrimers containing benzyl ethers can be fragmented upon mild oxidation. These systems may allow one to encapsulate guest molecules, then "break open" the dendrimer to release all guests incarcerated by the dendrimer. One of the most exciting features of dendrimers is their potential to serve as a host in drug delivery systems. Being able to deliver drugs to the target site may result in lower dosages and fewer side effects. Shabat and coworkers have functionalized dendrons with doxorubicin (DOX) and camptothecin. These drugs are attached to the dendrimer

by means of a self-immolative linker which is cleaved in the presence of antibody 38C2. Therefore the anticancer drugs are released upon exposure to antibody 38C2.[16] Several prodrugs have also been designed by de Groot and co-workers that specifically target tumor cells.[57-61] They recently began using dendrimers as the backbone of these prodrugs and de Groot's industrial group at Syntarga B.V. introduced a dendrimer that could release its end groups upon a single chemical event.[62] Considering this success with prodrugs in the past and this latest development, it is highly likely that dendrimers may play a crucial role in cancer treatment in the future.

It has been shown that the ability of dendrimers to host guest molecules leads to numerous possible uses. It is clearly evident that dendrimers will play an important role in future encapsulation and release chemistry. Most of the current dendrimer systems involve dynamic trapping in which the guests are able to freely diffuse in and out of the dendrimer. Our group is interested in creating a static trapping system in which guests cannot diffuse out of the dendritic cavities; true imprisonment of guests is the goal, as is the controlled, triggered release of guests. Thus, a major achievement would be to produce a dendrimer that can incarcerate guest molecules and release the guests only when stimulated by some well-defined chemical event. This desire led our group to produce poly(propylene imine) dendrimers functionalized with pyrrole along the periphery.

1.5 Pyrrole-Terminated Dendrimers

Pyrrole was chosen as the functional group for our dendrimers due to its ability to form oligomers when chemically[4-6,63-65] and electrochemically oxidized.[66-70] The presence of these oligomers at the periphery should afford a stimuli-responsive dendrimer capable of encapsulating guest molecules and releasing them upon command. Poly(pyrrole) was first synthesized in

1979[69] and has been the subject of numerous studies due to its superior conducting properties.[71,72]

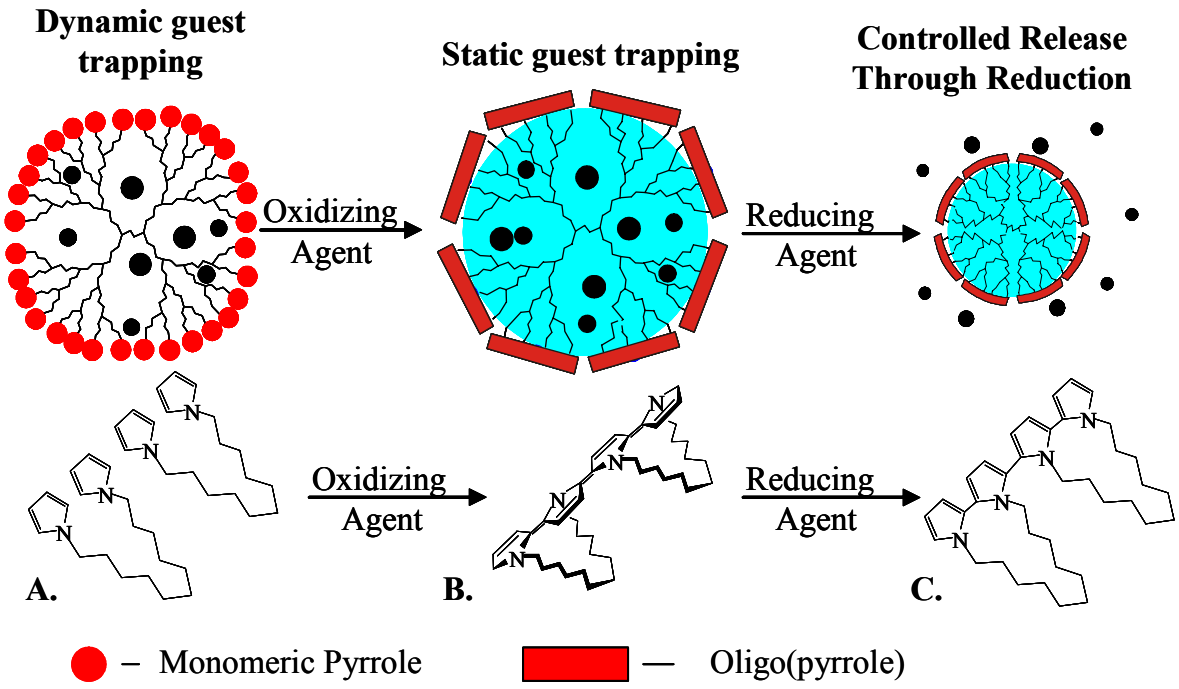

Figure 1.3 Scheme depicting the dynamic guest incarceration of the monomeric dendrimer (A), static guest trapping by the oxidized oligo(pyrrole)-terminated dendrimer (B), and the triggered release upon the reduction of the poly(pyrrole) oligomers (C).

To date there is still much debate over the initial coupling step in the pyrrole polymerization. It has been reported that the initial coupling step is between two radical cations,[73-76] two neutral radicals,[77,78] and a radical cation and a neutral monomer.[79,80] One belief that is fairly consistent throughout the literature is that individual monomeric pyrrole is added to the oligomers. Lacroix and co-workers have conducted molecular modeling experiments that predict lower dimerization rates for longer oligomer lengths. Their studies also suggested the presence of more defects and quick termination when large oligomers are oxidized, resulting in very short oligomers.[81]

It has also been observed that polymerization in aqueous environments is strongly affected by the pH. Kinetics studies revealed a slower reaction rate at higher pH.[4,76] Bjorklund believes the pyrrole cation radical is deprotonated at higher pH resulting in a neutral radical that is not involved in the oligomerization process.[4] It is also well known that unconjugated trimers are formed under acidic conditions[82] that do not form oligomers.[83] However, after dehydrogenation, these trimers form oligomers instantly.[84] Therefore it is our belief that we can form different length oligomers around the periphery of our dendrimers by adjusting the pH prior to oxidation with chemical oxidants.

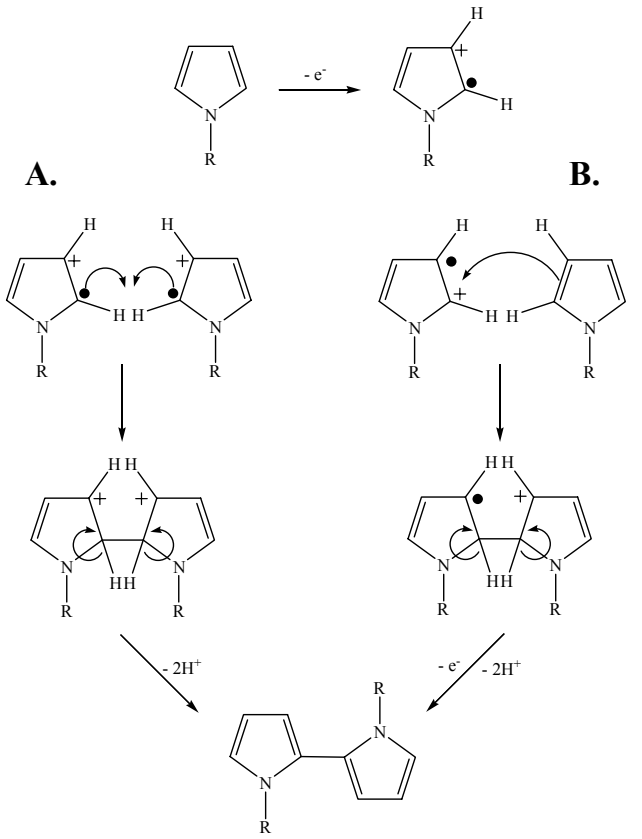

Figure 1.4 The proposed mechanisms for the polymerization of pyrrole in which the initial coupling step involves 2 cation radicals (A) and a cation radical and neutral monomer (B). The resulting dimer would then be oxidized, and couple with either a cation radical monomer or a neutral monomer.

Noble has shown that guests will partition into the core of a pyrrole-terminated dendrimer.[1] However, if oligo(pyrroles) are not present, the guests are quickly released from the core. Oligomerization of the periphery has proven to be an effective means to aid in retention of the guests; however, guests are still able to diffuse from the dendrimer, albeit at a 30% slower rate than in the monomeric state. Molecular modeling studies also revealed a change in the

dendrimer structure when the pyrroles are reversibly oxidized and reduced. A larger cavity volume is predicted when in the oxidized state and a smaller cavity volume is predicted when the pyrroles are reduced. Also, changes in porosity of the dendrimer were noted.[1] Therefore we would like to encapsulate guest molecules when the dendrimer is in the oxidized state and then release the guests upon reduction.

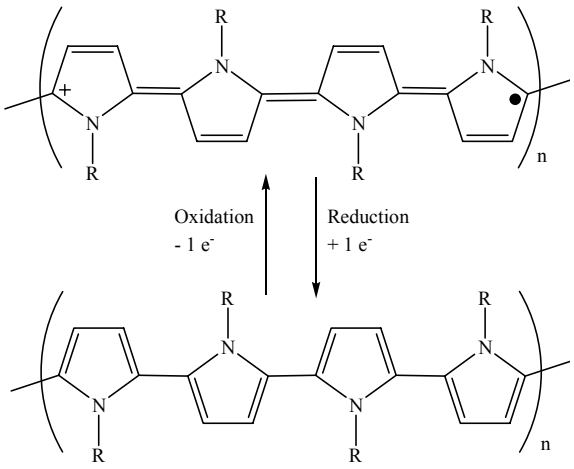

Figure 1.5 Schematic illustrating the reversible oxidation/reduction of oligopyrrole.

The hypothesis is that by increasing the length of the pyrrole oligomers, an increase in guest retainment can be achieved. The effect of solution parameters, such as pH and ionic strength, on the mobility of the pyrrole monomers was investigated here. To date it is unclear whether the mobility of the pyrrole monomers in the non-oligomeric dendrimer should be increased or decreased to yield longer oligomers in the product. ^{1}H NMR relaxation methods were used here to study the mobility of the pyrrole monomers and to determine which solution conditions yield longer oligo(pyrroles).

1.6 T_1 Relaxation Studies for Structural Characterization

Spin-lattice relaxation measurements have been conducted for determining the mobility of many structures such as dendrimers.[55,85-88] The T_1 data is obtained by measuring the length of time needed for the nuclear spins of a system to return to their original state after a 180 degree pulse. This is known as the inversion-recovery method for determining T_1. Large T_1 values are the result of nuclei needing longer periods of time to relax back to their original spin state. An increase in the T_1 value for small molecules means an increase in the mobility at that particular

area for a given molecule. The opposite is true for larger molecules. Therefore, it is often necessary to determine the effect temperature has on T_1 data to properly assess the type of molecule behavior (small versus large). The T_1 values are related to the rotational correlation time of the molecule. The correlation times can be decreased by heating the system which allows for determination of whether the systems being studied are behaving like small molecules or large molecules.[89] Once this has been determined, one can use T_1 data to estimate the relative mobility or rigidity at various locations of the system of interest.

Spin-lattice relaxation measurements were conducted on poly(ether ketone) dendrimers to determine the mobility of end groups as a function of the degrees of branching. Temperature studies led to the conclusion that the dendrimers were behaving like small molecules, and the mobility along the dendrimer periphery increased as the generation was increased, while the mobility in the interior was only slightly affected.[85] However, the T_1 data from Meijer's "dendritic box" suggested that the periphery of these hydrogen-bonded dendrimers behaved much like a solid shell at higher generations.[55] Ford also showed that his triethylenoxy methyl ether-terminated dendrimers demonstrated a decrease in mobility for all protons as the dendrimer generation increased.[86] They also demonstrated that the mobility of moieties increases when moving from the core of the dendrimer to the periphery.

Upon review of the literature, it is pertinent to conduct T_1 measurements on the system at hand as the mobility in all dendrimers is not the same. It is my desire to determine the effect of solution parameters, such as ionic strength and pH, on the mobility of the pyrrole monomers of our pyrrole-terminated dendrimers in aqueous media. In addition, I want to establish a relationship between pyrrole coupling efficiency and pyrrole mobility in the monomeric dendrimers. Once this relationship is determined, solution conditions can be optimized so that

longer pyrrole oligomers can be formed. Finally, the impact of oligomer length on encapsulation efficiency will be evaluated.

Further conclusions can also be drawn from T_1 relaxation data. Meijer used T_1 measurements to study the encapsulation of guests by thiourea-functionalized dendrimers. They were able to determine that the guests were only partially encapsulated inside the dendrimer as the T_1 values for some protons of the guests increased when the guest-dendrimer ratio was increased. Due to the fact that the mobility of a number of protons on each guest was unaffected, they were able to conclude that the guests were located along the periphery with some portion of the guest molecule protruding out of the dendrimer periphery and not encapsulated inside the core.[87] The T_1 values for these protons remained constant and correlated well with molecules in the bulk environment.

1.7 References

(1) Noble IV, C. O. *Pyrrole-Terminated Dendrimers for Use in Polymerizable Monolayers and Guest Encapsulation Systems, Louisiana State University, Baton Rouge,* 2001.

(2) Pavlov, G. M.; Korneeva, E. V.; Meijer, E. W. *Molecular Characteristics of Poly(Propylene Imine) Dendrimers as Studied with Translational Diffusion and Viscometry,* ***Colloid and Polymer Science*** **2002**, *280*, 416-423.

(3) Lyulin, A. V.; Davies, G. R.; Adolf, D. B. *Location of Terminal Groups of Dendrimers: Brownian Dynamics Simulation,* ***Macromolecules*** **2000**, *33*, 6899-6900.

(4) Bjorklund, R. B. *Kinetics of Pyrrole Polymerization in Aqueous Iron Chloride Solution,* ***Journal of the Chemical Society, Faraday Transactions 1: Physical Chemistry in Condensed Phases*** **1987**, *83*, 1507-1514.

(5) Schlenoff, J. B.; Fong, Y.; Shen, C. *Stoichiometry and Kinetics of Pyrrole Polymerization,* ***Macromolecules*** **1991**, *24*, 6791-6793.

(6) Stanke, D.; Hallensleben, M. L.; Toppare, L. *Oxidative Polymerization of Poly(2-(N-Pyrrolyl)Ethyl Methacrylate) with Iron Chloride,* ***Synthetic Metals*** **1995**, *72*, 95-98.

(7) Stanke, D.; Hallensleben, M. L.; Toppare, L. *Oxidative copolymerization of pyrrole and 2-(N-pyrrolyl)ethyl stearate with iron chloride in nitromethane,* ***Synthetic Metals*** **1995**, *72*, 167-171.

(8) Stanke, D.; Hallensleben, M. L.; Toppare, L. *Oxidative polymerization of some N-alkylpyrroles with ferric chloride,* ***Synthetic Metals*** **1995**, *73*, 267-272.

(9) Briber, R. M.; Bauer, B. J.; Hammouda, B.; Tomalia, D. A. *Small-Angle Neutron Scattering from Solutions of Dendrimer Molecules: Intermolecular Interactions,* ***Polymeric Materials Science and Engineering*** **1992**, *67*, 430-431.

(10) Young, J. K.; Baker, G. R.; Newkome, G. R.; Morris, K. F.; Johnson, C. S., Jr. *"Smart" Cascade Polymers. Modular Syntheses of Four-Directional Dendritic Macromolecules with Acidic, Neutral, or Basic Terminal Groups and the Effect of pH Changes on Their Hydrodynamic Radii,* ***Macromolecules*** **1994**, *27*, 3464-3471.

(11) Welch, P.; Muthukumar, M. *Tuning the Density Profile of Dendritic Polyelectrolytes,* ***Macromolecules*** **1998**, *31*, 5892-5897.

(12) Fischer, M.; Vogtle, F. *Dendrimers: From Design to Application - A Progress Report,* ***Angewandte Chemie, International Edition*** **1999**, *38*, 885-905.

(13) Hawker, C.; Frechet, M. J. *A New Convergent Approach to Monodisperse Dendritic Macromolecules,* ***Journal of the Chemical Society, Chemical Communications*** **1990**, 1010-1013.

(14) Li, S.; Szalai, M. L.; Kevwitch, R. M.; McGrath, D. V. *Dendrimer Disassembly by Benzyl Ether Depolymerization,* ***Journal of the American Chemical Society*** **2003**, *125*, 10516-10517.

(15) Szalai, M. L.; Kevwitch, R. M.; McGrath, D. V. *Geometric Disassembly of Dendrimers: Dendritic Amplification,* ***Journal of the American Chemical Society*** **2003**, *125*, 15688-15689.

(16) Shamis, M.; Lode, H. N.; Shabat, D. *Bioactivation of Self-Immolative Dendritic Prodrugs by Catalytic Antibody 38C2,* ***Journal of the American Chemical Society*** **2004**, *126*, 1726-1731.

(17) Okahata, Y.; Nakamura, G.; Noguchi, H. *Functional Capsule Membranes. Part 30. Concanavalin A-Induced Permeability Control of Capsule Membranes Corked with Synthetic Glycolipid Bilayers or Grafted with Synthetic Glycopolymers,* ***Journal of the Chemical Society, Perkin Transactions 2: Physical Organic Chemistry (1972-1999)*** **1987**, 1317-1322.

(18) Okahata, Y.; Ariga, K.; Seki, T. *Redox-Sensitive Permeation from a Capsule Membrane Grafted with Viologen-Containing Polymers,* ***Journal of the Chemical Society, Chemical Communications*** **1986**, 73-75.

(19) Shi, X.; Caruso, F. *Release Behavior of Thin-Walled Microcapsules Composed of Polyelectrolyte Multilayers,* ***Langmuir*** **2001**, *17*, 2036-2042.

(20) Balabushevich, N. G.; Tiourina, O. P.; Volodkin, D. V.; Larionova, N. I.; Sukhorukov, G. B. *Loading the Multilayer Dextran Sulfate/Protamine Microsized Capsules with Peroxidase,* ***Biomacromolecules*** **2003**, *4*, 1191-1197.

(21) Galow, T. H.; Ilhan, F.; Cooke, G.; Rotello, V. M. *Recognition and Encapsulation of an Electroactive Guest within a Dynamically Folded Polymer,* ***Journal of the American Chemical Society*** **2000**, *122*, 3595-3598.

(22) Sanji, T.; Nakatsuka, Y.; Ohnishi, S.; Sakurai, H. *Preparation of Nanometer-Sized Hollow Particles by Photochemical Degradation of Polysilane Shell Crosslinked Micelles and Reversible Encapsulation of Guest Mmolecules,* ***Macromolecules*** **2000**, *33*, 8524-8526.

(23) Sanji, T.; Nakatsuka, Y.; Kitayama, F.; Sakurai, H. *Encapsulation of Polysilane into Shell Cross-Linked Micelles,* ***Chemical Communications (Cambridge)*** **1999**, 2201-2202.

(24) Soo, P. L.; Luo, L.; Maysinger, D.; Eisenberg, A. *Incorporation and Release of Hydrophobic Probes in Biocompatible Polycaprolactone-block-poly(ethylene oxide) Micelles: Implications for Drug Delivery,* ***Langmuir*** **2002**, *18*, 9996-10004.

(25) Tang, Y.; Liu, S. Y.; Armes, S. P.; Billingham, N. C. *Solubilization and Controlled Release of a Hydrophobic Drug Using Novel Micelle-Forming ABC Triblock Copolymers,* ***Biomacromolecules*** **2003**, *4*, 1636-1645.

(26) Chattaraj, S. C.; Das, S. K. *Physicochemical Characterization of Influenza Viral Vaccine Loaded Surfactant Vesicles,* ***Drug Delivery*** **2003**, *10*, 73-77.

(27) Chung, M.-H.; Park, C.; Chun, B. C.; Chung, Y.-C. *Polymerized ion pair amphiphile vesicles with pH-sensitive transformation and controlled release property,* ***Colloids and Surfaces, B: Biointerfaces*** **2004**, *34*, 179-184.

(28) Qin, S.; Geng, Y.; Discher, D. E.; Yang, S. *Temperature-controlled assembly and release from polymer vesicles of poly(ethylene oxide)-block-poly(N-isopropylacrylamide),* ***Advanced Materials (Weinheim, Germany)*** **2006**, *18*, 2905-2909.

(29) Liu, Y.; Zhao, M.; Bergbreiter, D. E.; Crooks, R. M. *pH-Switchable, Ultrathin Permselective Membranes Prepared from Multilayer Polymer Composites,* ***Journal of the American Chemical Society*** **1997**, *119*, 8720-8721.

(30) Arkas, M.; Tsiourvas, D.; Paleos, C. M. *Functional Dendrimeric "Nanosponges" for the Removal of Polycyclic Aromatic Hydrocarbons from Water,* ***Chemistry of Materials*** **2003**, *15*, 2844-2847.

(31) Kimura, M.; Kato, M.; Muto, T.; Hanabusa, K.; Shirai, H. *Temperature-Sensitive Dendritic Hosts. Synthesis, Characterization, and Control of Catalytic Activity,* ***Macromolecules*** **2000**, *33*, 1117-1119.

(32) Furuta, P.; Brooks, J.; Thompson, M. E.; Frechet, J. M. J. *Simultaneous Light Emission from a Mixture of Dendrimer Encapsulated Chromophores: A Model for Single-Layer Multichromophoric Organic Light-Emitting Diodes,* ***Journal of the American Chemical Society*** **2003**, *125*, 13165-13172.

(33) Furuta, P.; Frechet, J. M. J. *Controlling Solubility and Modulating Peripheral Function in Dendrimer Encapsulated Dyes,* ***Journal of the American Chemical Society*** **2003**, *125*, 13173-13181.

(34) Paleos, C. M.; Tsiourvas, D.; Sideratou, Z.; Tziveleka, L. *Acid- and Salt-Triggered Multifunctional Poly(propylene imine) Dendrimer as a Prospective Drug Delivery System,* ***Biomacromolecules*** **2004**, *5*, 524-529.

(35) Miyazaki, M.; Obata, Y.; Abe, K.; Furusu, A.; Koji, T.; Tabata, Y.; Kohno, S. *Gene transfer using nonviral delivery systems,* ***Peritoneal Dialysis International*** **2006**, *26*, 633-640.

(36) Pardridge, W. M. *Nonviral gene transfer across the blood-brain barrier with trojan horse liposomes,* ***Gene Transfer*** **2007**, 701-710.

(37) Hoekstra, D.; Rejman, J.; Wasungu, L.; Shi, F.; Zuhorn, I. *Gene delivery by cationic lipids: in and out of an endosome,* ***Biochemical Society Transactions*** **2007**, *35*, 68-71.

(38) Huang, Y.-k. *Research progress on liposomes as drug delivery systems,* ***Zhongguo Yaoshi (Wuhan, China)*** **2005**, *8*, 549-550.

(39) Yan, Y.-l.; Zhou, L.-l. *Review on application of liposomes in nasal drug delivery system,* ***Zhongyao Xinyao Yu Linchuang Yaoli*** **2006**, *17*, 307-309.

(40) Xiang, T.-X.; Anderson, B. D. *Liposomal drug transport: A molecular perspective from molecular dynamics simulations in lipid bilayers,* ***Advanced Drug Delivery Reviews*** **2006**, *58*, 1357-1378.

(41) Angst, M. S.; Drover, D. R. *Pharmacology of drugs formulated with DepoFoam: a sustained release drug delivery system for parenteral administration using multivesicular liposome technology,* ***Clinical Pharmacokinetics*** **2006**, *45*, 1153-1176.

(42) Esposito, E.; Menegatti, E.; Cortesi, R. *Ethosomes and liposomes as topical vehicles for azelaic acid: A preformulation study,* ***Journal of Cosmetic Science*** **2004**, *55*, 253-264.

(43) Fluhr, J. W.; Barsom, O.; Gehring, W.; Gloor, M. *Antibacterial efficacy of benzoyl peroxide in phospholipid liposomes: a vehicle-controlled, comparative study in patients with papulopustular acne,* ***Dermatology (Basel)*** **1999**, *198*, 273-277.

(44) Date, A. A.; Naik, B.; Nagarsenker, M. S. *Novel drug delivery systems: potential in improving topical delivery of antiacne agents,* ***Skin Pharmacol Physiol FIELD Full Journal Title:Skin pharmacology and physiology FIELD Publication Date:2006*** **2006**, *19*, 2-16. FIELD Reference Number:95 FIELD Journal Code:101188418 FIELD Call Number:.

(45) Ikehara, Y.; Kojima, N. *Development of a novel oligomannose-coated liposome-based anticancer drug-delivery system for intraperitoneal cancer,* ***Current Opinion in Molecular Therapeutics*** **2007**, *9*, 53-61.

(46) Gabizon, A. A. *Applications of liposomal drug delivery systems to cancer therapy,* ***Nanotechnology for Cancer Therapy*** **2007**, 595-611, 591 plate.

47) Ristori, S.; Salvati, A.; Martini, G.; Spalla, O.; Pietrangeli, D.; Rosa, A.; Ricciardi, G. *Synthesis and Liposome Insertion of a New Poly(carboranylalkylthio)porphyrazine to Improve Potentiality in Multiple-Approach Cancer Therapy,* ***Journal of the American Chemical Society*** **2007**, *129*, 2728-2729.

(48) Buhleier, E.; Wehner, W.; Vogtle, F. *"Cascade"- and "Nonskid-Chain-Like" Syntheses of Molecular Cavity Topologies,* ***Synthesis*** **1978**, 155-158.

(49) Newkome, G. R.; Yao, Z.; Baker, G. R.; Gupta, V. K. *Micelles. Part 1. Cascade Molecules: A New Approach to Micelles. A [27]-Arborol,* ***Journal of Organic Chemistry*** **1985**, *50*, 2003-2004.

(50) Tomalia, D. A.; Baker, H.; Dewald, J.; Hall, M.; Kallos, G.; Martin, S.; Roeck, J.; Ryder, J.; Smith, P. *A New Class of Polymers: Starburst-Dendritic Macromolecules,* ***Polymer Journal (Tokyo, Japan)*** **1985**, *17*, 117-132.

(51) Baars, M. W. P. L.; Meijer, E. W. *Host-guest chemistry of dendritic molecules,* ***Topics in Current Chemistry*** **2000**, *210*, 131-182.

(52) Aulenta, F.; Hayes, W.; Rannard, S. *Dendrimers: a new class of nanoscopic containers and delivery devices,* ***European Polymer Journal*** **2003**, *39*, 1741-1771.

(53) Boas, U.; Heegaard Peter, M. H. *Dendrimers in drug research,* ***Chem Soc Rev FIELD Full Journal Title:Chemical Society reviews FIELD Publication Date:2004***, *33*, 43-63. FIELD Reference Number:158 FIELD Journal Code:0335405 FIELD Call Number:.

(54) Shoustikov, A. A.; You, Y.; Thompson, M. E. *Electroluminescence Color Tuning by Dye Doping in Organic Light-Emitting Diodes,* ***IEEE Journal of Selected Topics in Quantum Electronics*** **1998**, *4*, 3-13.

(55) Jansen, J. F. G. A.; de Brabander van den Berg, E. M. M.; Meijer, E. W. *Encapsulation of Guest Molecules into a Dendritic Box,* ***Science (Washington, D. C.)*** **1994**, *266*, 1226-1229.

(56) Archut, A.; Azzellini, G. C.; Balzani, V.; Cola, L.; Vogtle, F. *Toward Photoswitchable Dendritic Hosts. Interaction between Azobenzene-Functionalized Dendrimers and Eosin,* ***Journal of the American Chemical Society*** **1998**, *120*, 12187-12191.

(57) de Groot, F. M. H.; Broxterman, H. J.; Adams, H. P. H. M.; van Vliet, A.; Tesser, G. I.; Elderkamp, Y. W.; Schraa, A. J.; Kok, R. J.; Molema, G.; Pinedo, H. M.; Scheeren, H. W. *Design, synthesis, and biological evaluation of a dual tumor-specific motive containing integrin-targeted plasmin-cleavable doxorubicin prodrug,* ***Molecular Cancer Therapeutics*** **2002**, *1*, 901-911.

(58) de Groot, F. M. H.; Busscher, G. F.; Aben, R. W. M.; Scheeren, H. W. *Novel 20-Carbonate Linked Prodrugs of Camptothecin and 9-Aminocamptothecin Designed for Activation by Tumour-Associated Plasmin,* ***Bioorganic & Medicinal Chemistry Letters*** **2002**, *12*, 2371-2376.

(59) Damen, E. W. P.; Nevalainen, T. J.; van den Bergh, T. J. M.; de Groot, F. M. H.; Scheeren, H. W. *Synthesis of novel paclitaxel prodrugs designed for bioreductive activation in hypoxic tumour tissue,* ***Bioorganic & Medicinal Chemistry*** **2001**, *10*, 71-77.

(60) de Groot, F. M. H.; Loos, W. J.; Koekkoek, R.; van Berkom, L. W. A.; Busscher, G. F.; Seelen, A. E.; Albrecht, C.; de Bruijn, P.; Scheeren, H. W. *Elongated Multiple Electronic Cascade and Cyclization Spacer Systems in Activatible Anticancer Prodrugs for Enhanced Drug Release,* ***Journal of Organic Chemistry*** **2001**, *66*, 8815-8830.

(61) De Groot, F. M. H.; Damen, E. W. P.; Scheeren, H. W. *Anticancer prodrugs for application in monotherapy: targeting hypoxia, tumor-associated enzymes, and receptors,* ***Current Medicinal Chemistry*** **2001**, *8*, 1093-1122.

(62) de Groot, F. M. H.; Albrecht, C.; Koekkoek, R.; Beusker, P. H.; Scheeren, H. W. *"Cascade-release dendrimers" liberate all end groups upon a single triggering event in the dendritic core,* ***Angewandte Chemie, International Edition*** **2003**, *42*, 4490-4494.

(63) Groenendaal, L.; Peerlings, H. W. I.; van Dongen, J. L. J.; Havinga, E. E.; Vekemans, J. A. J. M.; Meijer, E. W. *Well-Defined Oligo(pyrrole-2,5-diyl)s by the Ullmann Reaction,* ***Macromolecules*** **1995**, *28*, 116-123.

(64) Martina, S.; Enkelmann, V.; Schlueter, A. D.; Wegner, G.; Zotti, G.; Zerbi, G. *Synthesis and Electrochemical and Spectroscopical Studies of 2,5-Pyrrole Oligomers and Well-Defined Short-Chain Poly(2,5-pyrrole),* ***Synthetic Metals*** **1993**, *55*, 1986-1101.

(65) Sigmund, W. M.; Weerasekera, G.; Marestin, C.; Styron, S.; Zhou, H.; Elsabee, M. Z.; Ruehe, J.; Wegner, G.; Duran, R. S. *Polymerization of Monolayers of 3-Substituted Pyrroles,* ***Langmuir*** **1999**, *15*, 6423-6427.

(66) McCarley, R. L.; Willicut, R. J. *Tethered Monolayers of Poly((N-pyrrolyl)alkanethiol) on Au,* ***Journal of the American Chemical Society*** **1998**, *120*, 9296-9304.

(67) Noble, C. O. I. V.; McCarley, R. L. *Pyrrole-Terminated Diaminobutane (DAB) Dendrimer Monolayers on Gold: Oligomerization of Peripheral Groups and Adhesion Promotion of Poly(pyrrole) Films,* ***Journal of the American Chemical Society*** **2000**, *122*, 6518-6519.

(68) Noble, C. O. I. V.; McCarley, R. L. *Surface-Confined Monomers on Electrode Surfaces. 7. Synthesis of Pyrrole-Terminated Poly(propylene imine) Dendrimers,* ***Organic Letters*** **1999**, *1*, 1021-1023.

(69) Diaz, A. F.; Kanazawa, K. K.; Gardini, G. P. *Electrochemical Polymerization of Pyrrole,* ***Journal of the Chemical Society, Chemical Communications*** **1979**, 635-636.

(70) Havinga, E. E.; Ten Hoeve, W.; Meijer, E. W.; Wynberg, H. *Water-Soluble Self-Doped 3-Substituted Polypyrroles,* ***Chemistry of Materials*** **1989**, *1*, 650-659.

(71) Ruehe, J.; Ezquerra, T.; Wegner, G. *Conducting Polymers from 3-Alkylpyrroles,* ***Makromolekulare Chemie, Rapid Communications*** **1989**, *10*, 103-108.

(72) Martina, S.; Enkelmann, V.; Wegner, G.; Schlueter, A. D. *Progress Toward the Development of a Chemical Synthesis for Poly(2,5-Pyrrole),* ***Synthetic Metals*** **1992**, *51*, 299-305.

(73) Genies, E. M.; Bidan, G.; Diaz, A. F. *Spectroelectrochemical Study of Polypyrrole Films,* ***Journal of Electroanalytical Chemistry and Interfacial Electrochemistry*** **1983**, *149*, 101-113.

(74) Andrieux, C. P.; Audebert, P.; Hapiot, P.; Saveant, J. M. *Observation of the Cation Radicals of Pyrrole and of Some Substituted Pyrroles in Fast-Scan Cyclic Voltammetry. Standard Potentials and Lifetimes,* ***Journal of the American Chemical Society*** **1990**, *112*, 2439-2440.

(75) Andrieux, C. P.; Audebert, P.; Hapiot, P.; Saveant, J. M. *Identification of the First Steps of the Electrochemical Polymerization of Pyrroles by Means of Fast Potential Step Techniques,* ***Journal of Physical Chemistry*** **1991**, *95*, 10158-10164.

(76) Guyard, L.; Hapiot, P.; Neta, P. *Redox Chemistry of Bipyrroles: Further Insights into the Oxidative Polymerization Mechanism of Pyrrole and Oligopyrroles,* ***Journal of Physical Chemistry B*** **1997**, *101*, 5698-5706.

(77) Shichiri, T.; Toriumi, M.; Tanaka, K.; Yamabe, T.; Yamauchi, J.; Deguchi, Y. *ESR Study for the Oxidation of Pyrrole in the Presence of a Spin Trap,* ***Synthetic Metals*** **1989**, *33*, 389-397.

(78) Lowen, S. V.; Van Dyke, J. D. *Mechanistic Studies of the Electrochemical Polymerization of Pyrrole: Deuterium Isotope Effects and Radical Trapping Studies,* ***Journal of Polymer Science, Part A: Polymer Chemistry*** **1990**, *28*, 451-464.

(79) Wei, Y.; Chan, C. C.; Tian, J.; Jang, G. W.; Hsueh, K. F. *Electrochemical Polymerization of Thiophenes in the Presence of Bithiophene or Terthiophene: Kinetics and Mechanism of the Polymerization,* ***Chemistry of Materials*** **1991**, *3*, 888-897.

(80) Satoh, M.; Imanishi, K.; Yoshino, K. *Characterization of Electrochemical Anodic Polymerization of Aromatic Compounds in Aprotic Solvents,* ***Journal of Electroanalytical Chemistry and Interfacial Electrochemistry*** **1991**, *317*, 139-151.

(81) Lacroix, J.-C.; Maurel, F.; Lacaze, P.-C. *Oligomer-Oligomer versus Oligomer-Monomer C2-C2' Coupling Reactions in Polypyrrole Growth,* ***Journal of the American Chemical Society*** **2001**, *123*, 1989-1996.

(82) Jones, R. A.; Bean, G. P. *The Chemistry of Pyrroles*; Academic Press, London, 1977.

(83) Lamb, B. S.; Kovacic, P. *Polymerization of Aromatic Nuclei. XXIII. Investigation of Oligomer and Pyrrole Red from Pyrrole and Trichloroacetic Acid,* ***Journal of Polymer Science, Polymer Chemistry Edition*** **1980**, *18*, 1759-1770.

(84) Rapoport, H.; Castagnoli, N., Jr.; Holden, K. G. *2,2':5',2''-Terpyrrole,* ***Journal of Organic Chemistry*** **1964**, *29*, 883-885.

(85) Kwak, S.-Y.; Lee, H. Y. *Molecular Relaxation and Local Motion of Hyperbranched Poly(ether ketone)s with Reference to Their Linear Counterpart. 1. Effect of Degrees of Branching,* ***Macromolecules*** **2000**, *33*, 5536-5543.

(86) Baille, W. E.; Malveau, C.; Zhu, X. X.; Kim, Y. H.; Ford, W. T. *Self-Diffusion of Hydrophilic Poly(propyleneimine) Dendrimers in Poly(vinyl alcohol) Solutions and Gels by Pulsed Field Gradient NMR Spectroscopy,* ***Macromolecules*** **2003**, *36*, 839-847.

(87) Boas, U.; Karlsson, A. J.; de Waal, B. F. M.; Meijer, E. W. *Synthesis and Properties of New Thiourea-Functionalized Poly(propylene imine) Dendrimers and Their Role as Hosts for Urea Functionalized Guests,* ***Journal of Organic Chemistry*** **2001**, *66*, 2136-2145.

(88) Chasse, T. L.; Sachdeva, R.; Li, Q.; Li, Z.; Petrie, R. J.; Gorman, C. B. *Structural Effects on Encapsulation as Probed in Redox-Active Core Dendrimer Isomers,* ***Journal of the American Chemical Society*** **2003**, *125*, 8250-8254.

(89) Levitt, M. H. *Spin Dynamics: Basics of Nuclear Magnetic Resonance*; John Wiley and Sons, LTD: New York, NY, 2001.

Chapter 2

Materials and Methods

2.1 Experimental

2.1.1 Chemicals

All solvents utilized were chromatographic grade or better and used without further purification unless otherwise stated. The following poly(propylene imine) dendrimers that were the focus of these studies were obtained from Aldrich and used as received: DAB-Am_4, poly(propylene imine) tetramine dendrimer, generation 1.0; DAB-Am_8, poly(propylene imine) octaamine dendrimer, generation 2.0; DAB-Am_{16}, poly(propylene imine) hexadecaamine dendrimer, generation 3.0; DAB-Am_{32}, poly(propylene imine) dotriacontaamine dendrimer, generation 4.0; and DAB-Am_{64}, poly(propylene imine) tetrahexacontaamine dendrimer, generation 5.0. DAB-Am_{32}, poly(propylene imine) dotriacontaamine dendrimer, generation 4.0 was also purchased from SyMO-Chem of the Netherlands. 6-aminocaproic acid (98%), 2,5-dimethoxytetrahydrofuran (98%), *N*-hydroxysuccinimide (99%), 1,3-dicyclohexylcarbodiimide (99%), triethylamine (99%), di-*tert*-butyldicarbonate (99%), iron(III) chloride (98%), iron(III) nitrate nonahydrate (99.99%), and ferrocenecarboxylic acid (97%) were also purchased from Aldrich and used as received. Phosphorous pentachloride (98%) was purchased from Fluka, tetrabutylamonnium fluoroborate was purchased from SACHEM (electric grade), and nile red (99.0%), potassium hydroxide (85%), sodium chloride (biological grade), sodium sulfate (99.2%), and magnesium sulfate (anhydrous) (98.0%) were purchased from Fisher and utilized without further purification. All water used had a resistivity of 18 MΩcm and was obtained by filtering distilled water with a Barnstead reverse osmosis system followed by charcoal filtration and ion exchange.

2.1.2 Synthetic Methods

All synthetic methods are described in Chapter 3.

2.1.3 Preparation of Au Substrates

Glass microscope slides purchased from Fisher (1" x 3" x 1 mm) were coated with gold (Au) and used for all electrochemical and reflection-absorbance infrared spectroscopy (RAIRS) analysis. To enhance adhesion of gold to the slides, one should refrain from touching the flat surfaces of the slides with a gloved hand. The slides were rinsed off thoroughly with acetone before being submerged in isopropanol (IPA) and sonicated for 30 minutes. The glass slides were then thoroughly washed with water and immersed in 3:1 98% sulfuric acid:30% hydrogen peroxide (piranha solution) for 30 minutes. ***Caution! Piranha solution is highly reactive and should be handled with extreme caution. Exposure of piranha solution to organic material (such as IPA from the previous step) will result in a violent exothermic reaction. This solution should be disposed of immediately after use.*** After removing the glass slides from the piranha solution, they were thoroughly rinsed with water and absolute ethanol before being dried under a stream of nitrogen or argon.

The cleaned slides were then placed in an Edwards 306A (Edwards, UK) cryogenically pumped vacuum chamber, in which they were placed under vacuum at pressures around 1 x 10^{-7} torr. Approximately 4.5 nm of chromium (Cr) was first deposited onto the glass slides at a rate of ~0.03 nm s^{-1} to serve as an adhesion layer for the gold layer to be deposited afterwards. After the Cr deposition, 200 nm of Au was evaporated onto the slides at a rate of ~0.15 nm s^{-1}. The gold slides were then allowed to cool to room temperature under vacuum before removal. All slides were stored in absolute ethanol until later use.[1] The thickness of the Cr and Au layers and the deposition rates were determined by an *in vacuo* quartz crystal microbalance.

2.1.4 Electrochemical Studies

Electrochemical studies were performed in normal three-electrode mode with a Princeton Applied Research Model 273A Potentiostat/Galvanostat and Yokogawa 3025 X-Y Recorder. Cyclic voltammograms were obtained from DAB-Fc_{16} and DAB-Am_{16} monolayers on gold electrodes immersed in 0.1 M tetrabutylammonium fluoroborate in acetonitrile. The potential was scanned versus a silver wire pseudoreference. The monolayers were prepared by immersing the electrodes for 5 hours in dendrimer solutions that were 0.05 M in end groups.

2.1.5 Dialysis

Dialysis tubing made of regenerated cellulose, purchased from Spectrum Laboratories, with a molecular weight cut off of 1000 daltons was used to purify dendrimers of generation 1–3, and a molecular weight cut off of 6,000–8,000 daltons was used for generations 4 and 5. Typically 20 mL of the analyte mixture was added to a dialysis membrane and the filled membrane was stirred in 800 mL of 50% acetone and 50% water. The dialysate was changed 6 times over 3 days.

2.2 Analysis

2.2.1 Gas Chromatography-Mass Spectrometry (GC-MS)

A Hewlett Packard Series II 5890 GC was used for analysis of all small organic compounds synthesized. The column used was a J&W DB-5 stationary phase column with a 0.25 μm film consisting of 5% phenyl and 95% dimethyl polysiloxane. The 30 m column had an inner diameter of 0.25 mm. Ultra high purity grade He was used as the carrier gas at 20 pounds per square inch. The instrument was used in electron ionization mode with a Hewlett Packard 5971A mass-selective quadrupole detector. The standard DB-5 method was used each time in

which the column temperature was held at 40 °C for 2 min, ramped to 280 °C at 20°C min^{-1}, and held at 280 °C for 24 min.

2.2.2 Matrix-Assisted Laser Desorption/Ionization Mass Spectrometry (MALDI-MS)

A Perseptive Biosystems Voyager linear time of flight mass spectrophotometer equipped with a nitrogen laser emitting at 337 nm was used to determine the molecular weight of the butoxycarbonyl- and ferrocene-terminated dendrimers. The matrix, 2,5 dihydroxybenzoic acid (DHB) was dissolved in 50/50 methanol/water and the analytes were prepared in methylene chloride (DCM) at a concentration of ~1.0 mg/mL. 1 μL of the matrix solution and 0.5 μL of the analyte solution were added to the MALDI target plate and allowed to co-crystallize. Analysis was conducted at pressures less than 10^{-5} Torr. A two-point calibration was used each time using the standards: Bradykinin (572.7 *m/z*), Angiotinsin I (1296.5 *m/z*), human adrenocorticotropic hormone fragment 18-39 (2465.7 *m/z*), insulin (bovine pancreas) (5732.5 *m/z*), and cytochrome C (12361.1 *m/z*).

2.2.3 Nuclear Magnetic Resonance

Three Bruker instruments were used for these studies: a DPX-250, ARX-300, and a DPX-400. The DPX-250 was typically used for quick analysis for confirmation of the proposed structure of small organic molecules synthesized in the lab. Structural analysis of pyrrole-terminated dendrimers was conducted on the ARX-300 and DPX-400. Experiments completed on these instruments include nuclear Overhauser effect spectroscopy (NOESY), rotational nuclear Overhauser effect spectroscopy (ROESY), T_1 studies, and T_2 studies.

NOESY studies were conducted in CD_2Cl_2 on the ARX-300 instrument. A 2 second delay between scans was used and 32 scans were acquired. The 90 degree pulse length was 6.35 μs. The mixing time was 0.15 seconds and line broadening was 1Hz in F2 and 3 Hz in F1.

ROESY studies were conducted in 1:1 Acetone-*d*6 DCl on the ARX-300 instrument as well. A 2 second delay between scans was used and 64 scans were acquired. The 90 degree pulse length was 6.85 μs. The mixing time was 0.18 s and line broadening was 0 Hz in both dimensions. 2048 data points were acquired in F2 and 512 slices were collected in F1 for all 2D spectra and zero filling was applied to yield a 2048 x 1024 data matrix.

T_1 and T_2 studies were both conducted on both the ARX-300 and DPX 400 instruments. The experimental parameters were held the same on each experiment with the exception of the 90 degree pulse length which varied with temperature and solvent and ranged from 6.3 to 7.5 μs on the 300 MHz spectrometer and 7.5 to 9 μs on the 400 MHz spectrometer. A 20 second delay between scans was employed and 16 scans were collected. The 180 degree pulse length for each experiment was approximately twice that of the 90 degree pulse length. The correct length was found prior to each experiment by determining the proper pulse length that resulted in peaks with null intensity.

2.2.4 Transmission Fourier-Transform Infrared Spectroscopy (FTIR)

Hydrogen bonding studies were completed on a Perkin Elmer 1760X FTIR with a triglycine sulfate (TGS) pyroelectric detector. A resolution of 4 cm^{-1} with normal apodization was used. A capillary film was studied through the use of a Spectra-tech solution cell with sodium chloride (NaCl) windows and a 50 μm Teflon spacer. All other transmission infrared studies were performed on a Thermo Nicolet Nexus 670 FTIR. The mercury-cadmium-telluride (MCT) detector was cooled with liquid nitrogen before use each time, and a reference blank was taken of a solvent cleaned potassium bromide (KBR) plate.

2.2.5 Reflection-Absorption Infrared Spectroscopy (RAIRS)

A Nicolet 740 FTIR with a liquid nitrogen-cooled MCT detector was used for all RAIRS studies of analytes on Au substrates. A versatile reflection accessory with retro-mirror attachment (VRA-RMA) from Harrick Scientific was used such that *p*-polarized light passing through a wire grid polarizer (Harrick Scientific) would strike the substrate at an angle of 86° with respect to the surface normal. The analysis chamber was contained in an Ar-filled poly(ethylene) glove bag, and the optical bench was purged with house nitrogen scrubbed with a homemade CO_2, water, and hydrocarbon scrubbing system. Background spectra were taken from a bare Au slide. A resolution of 4 cm^{-1} was used and 1024 scans were collected. [1]

2.2.6 Ultraviolet-Visible Spectroscopy (UV-vis)

A Varian Cary 50 Bio UV-Vis spectrophotometer containing a xenon flash lamp was used. A scan rate of 600 nm min^{-1} was employed, and the scan range varied from 200—1000 nm depending on the solvent. A background subtraction was conducted each time with the appropriate solvent (same solvent as sample) and quartz fluorescence cells with a 1 cm path length were utilized in all studies.

2.3 NMR Theory

Several NMR techniques were used to study the dendrimer structure as a function of its chemical environment. In order to grasp the meaning of the data acquired, it is necessary to have a basic understanding of the processes involved in the simplest NMR experiment. Protons are charged nuclei that rotate about an axis creating a magnetic moment. With no external magnetic field present, the nuclei and the resulting magnetic field are randomly aligned resulting in a net magnetic moment of zero intensity. However, when the sample is placed in the magnetic field of an NMR, the nuclei orient themselves either parallel (z axis) or antiparallel (-z axis) with the

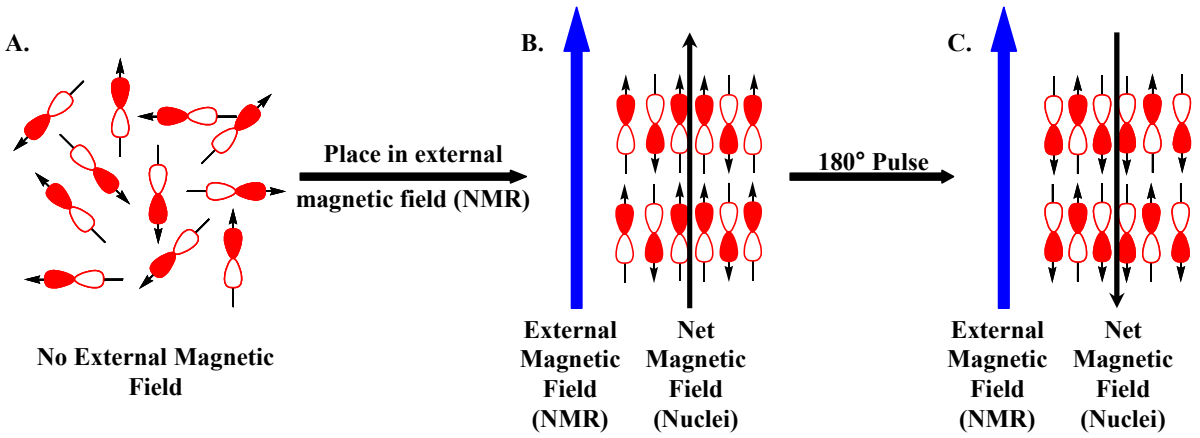

Figure 2.1 In the absence of an external magnetic field (A) the net magnetic field of a group of nuclei is zero as the orientations of the individual nuclei are randomly distributed. In the presence of an external field (B) the nuclei arrange themselves such that their magnetic moments are either parallel or antiparallel with respect to the external magnetic field resulting in a net field in the same orientation as that of the magnet. Applying a 180° pulse (C) inverts the orientation of all nuclei yielding a net magnetic field antiparallel to the external magnetic field.

instrument's magnetic field. This magnetic moment then precesses around the z axis at a certain frequency known as the Larmor frequency. Because the magnetic moment of the nuclei is extremely small when compared to that of the spectrometer's magnet, the nuclei's magnetic field must be rotated into the XY plane to facilitate detection. This can be done by applying a radiofrequency (RF) pulse with the same frequency as the Larmor frequency. Once the nuclei's magnetic moment is in the XY plane it rotates about the z-axis inducing an alternative current which can be measured by the instrument.[2]

As mentioned above, there are two different orientations in which the nuclei may exist prior to irradiation—parallel or antiparallel. The parallel orientation is the low energy state in which the nucleis' magnetic momentd is aligned with the magnetic field and the antiparallel orientation is the high energy state in which the nucleis' magnetic moment is oriented opposite to the magnetic field. The energy introduced by the RF pulse is absorbed by the nuclei in the low energy state and the orientation is inverted. As soon as irradiation by the RF pulse ceases, the

nuclei release this absorbed energy and relaxes back to the initial low energy state in the parallel orientation. This restoration of the initial magnetic moment along the z axis is known as longitudinal relaxation. The length of time it takes the longitudinal magnetization to increase by a factor of *e* (2.71828183) is known as the T_1 relaxation time constant.

Longitudinal relaxation is only one type of relaxation that can occur. When the magnetic moment is rotated to the XY plane it precesses about the z axis at its Larmor frequency. The transverse magnetization then dephases until net magnetization in the XY plane is zero. The T_2 relaxation time constant is defined as the length of time required for the transverse magnetization to decrease by a factor of *e*.

2.3.1 Proton Relaxation Studies

T_1 studies were conducted on Bruker ARX-300 and DPX-400 spectrometers using an inversion-recovery method. The 90° pulse length was determined by finding the duration of the 360° pulse length and dividing that value by 4. The pulse length for a 360° pulse is easily determined by varying the pulse length until no signal is detected in the XY plane. By finding the 360° pulse width, one does not have to wait long periods of time for the magnetic moment to relax back to its original orientation. A set of 16 τ values were used for relaxation delay parameters, ranging from 10 ms to 20 s. The largest τ value, 20 s, was used because this value was always at least five times that of the longest T_1 value for the molecules studied here. The values were carefully chosen such that the majority of the data points occurred when the peak intensity values were changing the most (10 ms to 1 sec). The dendrimer concentration for

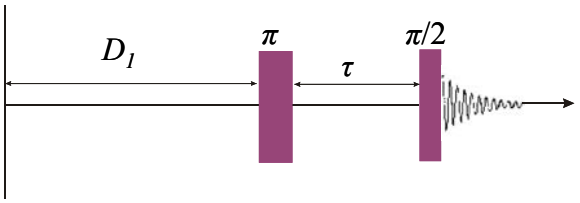

Figure 2.2 The inversion-recovery pulse sequence used in the determination of T_1 relaxation time constants.

each sample was 0.01 M in end groups. Dendrimers were dissolved in methylene chloride or in 1:1 d_6-acetone deuterium oxide (D_2O), and the T_1 values were determined as a function of temperature. In both cases, the initial temperature was near room temperature and then was decreased due to the low boiling points of both methylene chloride and acetone so as to prevent evaporation of the solvent. This was done by circulating liquid nitrogen vapor around the sample and then slowly heating the sample to the desired temperature. The T_1 relaxation time constant is determined by measuring the length of time needed for the nuclear spins of a system to return to their original state after a 180° pulse.

The magnetization is first inverted by a 180° pulse, the protons are allowed a period of time to relax to their original state, then a 90° pulse is applied placing the magnetization in the XY plane. By definition, the T_1 value is the length of time it takes the magnetization along the Z axis to increase by a factor of *e*. Large T_1 values are the result of nuclei needing longer periods of time to return back to their original spin state. An increase in the T_1 value for small molecules means an increase in the mobility at that particular area for a given molecule. The opposite is true for larger molecules. Therefore, it is often necessary to determine the effect temperature has on the T_1 data to properly assess the type of molecule behavior (small versus large). The T_1 values are related to the rotational correlation time of the molecule, the average time needed for the molecule to rotate by 1 radian, as is demonstrated in Figure 2.2.[3] The correlation times can be manipulated by heating and cooling the systems which

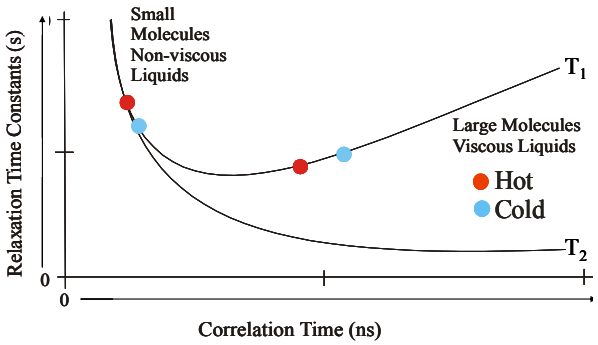

Figure 2.3 This figure is adaptated from Levitt[3] showing the relationship between relaxation time constants and the rotational correlation time of a given molecule.

allows for determination of whether the dendrimers being studied are behaving like small molecules or large molecules. Once this has been determined, one can use T_1 data to estimate the relative mobility or rigidity at various locations of the system of interest.

Often times the spin-spin relaxation time constant, T_2, is also determined to corroborate the calculated T_1 values. The T_2 time constant is the time it takes the transverse magnetization in the XY plane to decrease by a factor of *e*. In this experiment, the multi-echo spin-echo pulse sequence,[4] known as the Carr–Purcell–Meiboom–Gill (CPMG) pulse sequence, is used.[5] A 90° pulse is followed by a number of spin-echoes and then the transverse magnetization is measured. A single spin-echo is defined as two subsequent 180° pulses. This is repeated for an incremented number of spin-echoes beginning with two 180° pulses and then increasing the number of pulses until no transverse magnetization is measured. After the magnetic moment is oriented along the X axis, the spins dephase due to magnetic field inhomogeneities and T_2 processes. The spin echoes refocus the dephasing due to the inhomogeneities in the magnetic field, therefore the relaxation observed through the decrease in transverse magnetization is the result of T_2 processes only.

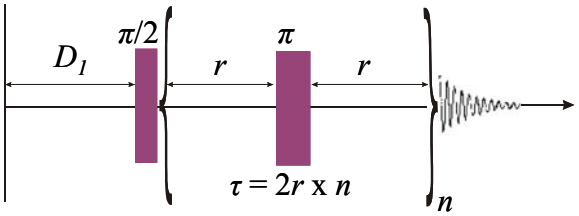

Figure 2.4 The CPMG pulse sequence used for the determination of transverse relaxation time constants.

The net magnetization along the z axis reaches zero only after the transverse magnetization completely dephases. Therefore, T_2 is always less than or equal to T_1. For small molecules T_2 is equal to T_1, and for larger molecules T_2 is much smaller than T_1. Therefore we can compare the T_1 and T_2 relaxation time constants at several temperatures to get a better understanding of the behavior of the molecule in question.

2.3.2 2-Dimensional NMR Studies

T_1 relaxation is a result of a net energy loss from the system, as energy is transferred from the excited nuclei to other nuclei in its environment referred to as the lattice. This energy transfer can involve nuclei on the molecule and solvent molecules, other molecules in solution, and between other nuclei on the same molecule. T_2 relaxation occurs through spin-spin relaxation: energy is transferred from one nucleus to another nucleus on the same molecule. Spin-spin relaxation results in the excitation of one or more nuclei after energy is transferred from a single, different nucleus previously excited. This leads to a phenomenon known as the nuclear Overhauser effect (NOE). Overhauser first described this phenomenon in the early 1950s and referred to it as dynamic nuclear polarization.[6] However, he was met with skepticism as numerous scientists believed this phenomenon violated the second law of thermodynamics. Several years passed before other researchers experimentally observed the NOE and Overhauser's proposal was finally accepted.[7,8]

The NOE is the change in intensity of a nuclear spin resulting from the simultaneous saturation of a second different spin.[2,9] The first experimental demonstration was conducted by Solomon in 1955 using HF.[7] Solomon observed a significant increase in the amplitude of the

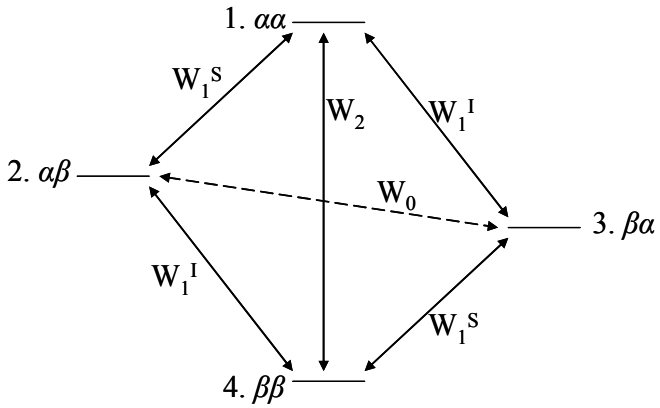

Figure 2.5 Energy level diagram for two spins-½ (IS), where $\alpha\beta$ denotes spin I is in the α spin state and spin S is in the β spin state.[9] The W's are possible spin-lattice transitions.

fluorine (^{19}F) resonance when a 180° pulse at hydrogen (^{1}H) frequency was applied. It was shown here that energy from an excited spin can be transferred to a nearby second spin. In 1972, data was published showing that NOEs could be negative as well.[10,11] The researchers observed a negative NOE for aromatic phenylalanine protons of bovine neurophysin. It was determined that the NOEs were negative for molecules with large correlation times and positive for molecules with short correlation times.

In order to better understand this phenomenon, a 2-spin system will be considered. After one of the spins is saturated, the spins will relax to their original states through several transitions observed in Figure 2.5: W_1^I, W_1^S, W_2, and W^0.[9] The absorption intensity of a given spin is defined by the populations in each energy level. For instance, at any given point in time the absorption intensity of the S resonance is proportional to the sum $(P_2\text{-}P_1) + (P_4\text{-}P_3)$ (where P_x (x = 1, 2, 3, or 4) denotes the population of spins in the x energy level) and the absorption intensity of the I resonance is proportional to the sum $(P_3\text{-}P_1) + (P_4\text{-}P_2)$. If spin S is saturated, the population in levels 1 and 2 will be equal, as well as the population in levels 3 and 4. The W_1^I and W_1^S transitions result in no net change in the populations because saturation has left the populations of these energy levels equal. The absorption intensity of spin I remains unchanged. However, the transition W_2 will result in an increase in P_4 and a decrease in P_1 leading to an increase in the absorption intensity of spin I. The W_0 transition will lead to an increase in P_2 and a decrease in P_3 resulting in a decrease in the absorption intensity of spin I.[9] While all transitions will occur simultaneously, the W_0 transition is the more dominant relaxation method for small molecules resulting in negative NOEs. The W_2 transition is the more dominant relaxation pathway for large molecules giving rise to positive NOEs.

Despite this huge discovery, the scientific community did not fully reap the benefits of this phenomenon until the introduction of the first 2-dimensional NOE experiment in 1979.[12-14] Swiss researchers created the pulse sequence employed by much of the magnetic resonance community today, known as NOESY (Nuclear Overhauser Effect Spectroscopy). As shown in Figure 2.6, the sequence consists of three 90° pulses separated by an evolution time (t_1) and the mixing time (t_m). The relaxation delay (D_1) for most NMR experiments is normally at least 5 times greater than the largest T_1 value to allow sufficient time for all nuclei to relax to their original orientation. The magnetization components are frequency labeled during t_1, and cross-relaxation occurs during the t_m. The signal is recorded immediately after the 3rd pulse (t_2) and the experiment is repeated for a given set of incremented t_1 values. The data is then processed in both dimensions (t_1,t_2) yielding a 2D spectrum providing a wealth of knowledge. If cross-relaxation does not occur between two nuclei during t_m, the frequency will be identical after t_1 and t_2 and no cross peaks will be observed. However, if cross-relaxation does occur, it will be evident by the presence of cross-peaks.[15] After this contribution it became possible to detect all spin-spin interactions in a given molecule by completing a single experiment.

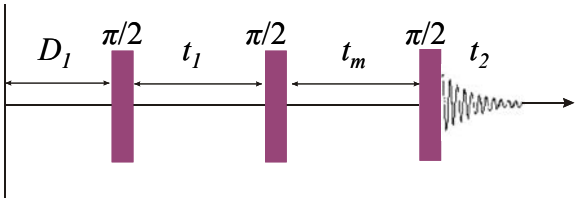

Figure 2.6 The pulse sequence used in NOESY experiments.

It is also important to mention the difference between NOE experiments and 2D NOE experiments. For molecules with short correlation times in the 2D experiment, an energy transfer occurs, resulting in a negative NOE. However, an energy exchange occurs in large molecules resulting in a positive NOE. The exact opposite is seen in standard Overhauser

saturation experiments, due to the fact that in saturation experiments negative magnetization is being transferred while 2D experiments involve the exchange of positive magnetization.[14]

Without overlooking the massive contribution of Ernst and his coworkers in the development of the NOESY experiment,[14] it is apparent that NOESY has its limitations. For molecules containing an intermediate correlation time, it is possible for energy transfer and energy exchange to simultaneously occur. In this scenario the intensities of the cross peaks may be extremely small, or even null. Bother-By et al. overcame this impediment by observing NOEs in the presence of a spin-locking field with an experiment they referred to as CAMELSPIN (cross-relaxation appropriate for minimolecules emulated by locked spins), known today as ROESY (Rotational Overhauser Effect Spectroscopy).[16]

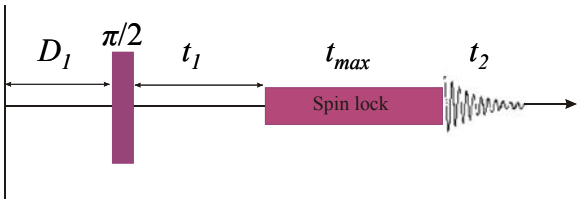

Figure 2.7 The pulse sequence used in ROESY experiments.

Just as the 2D NOE experiments were developed, the CAMELSPIN experiments were first conducted in one dimension. A reference spectrum is first acquired after a 90° pulse. Then after the t_1 interval, a spin locking field is applied along the x-axis during a relaxation period (t_{max}). Immediately after the field is removed the spectrum is acquired. Subtracting these two spectra allowed Bother-By to observe interactions not visible with NOESY. Repeating this experiment with incremental values of t_1 and a constant value for t_{max}, they were able to produce data extremely similar to that of NOESY experiments. There was one exception, all cross peaks were now positive.[16]

Transverse relaxation leading to NOEs in ROESY experiments occurs through the same relaxation pathways as the longitudinal relaxation in NOESY experiments. However, a

transverse relaxation in the NOESY experiment does not allow a NOE buildup because the spins dephase. The spin-locking field in ROESY experiments prevents the magnetic moments from precessing about the z-axis. Therefore the spins remain in phase and NOEs are allowed to build up. In the absence of a spin-locking field, the magnetic moments of the two spins are opposed to one another for as much time as they are aligned. Half of the time cross-relaxation increases the intensity of the second spin, while half of the time cross-relaxation decreases the intensity of the second spin. Transverse relaxation has a different dependence on molecular tumbling in that all molecules behave as though they are in the positive NOE regime. Therefore all NOE crosspeaks in the ROESY experiment are positive for all molecules.

2.4 Infrared Spectroscopy Studies

2.4.1 IR for Hydrogen Bonding Studies

Previously, IR spectroscopy has been used to show that amide-functionalized PPI dendrimers exhibit strong hydrogen bonding interactions in dichloromethane.[17] In that study, the extent of hydrogen bonding was assessed by comparing the intensities[18] of IR bands associated with N-H stretching for hydrogen-bonded amides and those associated with N-H stretching for non-hydrogen-bonded amides in PPI dendrimers. An alternative route is required for evaluating the extent of hydrogen bonding in dendrimers adsorbed on surfaces as the absorbance intensity strongly depends on theorientation of the bond with respect to the surface normal.[19]

It has been shown that the degree of H-bonding in proteins can be estimated by monitoring the band position (energy) of the amide I and amide II transitions.[20] A blue shift for the amide I transition and a red shift for the amide II transition were observed as hydrogen bonding increased. Because band location, rather than intensity, is used in this method, it is applicable for determining the extent of hydrogen bonding for molecules on surfaces. An

increase in hydrogen bonding is interpreted as a decrease in the distance between the amide functional groups.

2.4.2 Oligomer Length Studies

In 1994, Zerbi and coworkers suggested that the length of pyrrole oligomers could be estimated from their IR spectra.[21] They reported two characteristic vibrations in which they referred to as *T* bands and *B* bands that respectively correspond to the end group vibrations (*T*) and vibrations associated with pyrrole groups within the chains (*B*). The *T* band for the out-of-plane deformation modes was reported to occur in the 720-730 cm^{-1} region ($\omega(C\text{-}H)_{oop\text{-}ring}$) while in-plane deformation modes occur around 1065 cm^{-1} ($\omega(C\text{-}H)_{ip\text{-}ring}$). The out of plane and in plane deformations for the *B* modes are found at approximately 765 and 1035 cm^{-1}.

The intensities of these bands were compared to different pyrrole polymer lengths where the numbers of pyrroles were 3, 5, 7, and ~20 (Py3, Py5, Py7, and PPy). The intensities of the out-of-plane deformation bands at 764 (*B*) and 720 cm^{-1} (*T*) were similar for Py3. The *B* band (762 cm^{-1}) is much stronger than the *T* doublet (732 and 705 cm^{-1}) for Py5 and the *T* band (726 cm^{-1}) for Py7 is dominated by the *B* band (762 cm^{-1}). A very small *T* adsorption was observed for PPy on the lower frequency side of the *B* band (759 cm^{-1}). A similar trend for the in-plane deformation bands (Py3, 1060-1028; Py5 1064-1035; Py7, 1064-1037; PPy, 1065-1033 cm^{-1}) were also observed with respect to the peak intensity ratios. There was no significant difference in the band positions. Their work demonstrated that the number of individual pyrroles comprising a pyrrole-oligomer can be determined by monitoring the intensity of 4 key absorption bands in the IR spectra.

2.5 References

(1) Peanasky, J. S.; McCarley, R. L. *Surface-Confined Monomers on Electrode Surfaces. 4. Electrochemical and Spectroscopic Characterization of Undec-10-ene-1-thiol Self-Assembled Monolayers on Au,* ***Langmuir*** **1998**, *14*, 113-123.

(2) Neuhaus, D.; Williamson, M. P. *The Nuclear Overhauser Effect in Structural and Conformational Analysis*; VCH Publishers: New York, 1989.

(3) Levitt, M. H. *Spin Dynamics: Basics of Nuclear Magnetic Resonance*; John Wiley and Sons, LTD: New York, NY, 2001.

(4) Carr, H. Y.; Purcell, E. M. *Effects of diffusion on free precession in nuclear magnetic resonance experiments,* ***Physical Review*** **1954**, *94*, 630-638.

(5) Meiboom, S.; Gill, D. *Modified spin-echo method for measuring nuclear relaxation times,* ***Review of Scientific Instruments*** **1958**, *29*, 688-691.

(6) Overhauser, A. W. *Paramagnetic Relaxation in Metals,* ***Physical Review*** **1953**, *89*, 689-700.

(7) Solomon, I. *Relaxation Processes in a System of Two Spins,* ***Physical Review*** **1955**, *99*, 559-565.

(8) Carver, T. R.; Slichter, C. P. *Polarization of Nuclear Spins in Metals,* ***Physical Review*** **1953**, *92*, 212-213.

(9) Noggle, J. H. *The Nuclear Overhauser Effect; Chemical Applications*; Academic Press: New York, NY, 1971.

(10) Balaram, P.; Bothner-By, A. A.; Dadok, J. *Negative Nuclear Overhuaser Effects as Probes of Macromolecular Structure,* ***Journal of the American Chemical Society*** **1972**, *94*, 4015-4017.

(11) Balaram, P.; Bothner-By, A. A.; Breslow, E. *Localization of Tyrosine at the Binding Site of Neurophysin II by Negative Nuclear Overhouser Effects,* ***Journal of the American Chemical Society*** **1972**, *94*, 4017-4018.

(12) Meier, B. H.; Ernst, R. R. *Elucidation of Chemical Exchange Networks by Two-Dimensional NMR Spectroscopy: The Heptamethylbenzenonium Ion,* ***Journal of the American Chemical Society*** **1979**, *101*, 6441-6442.

(13) Jeener, J.; Meier, B. H.; Bachmann, P.; Ernst, R. R. *Investigation of Exchange Processes by Two-Dimensional NMR Spectroscopy,* ***Journal of Chemical Physics*** **1979**, *71*, 4546-4553.

(14) Macura, S.; Ernst, R. R. *Elucidation of Cross Relaxation in Liquids by Two-Dimensional NMR Spectroscopy,* ***Molecular Physics*** **1980**, *41*, 95-117.

(15) Kumar, A.; Ernst, R. R.; Wuethrich, K. *A Two-Dimensional Nuclear Overhauser Enhancement (2D NOE) Experiment for the Elucidation of Complete Proton-Proton Cross-Relaxation Networks in Biological Macromolecules,* ***Biochemical and Biophysical Research Communications*** **1980**, *95*, 1-6.

(16) Bothner-By, A. A.; Stephens, R. L.; Lee, J.; Warren, C. D.; Jeanloz, R. W. *Structure Determination of a Tetrasaccharide: Transient Nuclear Overhauser Effects in the Rotating Frame,* ***Journal of the American Chemical Society*** **1984**, *106*, 811-813.

(17) Bosman, A. W.; Bruining, M. J.; Kooijman, H.; Spek, A. L.; Janssen, R. A. J.; Meijer, E. W. *Concerning the Localization of End Groups in Dendrimers,* ***Journal of the American Chemical Society*** **1998**, *120*, 8547-8548.

(18) Gardner, R. R.; Gellman, S. H. *Evaluation of the Conformation-Directing Effects of Secondary Hydrogen-Bonding Interactions in Flexible Tetrapeptide Analogs,* ***J. Am. Chem. Soc.*** **1995**, *117*, 10411-10412.

(19) Porter, M. D. *IR external Reflection Spectroscopy: A Probe for Chemically Modified Surfaces,* ***Anal. Chem.*** **1988**, *60*, 1143A-1155A.

(20) Manas, E. S.; Getahun, Z.; Wright, W. W.; DeGrado, W. F.; Vanderkooi, J. M. *Infrared spectra of amide groups in alpha-helical proteins: Evidence for hydrogen bonding between helices and water,* ***Journal of the American Chemical Society*** **2000**, *122*, 9883-9890.

(21) Zerbi, G.; Veronelli, M.; Martina, S.; Schlueter, A. D.; Wegner, G. *Delocalization length and structure of oligopyrroles and of polypyrrole from their vibrational spectra,* ***Journal of Chemical Physics*** **1994**, *100*, 978-984.

Chapter 3

Functionalization of Amine-Terminated Diaminobutane (DAB) Dendrimers

3.1 Introduction

The dendrimers of choice for these studies are the poly(propylene imine), PPI, dendrimers due to their commercial availability and terminal primary amines that can be easily modified with almost any desired functional group using simple coupling techniques.[1-4] This characteristic of dendrimers is quite attractive as the overall properties of the dendrimer such as solubility,[1] electroactivity,[2] and spectroscopic response[5] are often determined by the functional groups located along the periphery. To date, PPI and poly(amido amine), PAMAM, dendrimers have been modified by a wide range of functional groups such as adamantylurea,[6] poly(ethylene glycol),[7] poly(*N*-isopropylacrylamide),[8] phenothiazines,[9] and ferrocene,[2,10,11] just to name a few. Of particular interest to the work at hand are peptide coupling reactions that have been used for addition of BOC and ferrocene to the periphery of dendrimers.[2,3,12] These coupling techniques lead to the formation of amide bonds that possess characteristic IR absorption bands that can be used to confirm functionalization and allow one to determine the relative extent of intra-dendrimer hydrogen bonding.

3.2 Synthesis of Ferrocene-Terminated Dendrimers (DAB-Fc$_x$, x=4, 8, 16, 32, and 64)

Commercially available amine-terminated poly(propylene imine) diaminobutane core dendrimers were functionalized with ferrocene end groups. The overall reaction included two steps: the conversion of ferrocene carboxylic acid (FcCOOH) into an acid chloride (FcCOCl)[13] and the reaction of the acid chloride with the amine-terminated dendrimers. FcCOOH was stirred for several minutes in benzene until the entire solid was dissolved. Approximately 1.2 equivalents of PCl_5 was added to the acid solution and allowed to stir in a glove box for 1 hour.

The solvent was removed under vacuum, and the red product was dissolved in dichloromethane (DCM). The organic solution was washed with NaOH until the lower aqueous layer was colorless and then washed once with water. The organic layer was dried with Na_2SO_4, filtered, and the solvent removed under vacuum. The red crystals were dissolved in pentane, filtered, and the solvent removed under vacuum. GC-MS confirmed the presence of a single product with a mass/charge (*m*/*z*) of 248, the same as the molecular weight of the ferrocenoyl chloride. Yields of 90% were typical for this reaction.

The second step is the functionalization of the dendrimer with ferrocene end groups. The acid chloride readily reacts with the amine functional groups located around the periphery of the dendrimer. The amine-terminated dendrimer, 1.2 equivalents of triethylamine, and FcCOCl for each primary amine were separately dissolved in DCM. The dendrimer and triethylamine solutions were transferred to an addition funnel and added dropwise to the FcCOCl solution. The solution was stirred until complete functionalization was confirmed by MALDI-MS (4 - 24 hours depending on the generation). After the dendrimer was completely functionalized, the solvent was removed under vacuum yielding a red powder. The resulting product was dissolved in a small amount of DCM, and the dendrimer was precipitated by the addition of hexanes. The solutions were centrifuged and the liquid decanted. The dendrimer was dissolved in DCM, dried with anhydrous sodium

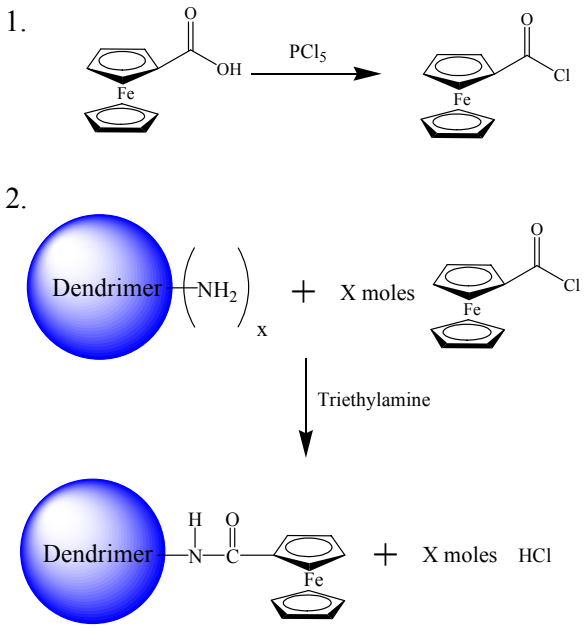

Figure 3.1 Schematic showing the synthesis of Ferrocene acid chloride and its addition to amine-terminated dendrimers.

sulfate, and again evaporated to dryness under vacuum. All of the dendrimers were transferred to vials and stored under argon at -20°C until further use. The MALDI-MS data indicated 100% conversion for generations 1-3 and >90% conversion for generations 4 and 5, as judged by the presence of molecular ion peaks for generations 1-3 and the presence of peaks at a slightly lower *m*/*z* than that of completely functionalized dendrimers of generations 4 and 5. While the protonated molecular ion peak was not observed for generations 4 and 5, neither were any peaks that would be characteristic of incompletely functionalized dendrimer.

3.3 Synthesis of Butoxycarbonyl-Terminated Dendrimers (DAB-BOC$_x$, x=4, 8, 16, 32, and 64)

Generations 1 through 5 of the DAB-dendrimers were also functionalized with butoxycarbonyl (BOC) end groups. A given amine-terminated dendrimer and triethylamine (Et_3N) were dissolved in methanol, while the *di-tert*-butyl dicarbonate [$O(BOC)_2$] was dissolved in a separate flask. For each dendrimer, 1.2 equivalents of $O(BOC)_2$ and triethylamine were used for each primary amine for functionalization. After all of the dendrimer and $O(BOC)_2$ were completely dissolved, the $O(BOC)_2$ solution was added to the dendrimer solution. The reaction was stirred, purged with argon, heated to approximately 75°C, and allowed to reflux until complete functionalization occurred, as determined by MALDI-MS. This ranged anywhere from 8 to 24 hours depending on the generation of the dendrimer.

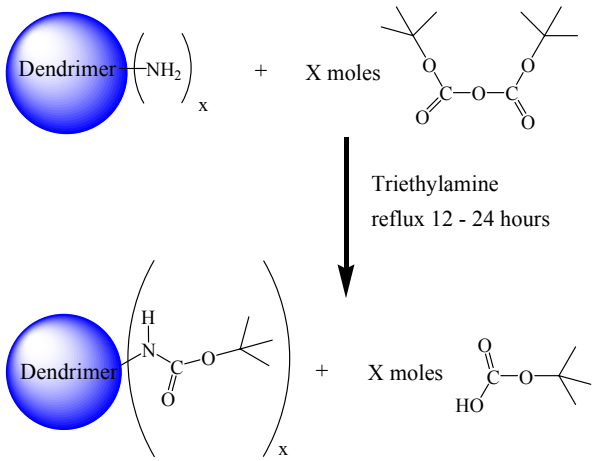

Figure 3.2 Functionalization of amine-terminated dendrimers with BOC groups.

Product analysis was conducted on IR and MALDI-MS instrumentation. When complete functionalization of the dendrimer was confirmed, the solvent was evaporated under vacuum. The resulting substance was dissolved in DCM and then washed 2 times with $NaHCO_3$, 2 times with NaCl, and 1 time with water. This purified organic solution was then dried with anhydrous sodium sulfate. Upon removal of the organic solvent the dendrimer was stored under argon in a freezer. Observance of only the protonated molecule in the MALDI mass spectra indicated complete functionalization for all 5 generations.

3.4 Synthesis of Pyrrole-Terminated Dendrimers

The primary amine of an amino acid was converted to pyrrole[14] utlitizing a Clausson-Kaas ring-closure reaction.[15-17] The pyrrole acid was then transformed into an activated ester which reacted readily with the terminal primary amines of PPI dendrimers. The direct conversion of the dendritic primary amines to pyrrole was not accomplished because too high concentration of primary amines leads to unclosed pyrrole rings.[18] Acid chloride derivatives of pyrrole were previously found to be unstable.[19]

3.4.1 Synthesis of *ω*-(*N*-pyrrolyl)-hexanoic Acid

A pyrrole-terminated alkanoic acid was formed via a ring-closure mechanism using 6-amino hexanoic acid and 2,5-dimethoxytetrahydrofuran.[16-18] The amino acid was dissolved in a degassed 10% acetic acid solution, the solution transferred to a three neck flask, and stirred at 45 °C. Once all of the amino acid was dissolved and the temperature was stable, one molar equivalent of 2,5-dimethoxytetrahydrofuran was canulated into the flask. The reaction mixture was allowed to stir for 2 hours. The product was extracted from the aqueous solution with an equal volume of methylene chloride 3 times. All organic extracts were combined and then washed with pH 2 HCl four times. The methylene chloride layer was then dried with anhydrous

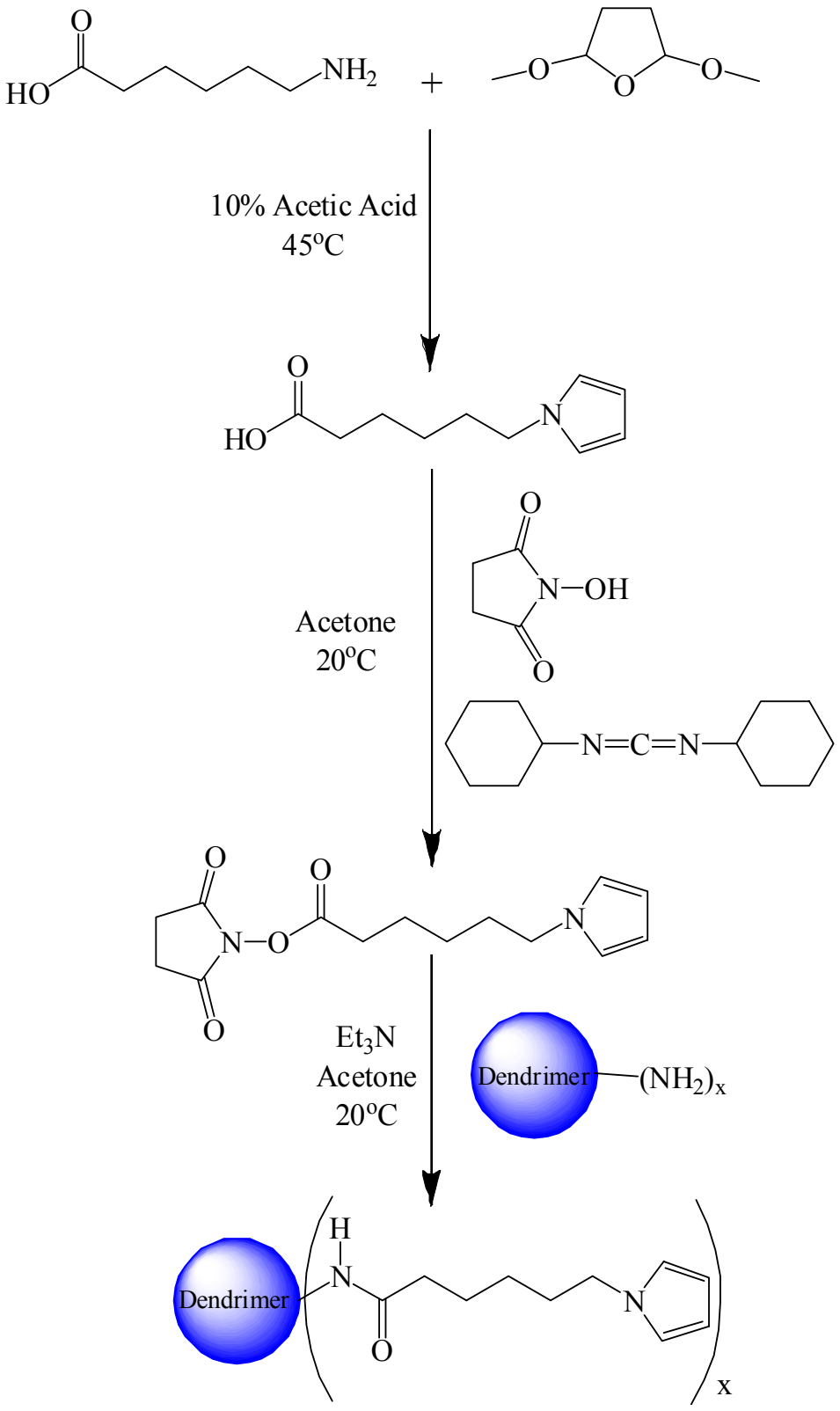

Figure 3.3 Synthesis route for converting primary amines along the dendrimer periphery to pyrrole moieties.

sodium sulfate and filtered. The solvent was removed under vacuum leaving a dark brown oil. Analysis with GC/MS confirmed the presence of the pyrrole acid only. Pure product was obtained with a 62.5% yield. ^{1}H NMR assignments for ω-(*N*-pyrrolyl)-hexanoic acid are: ^{1}H NMR (CD_2Cl_2, 250 MHz): δ 11.01 (bs, 1H, COO*H*), 6.66 (t, 2H, Py-2,5-*H*), 6.10 (t, 2H, Py-3,4-*H*), 3.87 (t, 2 H, -C*H*$_2$-Py), 2.60 (t, 2H, CO-C*H*$_2$-$(CH_2)_4$-Py), 1.79 (t, 2H, Py-CH_2-C*H*$_2$-$(CH_2)_3$-CO), 1.56 (m, 2H, CO-CH_2-C*H*$_2$-$(CH_2)_3$-Py), 1.28 (t, 2H, CO-$(CH_2)_2$-C*H*$_2$-$(CH_2)_2$-Py).

3.4.2 Synthesis of ω-(*N*-pyrrolyl)-1-hexanoic-succinimide Ester

In order to add the pyrrole hexanoic acid to the primary amines along the dendrimer periphery, an activated ester was necessary. The pyrrole acid, *N*-hydroxysuccinimide, *1,3*-dicyclohexylcarbodiimide, and triethylamine were each separately dissolved in acetone. Ten percent excess of *N*-hydroxysuccinimide and *1,3*-dicyclohexylcarbodiimide were used, while 2 equivalents of triethylamine was used. All solutions were purged for 30 minutes with nitrogen and then canulated into a large round bottom flask. The contents of the flask were magnetically stirred at room temperature for 12 hours. The mixture was then centrifuged and filtered to remove dicyclohexylurea (DCU). The solvent was then removed under vacuum, and the remaining solid was redissolved in acetonitrile. The acetonitrile containing the product was then allowed to stand in the freezer for 30 minutes. The solution was once again filtered to remove DCU and then washed with hexanes 10 times. The solvent was removed under vacuum yielding a light yellow wax. GC/MS was used to confirm the presence of a single product, ω-(*N*-pyrrolyl)-*1*-hexanoic-succinimide ester. Pure product was obtained with 88% yield. ^{1}H NMR assignments for ω-(*N*-pyrrolyl)-*1*-hexanoic-succinimide ester are: ^{1}H NMR (CD_2Cl_2, 250 MHz): δ 6.66 (t, 2H, Py-2,5-*H*), 6.10 (t, 2H, Py-3,4-*H*), 3.89 (t, 2 H, -C*H*$_2$-Py), 2.81 (s, 4H, NHS-3,4-H),

2.61 (t, 2H, CO-C*H*$_2$-(CH$_2$)$_4$-Py), 1.79 (t, 2H, Py-CH$_2$-C*H*$_2$-(CH$_2$)$_3$-CO), 1.56 (m, 2H, CO-CH$_2$-C*H*$_2$-(CH$_2$)$_3$-Py), 1.28 (t, 2H, CO-(CH$_2$)$_2$-C*H*$_2$-(CH$_2$)$_2$-Py).

3.4.3 Synthesis of DAB-Py$_x$ (*x*=4, 8, 16, 32, and 64)

The pyrrole succinimide ester adds readily to the primary amines along the periphery of the poly(propylene imine) dendrimers. In separate flasks, 1 equivalent of DAB-(NH$_2$)$_x$ and 1.2 equivalents of pyrrole ester per primary amine were dissolved in degassed acetone. After the entire dendrimer was dissolved, the pyrrole ester and 1.2 equivalents of triethylamine were added and allowed to stir for 24 hours under nitrogen at room temperature. The reaction mixture was filtered and the volume was reduced to 15-20 mL under vacuum. The pyrrole-functionalized dendrimers were isolated from other reactants and products by dialysis. Dialysis tubing made of regenerated cellulose, purchased from Spectrum Laboratories, with a molecular weight cut-off of 1000 was used to purify generations 1-3, and a molecular weight-cut off of 6,000-8,000 was used for generations 4 and 5. The dialysate used was a degassed solution composed of 50% acetone and 50% water and was changed every few hours over a time span of 3 days. The white milky solution in the dialysis bag was transferred to a flask and the solvent removed under vacuum. The yellow oil obtained was then redissolved in acetone and the solvent removed under vacuum resulting in a thick, yellow oil.

The resulting dendrimers were characterized with MALDI-MS and ^{1}H NMR. While well-defined molecular ion peaks for the completely functionalized dendrimer were obtained for generations 1-3 with a [M+H]$^+$ of 970 (969.4 calculated), 2078 (2079 calculated), and 4301 (3298.1 calculated) respectfully. MALDI data for the 4th generation dendrimer consisted of a broad peak centered at *m*/*z* 8460 with the most abundant peak at 8743 (8736.5 calculated). The data for generation 5 consisted of a broad peak centered at 17,000 (17612.9 calculated). ^{1}H

NMR suggests 100% conversion of the primary amines to pyrrole end groups for generations 1-3 and 90% conversion for generations 4 and 5 by comparing the peak integration of the internal $N(CH_2)_3$ protons to the pyrrole protons.

3.4.4 ^{1}H NMR Characterization Data for DAB-Py$_x$ (x = 4, 8, 16, 32, and 64)

DAB-Py$_4$: ^{1}H NMR (CD_2Cl_2, 250 MHz): δ 6.63 (t, 8H, Py-2,5-*H*), 6.06 (t, 8H, Py-3,4-*H*), 3.84 (t, 8 H, -C*H*$_2$-Py), 3.23 (q, 8H, C*H*$_2$-NH-C=O), 2.42 (m, 12H, N(C*H*$_2$)$_3$), 2.10 (t, 8H, CO-C*H*$_2$-(CH$_2$)$_4$-Py), 1.74 (p, 8H, CO-CH$_2$-C*H*$_2$-(CH$_2$)$_3$-Py), 1.58 (m, 8H, CO-(CH$_2$)$_3$-C*H*$_2$-CH$_2$-Py, 8H N-CH$_2$-C*H*$_2$-CH$_2$-N), 1.26 (m, 8H CO-(CH$_2$)$_2$-C*H*$_2$-(CH$_2$)$_2$-Py, 4H N-CH$_2$-C*H*$_2$-C*H*$_2$-CH$_2$-N).

DAB-Py$_8$: ^{1}H NMR (CD_2Cl_2, 250 MHz): δ 6.61 (s, 16H, Py-2,5-*H*), 6.06 (s, 16H, Py-3,4-*H*), 3.84 (t, 16 H, -C*H*$_2$-Py), 3.21 (q, 16H, C*H*$_2$-NH-C=O), 2.39 (m, 36H, N(C*H*$_2$)$_3$), 2.14 (t, 16H, CO-C*H*$_2$-(CH$_2$)$_4$-Py), 1.74 (p, 16H, CO-CH$_2$-C*H*$_2$-(CH$_2$)$_3$-Py), 1.58 (m, 16H, CO-(CH$_2$)$_3$-C*H*$_2$-CH$_2$-Py, 24H N-CH$_2$-C*H*$_2$-CH$_2$-N), 1.26 (m, 16H CO-(CH$_2$)$_2$-C*H*$_2$-(CH$_2$)$_2$-Py, 4H N-CH$_2$-C*H*$_2$-C*H*$_2$-CH$_2$-N).

DAB-Py$_{16}$: ^{1}H NMR (CD_2Cl_2, 250 MHz): δ 6.62 (t, 32H, Py-2,5-*H*), 6.05 (t, 32H, Py-3,4-*H*), 3.84 (t, 32 H, -C*H*$_2$-Py), 3.20 (q, 32H, C*H*$_2$-NH-C=O), 2.39 (m, 84H, N(C*H*$_2$)$_3$), 2.13 (t, 32H, CO-C*H*$_2$-(CH$_2$)$_4$-Py), 1.74 (p, 32H, CO-CH$_2$-C*H*$_2$-(CH$_2$)$_3$-Py), 1.58 (m, 32H, CO-(CH$_2$)$_3$-C*H*$_2$-CH$_2$-Py, 56H N-CH$_2$-C*H*$_2$-CH$_2$-N), 1.30 (m, 32H CO-(CH$_2$)$_2$-C*H*$_2$-(CH$_2$)$_2$-Py, 4H N-CH$_2$-C*H*$_2$-C*H*$_2$-CH$_2$-N).

DAB-Py$_{32}$: ^{1}H NMR (CD_2Cl_2, 300 MHz): δ 6.61 (s, 64H, Py-2,5-*H*), 6.05 (s, 64H, Py-3,4-*H*), 3.83 (t, 64 H, -C*H*$_2$-Py), 3.19 (q, 64H, -C*H*$_2$-NH-C=O), 2.39 (m, 180H, N(C*H*$_2$)$_3$), 2.13 (t, 64H, CO-C*H*$_2$-(CH$_2$)$_4$-Py), 1.74 (m, 64H, CO-CH$_2$-C*H*$_2$-(CH$_2$)$_3$-Py), 1.58 (m, 64H, CO-(CH$_2$)$_3$-C*H*$_2$-CH$_2$-Py, 120H N-CH$_2$-C*H*$_2$-CH$_2$-N), 1.30 (m, 64H CO-(CH$_2$)$_2$-C*H*$_2$-(CH$_2$)$_2$-Py, 4H N-CH$_2$-C*H*$_2$-C*H*$_2$-CH$_2$-N).

DAB-Py$_{64}$: ^{1}H NMR (CD_2Cl_2, 250 MHz): δ 6.61 (s, 128H, Py-2,5-*H*), 6.05 (s, 128H, Py-3,4-*H*), 3.82 (t, 128 H, -CH_2-Py), 3.20 (m, 128H, CH_2-NH-C=O), 2.38 (m, 372H, N(CH_2)$_3$), 2.01 (t, 128H, CO-CH_2-(CH$_2$)$_4$-Py), 1.74 (m, 128H, CO-CH$_2$-CH_2-(CH$_2$)$_3$-Py), 1.58 (m, 128H, CO-(CH$_2$)$_3$-CH_2-CH$_2$-Py, 248H N-CH$_2$-CH_2-CH$_2$-N), 1.26 (m, 128H CO-(CH$_2$)$_2$-CH_2-(CH$_2$)$_2$-Py, 4H N-CH$_2$-CH_2-CH_2-CH$_2$-N).

3.5 References

(1) Pan, Y.; Ford, W. T. *Dendrimers with Both Hydrophilic and Hydrophobic Chains at Every End,* ***Macromolecules*** **1999**, *32*, 5468-5470.

(2) Takada, K.; Diaz, D. J.; Abruna, H. D.; Cuadrado, I.; Casado, C.; Alonso, B.; Moran, M.; Losada, J. *Redox-Active Ferrocenyl Dendrimers: Thermodynamics and Kinetics of Adsorption, In-Situ Electrochemical Quartz Crystal Microbalance Study of the Redox Process and Tapping Mode AFM Imaging,* ***Journal of the American Chemical Society*** **1997**, *119*, 10763-10773.

(3) Jansen, J. F. G. A.; de Brabander van den Berg, E. M. M.; Meijer, E. W. *Encapsulation of Guest Molecules into a Dendritic Box,* ***Science (Washington, D. C.)*** **1994**, *266*, 1226-1229.

(4) Stephan, H.; Spies, H.; Johannsen, B.; Kauffmann, C.; Voegtle, F. *pH-Controlled Inclusion and Release of Oxyanions by Dendrimers Bearing Methyl Orange Moieties,* ***Organic Letters*** **2000**, *2*, 2343-2346.

(5) James, T. D.; Shinmori, H.; Takeuchi, M.; Shinkai, S. *A Saccharide 'Sponge'. Synthesis and Properties of a Dendritic Boronic Acid,* ***Chemical Communications (Cambridge)*** **1996**, 705-706.

(6) Versteegen, R. M.; Van Beek, D. J. M.; Sijbesma, R. P.; Vlassopoulos, D.; Fytas, G.; Meijer, E. W. *Dendrimer-Based Transient Supramolecular Networks,* ***Journal of the American Chemical Society*** **2005**, *127*, 13862-13868.

(7) Paleos, C. M.; Tsiourvas, D.; Sideratou, Z.; Tziveleka, L. *Acid- and Salt-Triggered Multifunctional Poly(propylene imine) Dendrimer as a Prospective Drug Delivery System,* ***Biomacromolecules*** **2004**, *5*, 524-529.

(8) Kimura, M.; Kato, M.; Muto, T.; Hanabusa, K.; Shirai, H. *Temperature-Sensitive Dendritic Hosts. Synthesis, Characterization, and Control of Catalytic Activity,* ***Macromolecules*** **2000**, *33*, 1117-1119.

(9) Christensen, J. B.; Nielsen, M. F.; Van Haare, J. A. E. H.; Baars, M. W. P. L.; Janssen, R. A. J.; Meijer, E. W. *Synthesis and Properties of Redox-Active Dendrimers Containing Phenothiazines,* ***European Journal of Organic Chemistry*** **2001**, 2123-2128.

(10) Cuadrado, I.; Moran, M.; Casado, C. M.; Alonso, B.; Lobete, F.; Garcia, B.; Ibisate, M.; Losada, J. *Ferrocenyl-Functionalized Poly(propylenimine) Dendrimers,* ***Organometallics*** **1996**, *15*, 5278-5280.

(11) Yoon, H. C.; Hong, M.-Y.; Kim, H.-S. *Affinity Biosensor for Avidin Using a Double Functionalized Dendrimer Monolayer on a Gold Electrode,* ***Analytical Biochemistry*** **2000**, *282*, 121-128.

(12) Wysong, C. L.; Yokum, T. S.; Morales, G. A.; Gundry, R. L.; McLaughlin, M. L.; Hammer, R. P. *4-Aminopiperidine-4-carboxylic Acid: A Cyclic a,a-Disubstituted Amino Acid for Preparation of Water-Soluble Highly Helical Peptides,* ***Journal of Organic Chemistry*** **1996**, *61*, 7650-7651.

(13) Pauson, P. L.; Watts, E. E. *Ferrocene Derivatives. XIII. Some Ferrocenylethylene and -Acetylene Derivatives,* ***Journal of the Chemical Society*** **1963**, 2990-2996.

(14) Noble, C. O. I. V.; McCarley, R. L. *Surface-Confined Monomers on Electrode Surfaces. 7. Synthesis of Pyrrole-Terminated Poly(propylene imine) Dendrimers,* ***Organic Letters*** **1999**, *1*, 1021-1023.

(15) Elming, N.; Clauson-Kaas, N. *The Preparation of Pyrroles from Furans,* ***Acta Chemica Scandinavica*** **1952**, *6*, 867-874.

(16) Schalkhammer, T.; Mann-Buxbaum, E.; Pittner, F.; Urban, G. *Electrochemical Glucose Sensors on Permselective Nonconducting Substituted Pyrrole Polymers,* ***Sensors and Actuators, B: Chemical*** **1991**, *B4*, 273-281.

(17) Seino, H.; Ishii, Y.; Hidai, M. *1-Pyrrolylimido Complexes of Molybdenum and Tungsten: Synthesis of Pyrrole from Molecular Dinitrogen and Unusual b-Regioselective Substitution Reactions of the Pyrrole Ring on a Metal Complex,* ***Journal of the American Chemical Society*** **1994**, *116*, 7433-7434.

(18) Seino, H.; Ishii, Y.; Sasagawa, T.; Hidai, M. *Synthesis and Reactivities of Pyrrolylimido Complexes of Molybdenum and Tungsten: Formation of Pyrrole and N-Aminopyrrole from Molecular Nitrogen,* ***Journal of the American Chemical Society*** **1995**, *117*, 12181-12193.

(19) Noble IV, C. O.; Louisiana State University: Baton Rouge, 2001.

Chapter 4

Determining the Location of End Groups on DAB Dendrimers

4.1 Introduction

The ability of macromolecules to encapsulate smaller molecular guests has been the focus of a significant portion of efforts in the scientific community. Of interest here is the formation of gated dendrimer hosts, that is, dendrimers whose ability to trap guests can be manipulated through external stimuli. In this approach, it is propsed that smart dendrimers can be constructed by appending at the periphery of the dendrimer, monomers whose oligomers can have their backbone conformation changed through electron-transfer reactions. In order to create a highly efficient dendrimer/host system based on such a redox-stimuli-responsive mechanism, some basic properties of peripherally functionalized dendrimers must first be defined.

It has been shown that the majority of end groups are located along the periphery of poly(propylene imine) dendrimers.[1] Thus, one would postulate that as dendrimers become larger, the end groups would be forced together in closer proximity to one another. However, there is evidence that significant backfolding takes place in poly(amido amine), PAMAM, dendrimers,[2] resulting in the end groups being located inside the dendrimer.

The major goal of the present studies is determination of PPI dendrimer functional group location with respect to one another as a function of dendrimer generation in solution and when adsorbed on gold surfaces. In this work, the existence of hydrogen bond interactions in functionalized PPI dendrimers has been demonstrated by the presence of bands correlating to hydrogen bonded C=O and N-H stretches in their IR spectra.[3] By measuring the relative extent of hydrogen bonding for several generations, a qualitative assessment of the distance between end groups as a function of dendrimer generation can be made.

4.2 Monitoring Hydrogen Bonding of Dendrimers in Solution with IR

Previously, an IR spectroscopy study demonstrated that amide-functionalized PPI dendrimers exhibit strong hydrogen bonding interactions in dichloromethane.[4] In that study, the extent of hydrogen bonding was assessed by comparing the intensities of IR bands associated with N-H stretching for hydrogen-bonded amides and those associated with N-H stretching for non-hydrogen-bonded amides in PPI dendrimers.[5] An alternative route is required for evaluating the extent of hydrogen bonding in dendrimers adsorbed on surfaces.[6]

It has been shown that the degree of H-bonding in proteins can be evaluated by monitoring the band position (frequency)[7] of the amide I and amide II transitions.[7] This method is applicable for determining the extent of hydrogen bonding for molecules in solution and on surfaces. By monitoring the band positions of the amide I and amide II transitions of amide-functionalized PPI dendrimers, it is shown here that the amide-linked functionalities at the terminal ends of the PPI chains in PPI dendrimers exhibit increased hydrogen bonding with increased generation. This increase in hydrogen bonding is interpreted as resulting from a decrease in the distance between the amide functional groups.

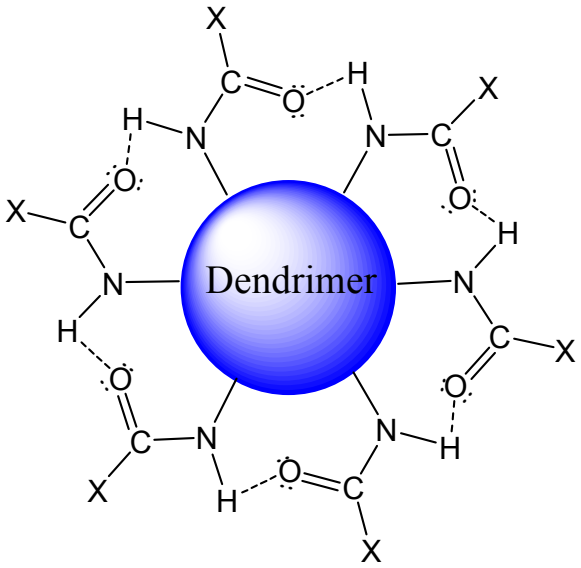

Figure 4.1 Graphic illustrating the intradendrimer hydrogen-bonding between the amide functionalities.

A distinct trend in the IR spectra with respect to generation was observed for ferrocene-terminated PPI dendrimers and BOC-terminated PPI dendrimers in solution (Figure 4.2), and BOC-terminated PPI dendrimers adsorbed to gold substrates (Figure 4.6). A red shift was

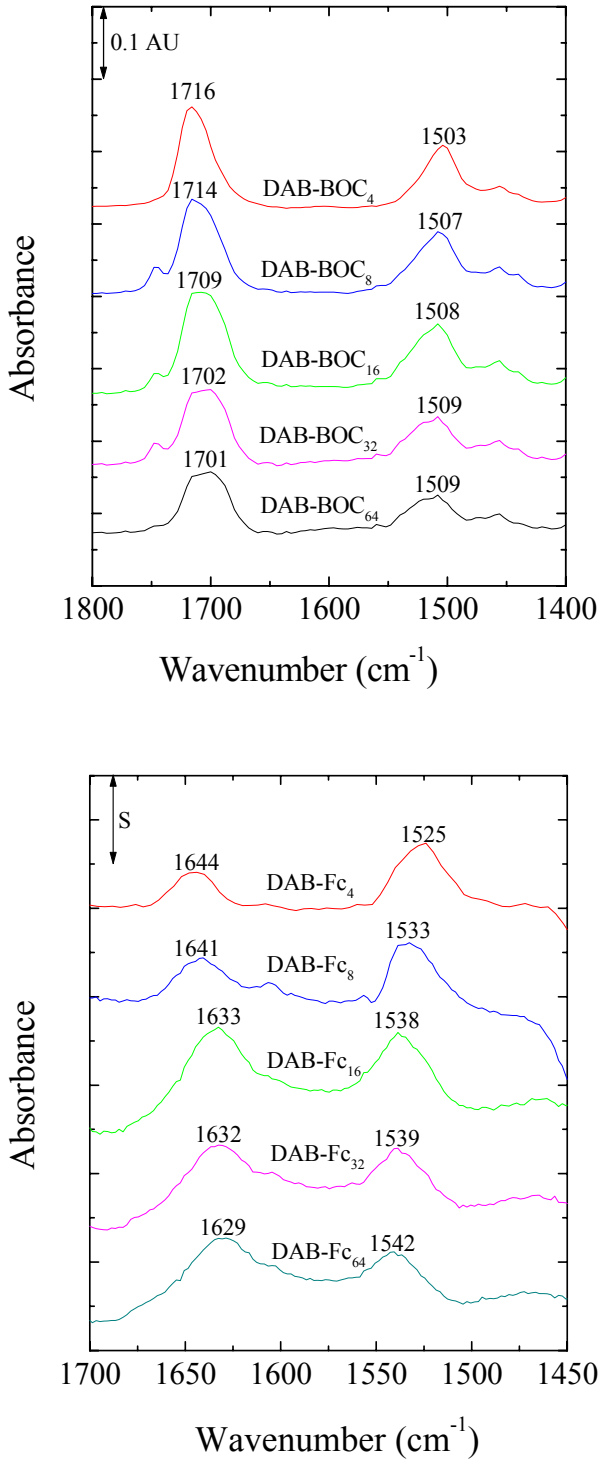

Figure 4.2 Infrared data of BOC and ferrocene-terminated dendrimers in CCl_4 with an end group concentration of 40 x 10^{-3} M for all generations and a path length of 50 μm. S=0.02 AU for DAB-Fc_4 and 0.1 AU for all others.

observed for the amide I absorption band (1629 – 1716 cm^{-1}) while a blue shift was observed for the amide II band (1503 – 1542 cm^{-1}). As a result, more extensive hydrogen bonding is observed for higher generation dendrimers in the IR spectra in Figure 4.2. This increase in hydrogen bonding is interpreted as a decrease in the distance between functional groups. Therefore, as dendrimer generation increases, the functional groups along the periphery are forced closer to one another.

4.3 Adsorption to Gold Substrates

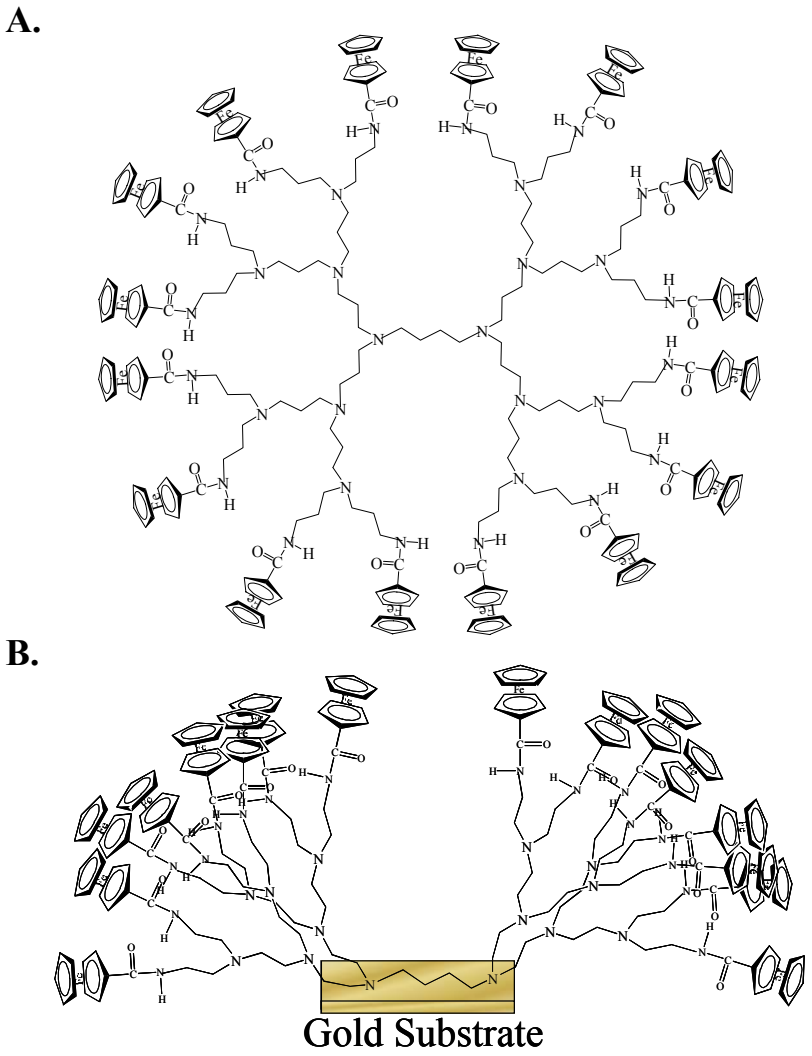

Figure 4.3 Schematic depicting the change in structure when a third generation ferrocene-terminated dendrimer in solution (A) adsorbs to a gold surface through its tertiary amines (B).

It has been observed that fully functionalized PPI dendrimers with no primary amines present along the periphery adsorb quite well to gold substrates, suggesting binding of such molecules to the gold occurs through the core tertiary amines. However, it has been reported that the primary amine end groups of PAMAM dendrimers direct their adsorption to gold surfaces.[8] Due to the flexibility of dendrimers,[9,10] it is also possible that binding of PPI dendrimers to gold surfaces occurs by means of the tertiary amines, the primary amines, or both in unfunctionalized PPI dendrimers. Previous surface studies include amine-terminated[9] and modified dendrimers[11-13] whose functional groups along the periphery are directly involved in the adsorption process. The dendrimers in our studies possess functional groups which do not adsorb to gold, therefore adsorption occurs by means of the tertiary amines.[14] In such a scenario, binding through the tertiary amines may result in deformation of the dendrimer, thereby forcing the end groups closer together. Reflection-absorption IR spectroscopy (RAIRS) and cyclic voltammetry were used to monitor surface reactions to investigate these possibilities.

4.3.1 Reactivity of Amine-Terminated Dendrimers Adsorbed to Gold Substrates

In order to study the binding characteristics of amine-terminated dendrimers to gold substrates, surface reactions were monitored via cyclic voltammetry, (Figure 4.4). Both DAB-Am_{16} and fully functionalized DAB-Fc_{16} were adsorbed to gold electrodes, and the cyclic voltammograms were taken of each. An electrode with DAB-Am_{16} adsorbed to the surface was then immersed into DCM that was 5×10^{-3} M in ferrocenoyl chloride. The cyclic voltammogram of this electrode was obtained and suggested functionalization was achieved. The anodic and cathodic peak currents for the fully functionalized dendrimer and the surface derivatized dendrimer were very similar, suggesting each surface contained similar quantities of ferrocene. However, the larger double-layer capacitance for DAB-Am_{16} reacted with ferrocenoyl chloride

suggests a difference in surface packing. The cause could be a more close-packed dendrimer layer than that of the DAB-Fc_{16}, which must distort in order to bind through the tertiary amines. This would result in a higher surface coverage for DAB-Am_{16} than DAB-Fc_{16}. Therefore if complete functionalization is achieved, the surface reaction should yield larger anodic and cathodic peak currents. The similarity of the values indicates that the surface reaction is not complete and complete functionalization is not achieved under these conditions.

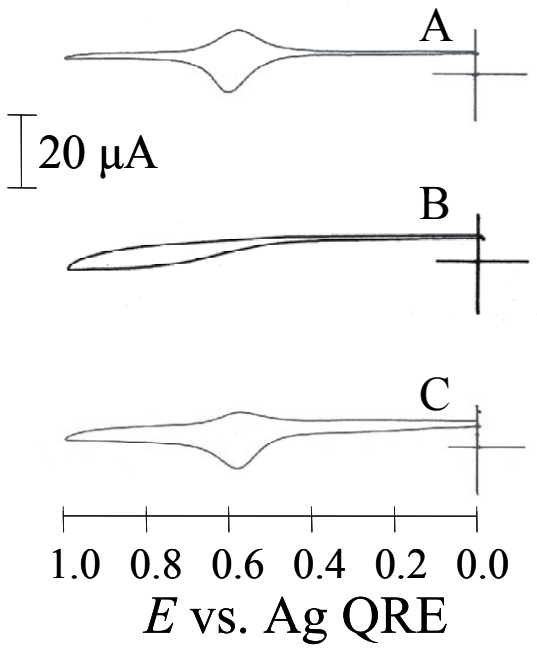

Figure 4.4 Cyclic Voltammetry of DAB dendrimers on Au surfaces: A, functionalized before adsorption (from 0.5 x 10^{-3} M DCM solution of DAB-Fc16); B, unfunctionalized (from 0.5 x 10^{-3} M DCM solution of DAB-Am16); and C, functionalized after adsorption by immersing electrodes containing adsorbed DAB-Am_{16} layers in a 50 x 10^{-3} M ferrocene acid chloride solution in DCM for 5 hours (DAB-Fc*y*). The area of the working electrode was 0.172 cm^2 and the scan rate was 0.1 V s^{-1}.

In order to further investigate the results obtained from cyclic voltammetry, reflection-absorption infrared spectroscopy (RAIRS) data were obtained for DAB-Am_{16} adsorbed to a gold slide (Au/Cr/SiO_2). This slide was then immersed in a ferrocene acid chloride solution and the RAIR spectrum was promptly obtained. The data in Figure 4.5 shows the presence of amide I (1630 cm^{-1}) and amide II (1540 cm^{-1}) bands demonstrating that surface functionalization was achieved. However, because the absorption band corresponding to the C-N stretch of primary amines is still present (1460 cm^{-1}), it is clear that the primary amines are not completely converted to ferrocene-amide functional groups. This suggests that the amine-terminated dendrimers are binding to gold surfaces by means of the

primary amines—to some degree—and these bound amines are not available for functionalization. However, incomplete functionalization could also be the result of a periphery overcrowded with bulky ferrocene end groups and not a result of binding through the primary amines. Thus it is possible that the adsorption process involves both primary and tertiary amines for DAB-Am$_x$.

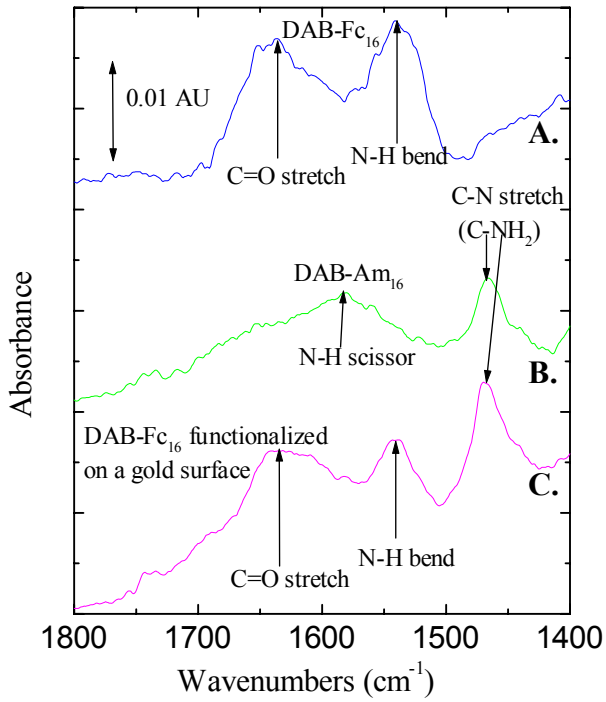

Figure 4.5 RAIR spectra of A. DAB-Fc$_{16}$ dendrimer on gold, B. DAB-Am$_{16}$ on gold, and C. DAB-Am$_{16}$ functionalized with ferrocene acid chloride after being adsorbed on the Au surface (DAB-Fc$_y$).

4.3.2 Hydrogen Bonding Studies of Dendrimers Adsorbed to Gold Substrates

In order for the tertiary amines to be available for adsorption to gold substrates, distortion of the dendrimer structures must occur. This distortion may force the dendrimer end groups in closer proximity of one another. Therefore RAIRS data was obtained for ferrocene and BOC-terminated dendrimers adsorbed to gold surfaces. The RAIRS data for both dendrimers show an increase in hydrogen bonding as the number of functional groups increases. In particular the

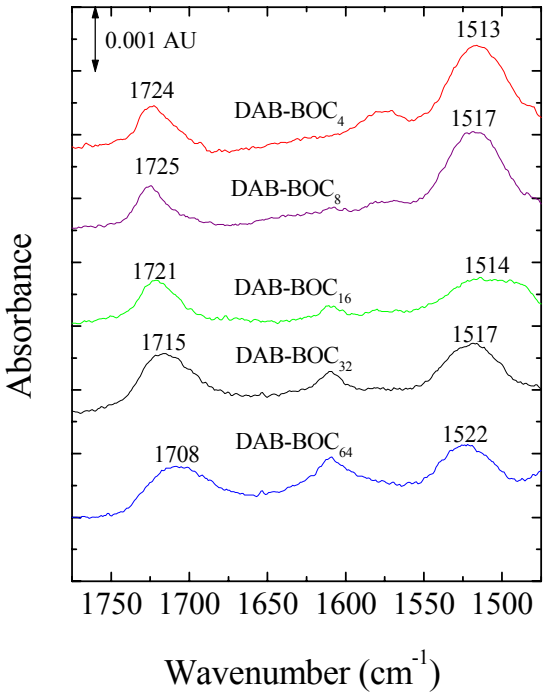

Figure 4.6 RAIR spectra of BOC-terminated dendrimer monolayers adsorbed to gold from dendrimer solutions with an end group concentration of 0.5 x 10^{-3} M in DCM for 5 hours.

data from the BOC-terminated dendrimers is very similar to that of the IR data from the dendrimers in solution. While it is evident the hydrogen bonding interactions are stronger for the larger ferrocene-terminated dendrimers, the trend is not as consistent as that of the solution data or the surface data from the BOC-terminated dendrimers. It is believed this is due to the size of the functional group. The ferrocene along the periphery of the dendrimer is more bulky compared to the BOC groups. This bulkiness may prevent the end branches of the dendrimer from approaching one another, reducing hydrogen bonding interactions. The relatively smaller size of the BOC groups allows the amide groups to readily interact with one another resulting in a larger degree of hydrogen bonding as dendrimer generation increases. However, it is still apparent that the distance between end groups decreases when dendrimer generation increases for both dendrimers.

4.4 Conclusions

As is evident by the IR studies as a function of generation, the dendritic end groups are forced into closer proximity as generation increases for PPI dendrimers. This was deduced from the fact that an increase in hydrogen bonding was observed for the higher generation dendrimers. This also supports the hypothesis that the end groups are located along the periphery of the dendrimer. If the branches are backfolded in the interior of the dendrimer, one would expect to see little change in the IR spectra as a function of generation.

Another aspect of this study was the investigation of surface adsorption properties of both functionalized and unfunctionalized dendrimers. Fully functionalized dendrimers adsorbed extremely well to gold surfaces suggesting adsorption occurs through the tertiary amines because there are no primary amines available. We were also able to determine through surface reactions that some primary amines were available for functionalization when unsubstituted dendrimers were adsorbed. However, complete functionalization did not occur, and therefore it is possible that the primary amines are involved in the adsorption process. It is also possible that the dendrimer structure becomes distorted to allow adsorption through the tertiary amines. If this occurs the distortion may lead to significant crowding of the end groups making it sterically difficult for the functional groups to approach the primary amines. Further studies will be necessary to determine which scenario is occurring, or if it is a combination of the two.

4.5 References

(1) Pavlov, G. M.; Korneeva, E. V.; Meijer, E. W. *Molecular characteristics of poly(propylene imine) dendrimers as studied with translational diffusion and viscometry,* ***Colloid and Polymer Science*** **2002**, *280*, 416-423.

(2) Lyulin, A. V.; Davies, G. R.; Adolf, D. B. *Location of Terminal Groups of Dendrimers: Brownian Dynamics Simulation,* ***Macromolecules*** **2000**, *33*, 6899-6900.

(3) Bosman, A. W.; Janssen, R. A. J.; Meijer, E. W. *Five Generations of Nitroxyl-Functionalized Dendrimers,* ***Macromolecules*** **1997**, *30*, 3606-3611.

(4) Bosman, A. W.; Bruining, M. J.; Kooijman, H.; Spek, A. L.; Janssen, R. A. J.; Meijer, E. W. *Concerning the Localization of End Groups in Dendrimers,* ***Journal of the American Chemical Society*** **1998**, *120*, 8547-8548.

(5) Gardner, R. R.; Gellman, S. H. *Evaluation of the Conformation-Directing Effects of Secondary Hydrogen-Bonding Interactions in Flexible Tetrapeptide Analogs,* ***J. Am. Chem. Soc.*** **1995**, *117*, 10411-10412.

(6) Porter, M. D. *IR external reflection spectroscopy: a probe for chemically modified surfaces,* ***Anal. Chem.*** **1988**, *60*, 1143A-1155A.

(7) Manas, E. S.; Getahun, Z.; Wright, W. W.; DeGrado, W. F.; Vanderkooi, J. M. *Infrared spectra of amide groups in alpha-helical proteins: Evidence for hydrogen bonding between helices and water,* ***Journal of the American Chemical Society*** **2000**, *122*, 9883-9890.

(8) Rahman, K. M. A.; Durning, C. J.; Turro, N. J.; Tomalia, D. A. *Adsorption of Poly(amidoamine) Dendrimers on Gold,* ***Langmuir*** **2000**, *16*, 10154-10160.

(9) Tokuhisa, H.; Zhao, M.; Baker, L. A.; Phan, V. T.; Dermody, D. L.; Garcia, M. E.; Peez, R. F.; Crooks, R. M.; Mayer, T. M. *Preparation and Characterization of Dendrimer Monolayers and Dendrimer-Alkanethiol Mixed Monolayers Adsorbed to Gold,* ***J. Am. Chem. Soc.*** **1998**, *120*, 4492-4501.

(10) Tsukruk, V. V.; Rinderspacher, F.; Bliznyuk, V. N. *Self-Assembled Multilayer Films from Dendrimers,* ***Langmuir*** **1997**, *13*, 2171-2176.

(11) Nijhuis, C. A.; Huskens, J.; Reinhoudt, D. N. *Binding Control and Stoichiometry of Ferrocenyl Dendrimers at a Molecular Printboard,* ***Journal of the American Chemical Society*** **2004**, *126*, 12266-12267.

(12) Hong, M.-Y.; Yoon, H. C.; Kim, H.-S. *Protein-Ligand Interactions at Poly(amidoamine) Dendrimer Monolayers on Gold,* ***Langmuir*** **2003**, *19*, 416-421.

(13) Rolandi, M.; Suez, I.; Dai, H.; Frechet, J. M. J. *Dendrimer Monolayers as Negative and Positive Tone Resists for Scanning Probe Lithography,* ***Nano Letters*** **2004**, *4*, 889-893.

(14) Noble, C. O. I. V.; McCarley, R. L. *Pyrrole-terminated diaminobutane (DAB) dendrimer monolayers on gold: Oligomerization of peripheral groups and adhesion promotion of poly(pyrrole) films,* ***Journal of the American Chemical Society*** **2000**, *122*, 6518-6519.

Chapter 5

Structural Characterization of DAB-Py_{32}

5.1 Introduction

Several different NMR techniques were utilized under different environmental conditions in order to gain a better understanding of the structure of pyrrole-terminated dendrimers. Both NOESY (Nuclear Overhauser Effect Spectroscopy) and ROESY (Rotational Overhauser Effect Spectroscopy) data were obtained which yielded information as to the location of the pyrrole functionalities. If the pyrrole groups are located in the interior of the dendrimer, encapsulation of guests may be difficult. An ideal phenomenon would be one in which the pyrrole units were extended outward along the periphery of the dendrimer, making way for the desired guest to occupy any internal cavities.

Relaxation experiments also provide useful information in deducing the relative mobility of the terminal groups. It is currently unknown as to whether rigid or mobile pyrrole monomers are more likely to form oligomers. We are interested in determining whether the pH of the solution has an effect on the rigidity of the pyrrole groups prior to coupling. An ideal scenario would be one in which we are able to control the number of pyrrole monomers involved in the pyrrole oligomers by altering the pH. Noble has already demonstrated that pyrrole-terminated dendrimers possessing an oligomeric periphery are more efficient in the retention of entrapped guests than dendrimers whose periphery is in the monomeric state.[1] He has also shown that reducing the oligomers results in the dendrimers quickly expelling the incarcerated molecules. We would like to determine whether longer or shorter oligomers will aid in retention of guests incarcerated by the dendrimer, and how controlling the length of the oligomers will affect the release properties of guests.

5.2 2-Dimensional NMR studies

The 2D NMR techniques used for structural characterization were NOESY and ROESY. Both techniques are extremely useful in determining chemical structure, but in most situations one of the experiments is preferred over the other. The sense of the cross peaks observed in NOESY data depends on the rotational correlation time of the molecule being studied. If the diagonal is phased negative, positive cross peaks are obtained for molecules with small correlation times while negative cross peaks are obtained for molecules with large correlation times.[2] Chemical exchange results in negative cross-peaks as well and are indistinguishable from negative NOEs arising from large molecules. Molecules with an intermediate correlation time may yield cross peaks with zero intensity. Because ROESY experiments yield NOE cross peaks that are always positive, NOEs that go undetected in NOESY can be observed in ROESY data.[3] Another advantage of ROESY is the ability to distinguish between cross peaks resulting from exchange and NOEs as they are opposite in phase. Therefore, NOESY is preferred for small molecules while ROESY is preferred for intermediate to large molecules. However, the main drawback with ROESY is its similarity with TOCSY (total correlated spectroscopy) experiments. Both experiments utilize the same pulse program, with the exception that TOCSY utilizes a higher power spin-lock. If one uses a spin-lock power that is too high, TOCSY peaks may be present in ROESY spectra.

The 4th-generation pyrrole-terminated dendrimer was the focus of these studies because this was the dendrimer used in future encapsulation studies. NOESY experiments were conducted on DAB-Py_{32} in deuterated methylene chloride (CD_2Cl_2), although no through-space interactions were observed in the form of cross peaks between pyrrole protons and protons located in the interior of the dendrimer. However, as discussed previously, this does not mean

that backfolding is not taking place, because the sign of the NOE can be different for small[4] and large molecules,[5,6] or null for intermediate-sized molecules.[3] Therefore, ROESY experiments were performed to determine if this phenomenon was occurring.

Because the pyrrole-terminated dendrimers used in our studies are only slightly soluble in water (~20 x 10^{-6} M), we believed if any backfolding occurs it will be most significant in aqueous solutions. At lower pH, the interior tertiary amines are protonated,[7] causing the dendrimer branches to spread out as far as possible due to charge repulsions.[8] However, at higher pH this should be less of a factor in regards to the location of the pyrrole functionalities. Several groups have shown that PAMAM dendrimer size increases as the pH is lowered and tertiary amines become protonated.[9-11] Therefore, ROESY data was obtained for DAB-Py_{32} in both pD 2 DCl and in neutral D_2O to determine if the smaller dendrimer diameters are the result of backfolding.

Surprisingly NOESY data in organic solvents and both ROESY data sets in aqueous solvents were extremely similar between the pyrrole protons and other protons on the dendrimer; however, there were no crosspeaks between protons located in the interior of the dendrimer and the pyrrole functional groups along the periphery. Crosspeaks were observed between peaks associated with the pyrrole protons and peaks located at 1.29, 2.16 and 3.85 ppm, which correspond to protons located on the hexyl chain linking the pyrrole to the dendrimer.

If significant backfolding were occurring, we would expect to see crosspeaks between the pyrrole protons at 6.2 and 6.6 ppm and the peaks found at 2.4 and 1.6 ppm that correlate with methylene protons, which are found throughout the interior of the dendritic structure. Because no through-space interactions are observed between pyrrole protons and these methyelene protons, it is believed that the majority of the end groups are located along the periphery of the

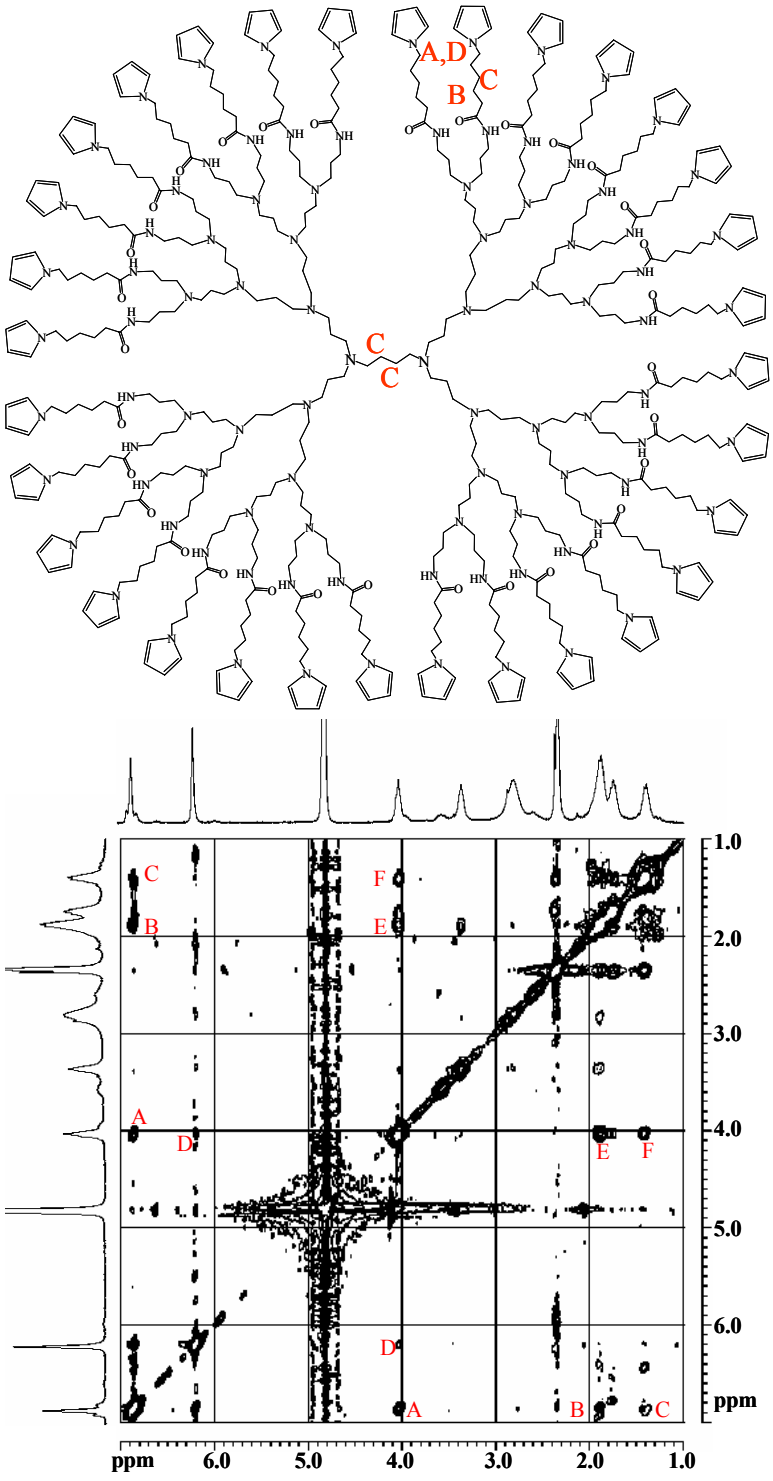

Figure 5.1 ROESY data obtained from a 1:1 *d*6-Acetone D_2O solution in which the concentration was 0.01 M in end groups.

dendrimer. However, due to the numerous crosspeaks present in the spectra it is apparent that the pyrroles are located in several different environments and are not exclusively extended outward. Through-space interactions were observed between pyrrole protons and protons on the hexyl chain linking the pyrrole to the dendrimer and between the methylene adjacent to the pyrrole and methylene protons on the hexyl linker.

5.3 NMR Relaxation Measurements

5.3.1 T_1 Studies in Organic Solvents

Spin-lattice relaxation experiments were conducted for generations 1–5 of pyrrole-terminated dendrimers on 300 and 400 MHz spectrometers in deuterated methylene chloride. On the 300 MHz instrument, the T_1 relaxation time constant was calculated for each proton on all dendrimer generations at room temperature. The T_1 values were also determined at several different temperatures for the 4th-generation dendrimer in order to determine whether the data

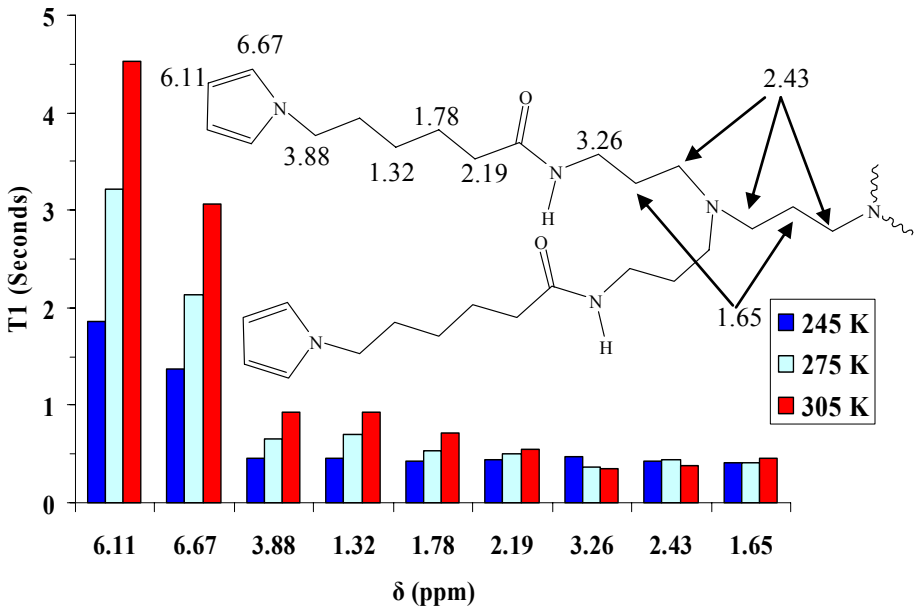

Figure 5.2 T_1 data collected at various temperatures on an ARX-300 MHz instrument for DAB-Py$_{32}$ in CD_2Cl_2 with an end group concentration of 0.01 M.

was consistent with that of a small molecule or a large molecule. Relaxation values are a function of a molecules size, or its rotational correlation time. Increasing the temperature results in faster tumbling and decreases the correlation time. In general, the T_1 value for small molecules increases as the correlation time is decreased or as the temperature is increased. For large molecules the relaxation time is directly related to its correlation time and increases as the temperature is decreased. By measuring the relaxation values at different temperatures, it is possible to deduce whether or not the dendrimers behave like small or large molecules. This is an important step in order to interpret relaxation data. For small molecules, an increase in T_1 is characteristic of an increase in mobility, whereas it is the opposite is true for large molecules.

The T_1 values for protons located along the periphery of the dendrimer increased with temperature, while protons in the interior of the dendrimer were relatively unaffected. This suggests the periphery of the dendrimer (pyrrole and the hexyl linker) behaves like a small molecule while the interior of the dendrimer (all protons interior to the amide bonds) is more characteristic of a large molecule (Figure 5.2). Therefore, an increase in the T_1 values for a proton located along the periphery is the result of an increase in mobility for that proton. After completion of the temperature studies, T_1 relaxation data was obtained at room temperature for all 5 generations of pyrrole-termianted dendrimers (Figure 5.3). The T_1 values for identical protons on different generation dendrimers located along the periphery decreased as dendrimer generation increased. Therefore, it was found that the mobility along the periphery of the dendrimer decreases with increasing dendrimer generation. This corroborates the previous results obtained from hydrogen-bonding studies of similarly substituted PPI dendrimers (Chapter 4) utilizing FTIR. As the generation increases, the external moieties become closer together, restricting mobility.

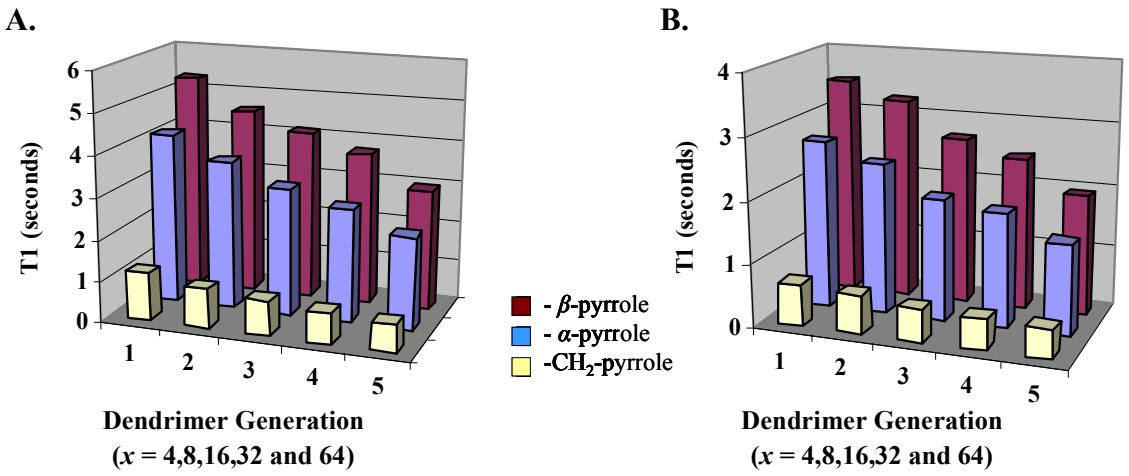

Figure 5.3 T_1 data acquired with an ARX-300 MHz spectrometer as a function of generation for DAB-Py$_x$ (x = 4, 8, 16, 32, and 64) in CD_2Cl_2 (A) and 1:1 *d*6-Acetone pD 2 DCl (B) with an end-group concentration of 0.01 M for all solutions.

Further T_1 determinations were carried out on the 400 MHz spectrometer, because the temperature control on this instrument is more accurate than that on the lower field instrument. T_1 data as a function of temperature were obtained for each generation dendrimer because it was not known as to whether the interior of the lower generation dendrimers would demonstrate large molecule behavior as the 4th-generation did. Another interest was to determine whether or not the periphery of the dendrimer would behave more like a large molecule for the 5th-generation dendrimer as the mobility is further restricted due to the decreasing distance between the end groups as generation increases.

Generations 2–5 yielded similar results as is seen in Figures 5.4–5.6. While the T_1 values were significantly different for most of the protons, the temperature trends were essentially the same. All four generations (2–5) depicted a small-molecule behavior along the periphery of the dendrimer and large-molecule behavior within the interior of the dendrimer, as discussed above for the 4th-generation dendrimer. For DAB-Py$_4$, the T_1 value for all protons increased with temperature, pointing to small-molecule behavior. Another interesting observation was that the

T_1 values for the protons located along the periphery of the dendrimer were significantly larger than the values for the protons in the dendrimer interior. Therefore, it was concluded that mobility increases from the core outward towards the periphery.

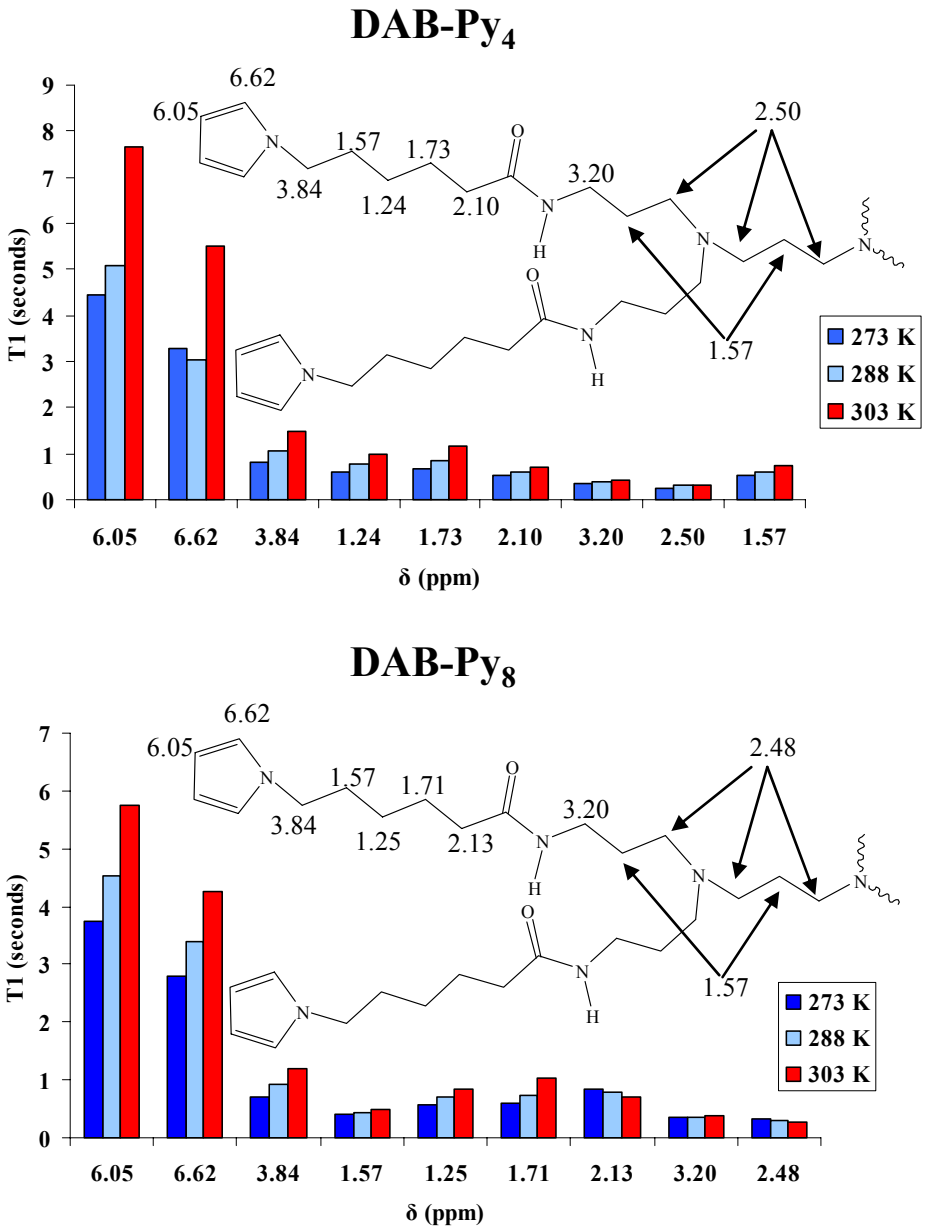

Figure 5.4 T_1 data acquired on a DPX-400 MHz spectrometer as a function of temperature for DAB-Py_4 and DAB-Py_8 in CD_2Cl_2 with an end group concentration of 0.01 M.

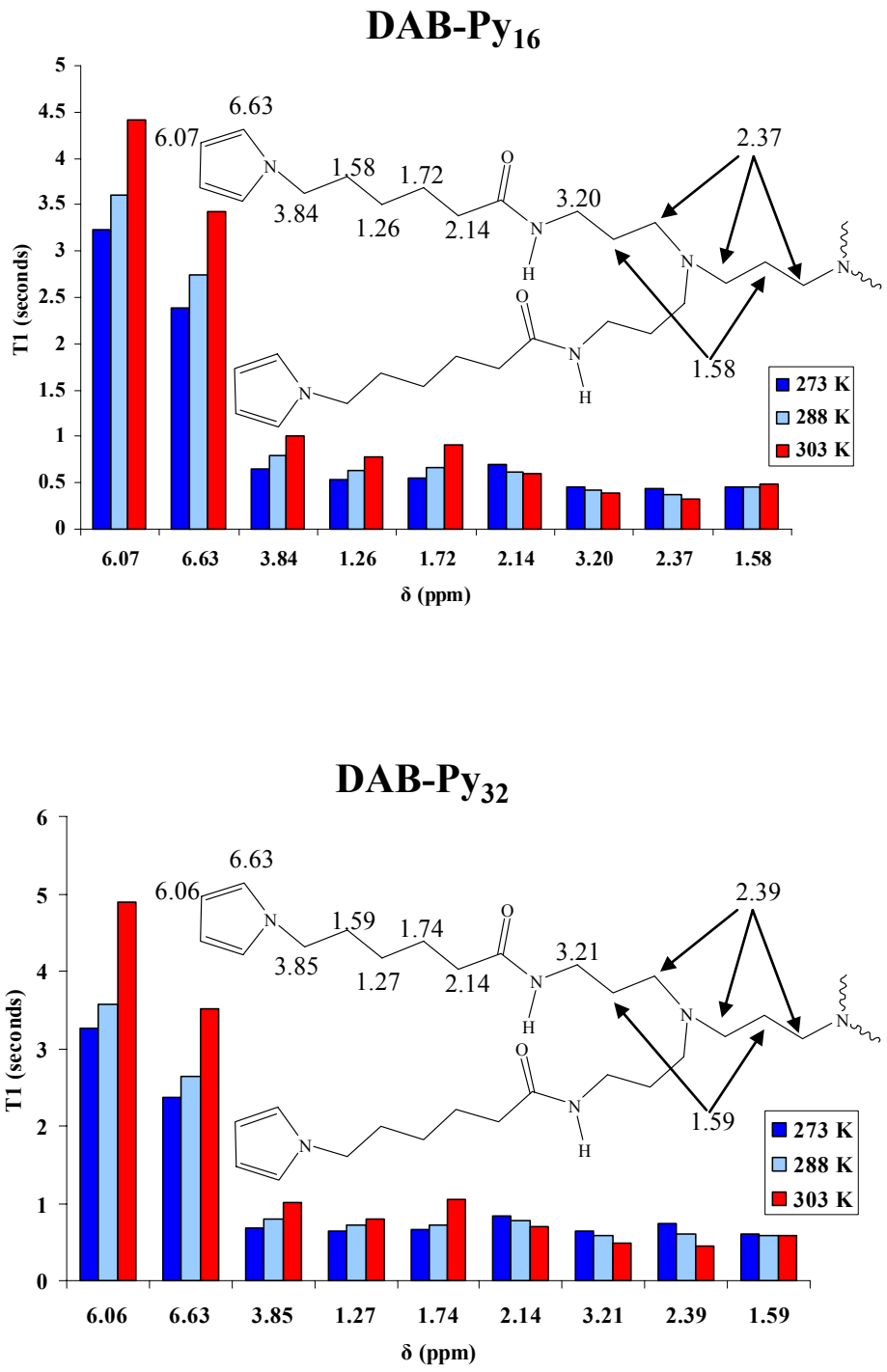

Figure 5.5 T_1 data acquired on a DPX-400 MHz spectrometer as a function of temperature for DAB-Py_{16} and DAB-Py_{32} in CD_2Cl_2 with an end group concentration of 0.01 M.

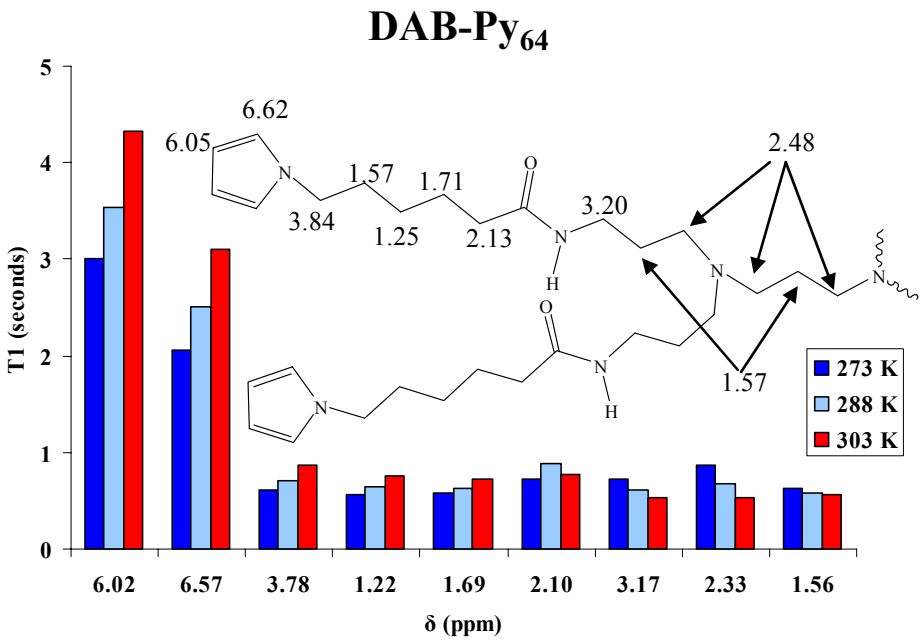

Figure 5.6 T_1 data acquired on a DPX-400 MHz spectrometer as a function of temperature for DAB-Py_{64} in CD_2Cl_2 with an end group concentration of 0.01 M.

5.3.2 T_1 studies in Aqueous Solutions

Of particular interest is the behavior of the pyrrole-terminated dendrimers in aqueous solutions, as encapsulation experiments discussed in Chapter 6 are conducted under these conditions. On the 300 MHz spectrometer, T_1 values were determined for all protons on generations 1–5 pyrrole-terminated dendrimers at 298 K. Temperature studies were also conducted on the 4th-generation dendrimer dissolved in a 1:1 solution of pD 2 DCl and deuterated acetone. Therefore, the pD values reported in these studies are the -log [D^+] prior to adding acetone.

As is seen in Figure 5.7 the trends in the data were similar to those acquired in CD_2Cl_2. The temperature studies suggest the periphery of the dendrimers exhibit small molecule behavior while the interior is more characteristic of a large molecule. Relaxation times along the periphery decreased with increasing dendrimer generation, suggesting mobility along the

periphery is more restricted for larger dendrimers. The T_1 values for internal protons remained relatively unchanged. Again the relaxation values increased from the core outward towards the periphery, allowing one to conclude that protons located along the periphery of the dendrimer are more mobile than those located in the interior regions of the dendrimer in aqueous environments.

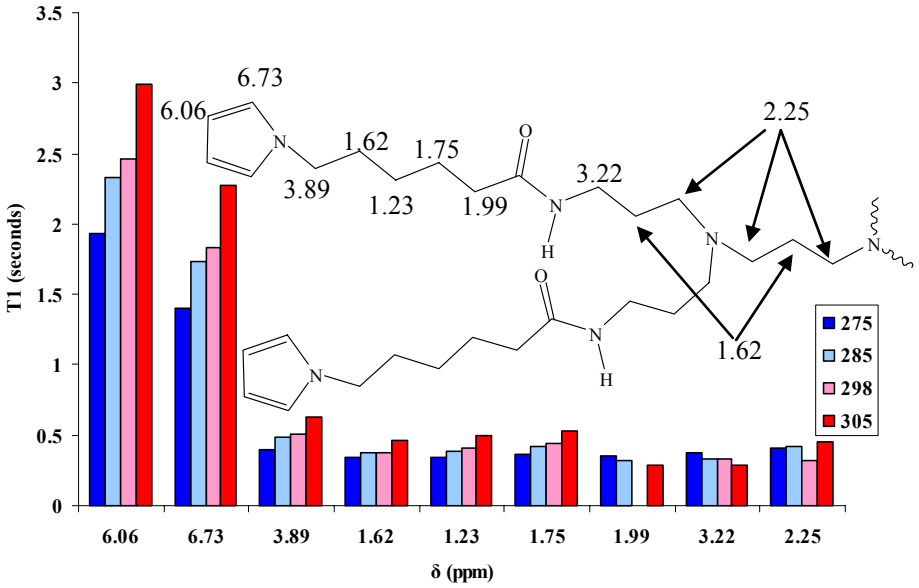

Figure 5.7 T_1 data collected at various temperatures on the ARX-300 MHz spectrometer for DAB-Py_{32} in 1:1 pD 2 DCl *d*6-Acetone with an end group concentration of 0.01 M.

Further temperature studies were conducted on all 5 generations of pyrrole-terminated dendrimers on the 400 MHz instrument to determine whether the small- molecule/large-molecule behavior was dependent upon the dendrimer generation. These results were also similar to those obtained in CD_2Cl_2. All protons depicted small molecule behavior for generation 1 along with protons located along the periphery of the dendrimer for generations 2–5, while protons located along the interior of the dendrimer of generations 2–5 displayed large molecule behavior. The only difference in the data is that the methylene adjacent to the carbonyl on the hexyl linker displayed large molecule characteristics in aqueous solutions for generations 2–5.

5.3.3 Effect of pD on T_1

Because one of the major objectives in this work is to observe the encapsulation properties at various pH and ionic strengths, the effect of pD on spin-lattice relaxation was also investigated. Several aqueous solutions were prepared with various concentrations of DCl. To these solutions, an equal volume of dendrimer solution in deuterated acetone with a concentration of 0.02 M in end groups was added resulting in a final concentration of 0.01 M in end groups. The pD of the samples used ranged from 1.2 to 6 and were analyzed on the 300 MHz instrument. A distinct trend in the T_1 values was observed for the pyrrole protons. The relaxation time at lower pD was much longer than those values at high pD suggesting a more rigid structure at higher pD. There was no significant difference in the relaxation rates of the other dendritic protons. These findings are contrary to those in the literature which suggest a more rigid structure exists at lower pH upon protonation of the tertiary amines.[7,12]

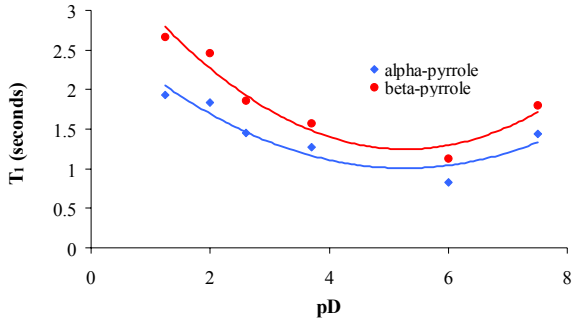

Figure 5.8 Effect of pD on the relaxation rate for pyrrole protons on DAB-Py_{32}. The T_1 data were acquired on an ARX-300 with an end-group concentration of 0.01 M.

Analysis of the data acquired from the 400 MHz instrument proved to be more difficult. It was imperative to conduct temperature studies at different pD to ensure that the small molecule/large molecule behavior remained unchanged, and interpretation of the data was still accurate as the pD was adjusted. The behavior of DAB-Py_{32} at pD 2 had already been observed, so samples were prepared as discussed above with aqueous solutions that were pD 4 and pD 7. The spin-lattice relaxation time constants were then determined at different temperatures in each solution. One of the first things noticed was the appearance of small shoulders near two of the

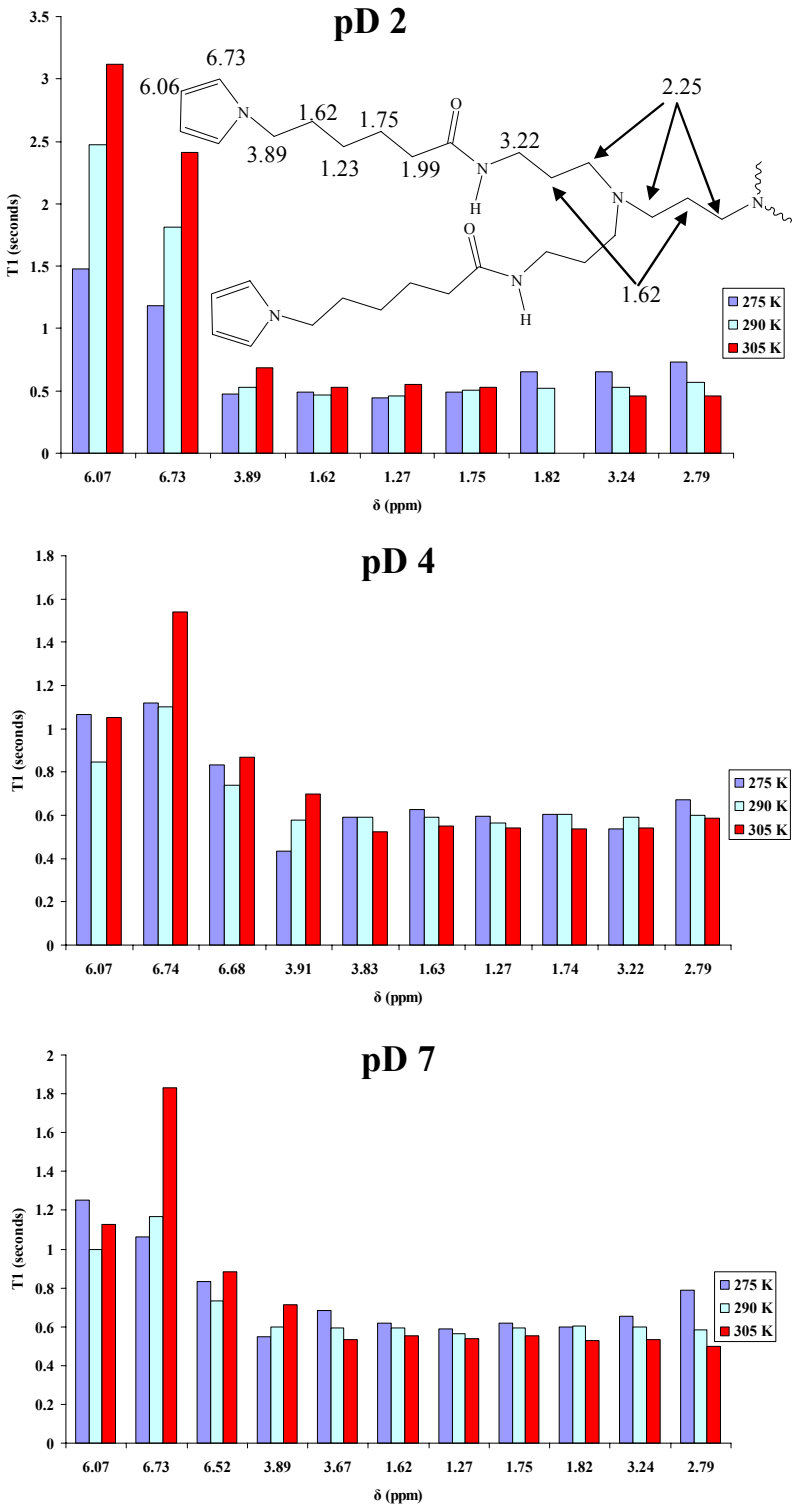

Figure 5.9 T_1 data acquired on a DPX-400 spectrometer at different temperatures in which the samples were dissolved in 1:1 *d*6-Acetone D_2O with a pD of 2, 4, and 7 with an end-group concentration of 0.01 M.

peaks. Previously, in organic and in pD 2 solutions, the *alpha*-pyrrole protons and the protons on the methylene chain adjacent to the pyrrole were narrow and contained no shoulders located downfield or upfield of the larger peak. Raising the pD results in the growth of a small shoulder located just downfield from these peaks. The T_1 values for the *alpha*-pyrrole protons and the methylene protons adjacent to pyrrole increased with temperature. However, the remaining protons, including the two shoulders, demonstrated large molecule behavior. There was no distinct trend for protons at the *beta* position.

We believe the presence of these shoulders can be explained by the previous ROESY data obtained on these dendrimers. Several cross peaks were observed in the ROESY data suggesting the pyrrole moieties are located in multiple environments. As noted above, previous T_1 studies showed that the relaxation times were greatly dependent on proton location on the dendrimer. The peaks correlating to protons demonstrating small molecule behavior are those extended outward along the periphery of the dendrimer, while the smaller shoulders demonstrating large molecule behavior result from the end groups backfolded somewhat into the dendrimer. Because the two peaks were resolved for the *alpha*-protons and the methylene protons we are able to see both trends. I believe the two peaks are simply overlapping for the proton in the *beta* position and this is why no distinct trend is observed in the T_1 versus temperature graphs. This scenario is also supported by the T_2 data discussed below.

5.3.4 T_2 Determination

Often the spin-spin relaxation time is also measured to support T_1 results. As discussed previously, it is imperative to determine whether a given proton is demonstrating small or large molecule behavior in order to correctly interpret the relaxation data. One simple method is to acquire T_1 data at multiple temperatures and determine the effect temperature has on the

relaxation time, as we have already done. When compared with T_1 values obtained, T_2 values also provide insight as to small or large molecule behavior.

As is the case with spin-lattice relaxation, spin-spin relaxation is dependent upon correlation time. However, the spin-spin relaxation time constant decreases as the rotational correlation time increases for both small and large molecules. When the net magnetization is placed in the XY plane after a 90° pulse, two processes simultaneously occur: the magnetization in the XY plane dephases and goes to zero and longitudinal magnetization grows as it reaches the equilibrium value prior to the pulse. The longitudinal magnetization never reaches its equilibrium value prior to complete dephasing of the transverse magnetization. Therefore T_2 is always equal to or less than T_1.

For small molecules T_2 is equal to T_1. Therefore one can determine T_2 relaxation times and compare them with the T_1 values to conclude as to whether the molecules were demonstrating small or large molecule characteristics. T_2 data was obtained for DAB-Py_{32} in CD_2Cl_2 to support our T_1 data. After conducting an exponential decay fit on the data, T_2 values were obtained that were substantially larger than the T_1 values determined under the same conditions.

As an alternative to using the Bruker software to complete the calculations, the individual rows in the 2D-data set were extracted and processed individually. The rows correlating with *tau* = 0.12, 0.4, and 0.8 seconds are shown in Figure 5.10. After processing the first row, insufficient shimming was a concern, as there seemed to be significant asymmetry for some of the peaks. However, after processing further rows with longer *tau* values, it was clear what was occurring. What appears to be significant asymmetry in the peaks toward lower ppm values at short *tau* values, is actually the result of identical protons being located in multiple environments. This

was not evident until rows with larger *tau* values were processed. As the peak intensity decays over time, the peaks associated with the numerous components are resolved. These individual components are only observed in the individual rows in the T_2 data set. Numerous 1D studies have been conducted on this dendrimer under the same conditions and the pyrrole protons always yielded 2 single narrow peaks. These additional peaks are not observed in 1D data sets because the FID is obtained almost immediately after the magnetization is rotated into the XY plane. There is insufficient time for the individual peaks to diphase and become resolved with respect to one another.

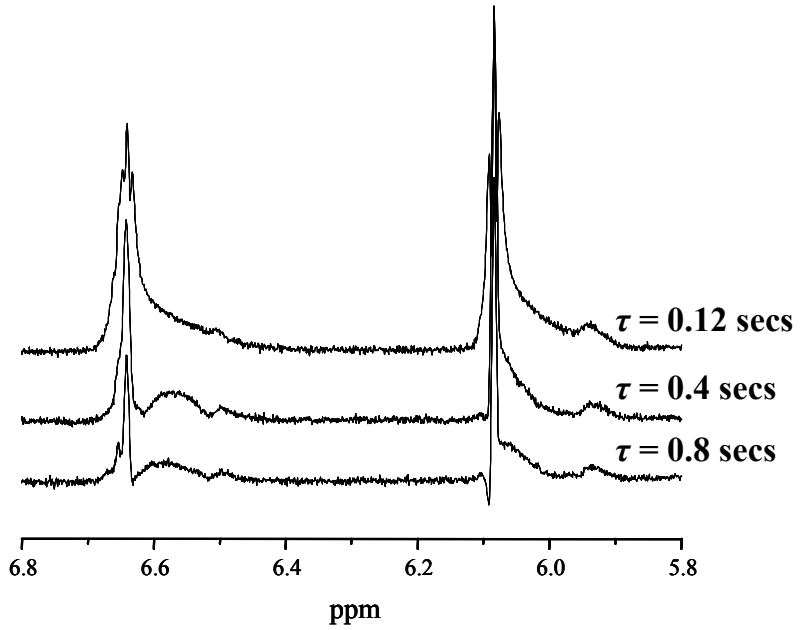

Figure 5.10 The 1-D rows extracted from the T_2 data file acquired on a DPX-400 of DAB-Py_{32} dissolved in CD_2Cl_2 with an end-group concentration of 0.01 M.

Due to the presence of numerous components, it was impossible to calculate accurate T_2 values. The individual peaks were not resolved at short *tau* values and decayed too quickly to obtain enough data points for an accurate determination of the spin-spin relaxation. While we were unable to calculate accurate T_2 values, we are unaware of any work in the literature showing such a phenomenon. There are several studies available with published T_2 values, but

none have mentioned any proton being in such different environments. The importance of these studies is the fact that these multiple components go unnoticed when simple 1-D data is acquired, or when the Bruker software is used to complete the calculations.

As discussed in Section 5.2 several through-space interactions were observed between pyrrole protons and methylene protons located on the hexyl chain through which the pyrrole is attached to the dendrimer. Through-space interactions were observed for 3 different methylene protons suggesting the pyrrole functionalities are located in several environments. Further T_1 studies revealed a distinct trend in relaxation times as a function of proton location. Protons towards the interior regions of the dendrimer had shorter relaxation values, while protons near the periphery of the dendrimer had longer relaxation values. In 1D studies, the FID is taken almost immediately after the magnetization is transferred to the XY plane and the protons are not given sufficient time to dephase. Therefore, the result is a single broad peak in the NMR spectra.

While the chemical shifts remain relatively the same, the relaxation values for each proton can be different. In fact it was observed that two chemically identical protons, both located on the same position on pyrrole, depicted both small-molecule behavior and large-molecule behavior. T_1 studies revealed that protons in the interior regions of the dendrimer depicted large-molecule behavior, while protons located along the periphery depicted small-molecule behavior. Therefore, interpretation of these results allows one to conclude that some of the pyrrole functionalities are located along the periphery of the dendrimer, while some are located towards the interior regions of the dendrimer. To what extent the pyrrole groups are backfolding into the dendrimer remains unclear. 2D NMR studies suggest the terminal groups are predominately located along the periphery with some of the pyrroles interacting with

methylene groups on the hexyl linker. There is no evidence to suggest the pyrroles units are backfolded into the interior cavities of the dendrimer.

If the dendrimers are in fact backfolded into the interior cavities of the dendrimer, encapsulation may prove difficult. However, if the dendrimers are collapsing about the periphery, encapsulation efficiency may be enhanced as guests may be sterically prevented from exiting the dendrimer. These scenarios were investigated and are discussed further in Chapter 6.

5.4 Oligomerization of Pyrrole End Groups

Pyrrole has numerous properties that make it attractive to researchers, but its ability to form oligomers in the presence of chemical oxidants is most significant to this work. Specifically their ability to form oligomers after being attached to high-generation dendrimers is the most attractive asset. Noble[1] and Morara[13] have demonstrated the ability of dendrimers possessing an oligo-pyrrole periphery to retain guest molecules in the core. The aim of the work in this dissertation is to determine whether different length oligomers can be made by altering the pH and whether the encapsulation properties of the dendrimers are related to the length of these oligomers.

A stock solution of DAB-Py_{32} in acetone was prepared that was 0.02 M in end groups. This solution was added to an equal portion of aqueous solvent (pH = 2, 4, or 7) and the acetone was removed under vacuum. An equal volume of 0.2 M $Fe(NO_3)_3 \cdot 9H_2O$ was then added and the reaction was allowed to progress for 12 hours. Methanol was then added to reduce the oxidized pyrroles, and the solution was stirred for an additional 24 hours. The oligo-pyrrole-terminated dendrimer was then extracted with chloroform. The volume of the organic solution was then decreased to increase the concentration of the dendrimer. The solution was added to a gold coated microscope slide and the solvent was allowed to evaporate under a steady stream of

nitrogen. A blank gold slide prepared in the same batch as the one used above was used as a reference on the FTIR. Finally RAIRS was conducted on the oligo(pyrrole)-terminated dendrimer.

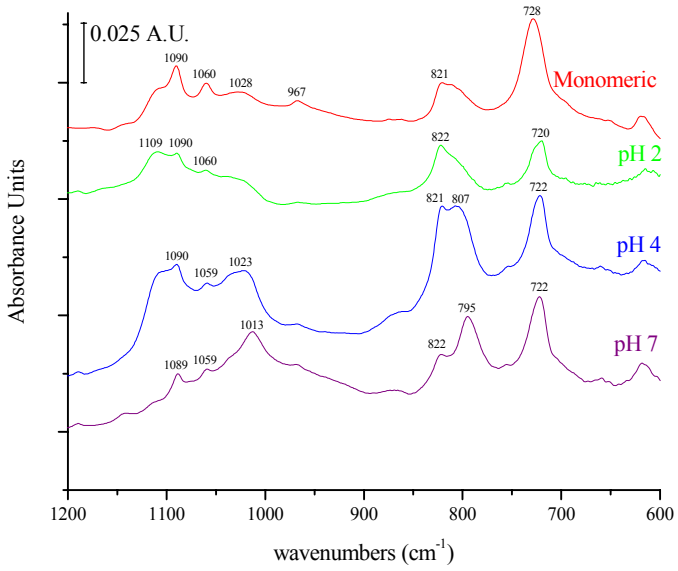

Figure 5.11 RAIR spectra obtained from DAB-Py_{32} oligomerized at pH 2, 4, and 7.

Zerbi prepared and isolated oligo(pyrrole)s of different repeat unit length and acquired IR spectra of each polymer. They reported a direct correlation between to characteristic bands, which they referred to as *T* bands and *B* bands, with that of the oligomer length. *T* bands correspond to end group vibrations and are found in the 720-730 cm^{-1} region (ω(C-H)$_{oop\text{-}ring}$) and around 1065 cm^{-1} (ω(C-H)$_{ip\text{-}ring}$). *B* bands correspond to pyrrole groups within the oligo(pyrrole) chains and are found at approximately 765(ω(C-H)$_{oop\text{-}ring}$) and 1035 cm^{-1}(ω(C-H)$_{ip\text{-}ring}$).[14] When monomeric pyrroles are present the intensities of the *B* bands are dominated by that of the *T* bands. When oligomers are formed, the intensities of the *B* bands increase and the intensities of the *T* bands decrease. By comparing the relative intensities of these two bands, Zerbi was able to estimate the length of the oligo(pyrrole)s formed.[14] Using this approach it can be seen in Figure

5.11 that longer oligomers were formed at higher pH. The intensities of the *T* and *B* bands were similar for the oxidation conducted in pH 2 HCl, while the *T* band intensity increased as the pH was increased to 7. This suggests that trimers were formed at pH 2 and oligomers containing up to 7 pyrroles were formed at pH 7. While it is difficult to put an exact number on the oligomer lengths, it is quite obvious that the *B* band/*T* band ratio increased with pH suggesting larger oligomers were formed at higher pH.[14]

T_1 studies conducted in aqueous solutions revealed a more rigid structure at increasing pH. Therefore, upon initial glance it appears as though reducing mobility results in longer oligomers. While this is the case with this particular system, it remains unclear as to the exact reason for the formation of longer oligomers. This increase in oligomer length could in fact be directly related to an increase in mobility. However, these same relaxation studies also suggest the pyrrole functionalities are located in multiple environments with some of them collapsed into the inner portions of the periphery. This collapsing may force the end groups closer to one another and may be the true reason longer oligomers were formed at higher pH.

5.5 Conclusions

The results of the NMR studies suggest that the pyrrole functional groups are located in multiple environments. 2D NMR experiments were conducted that resulted in no significant confirmation that the pyrrole groups are backfolded into the core of the dendrimer. Evidence was observed however, that shows the pyrrole groups are in close proximity to multiple protons located on the hexyl linker. T_2 relaxation experiments supported this data as numerous peaks were observed as the transverse magnetization decayed.

T_1 studies conducted at multiple temperatures suggested the periphery of the dendrimers possess small molecule characteristics while the protons located throughout the interior of the

dendrimer display a large molecule behavior. The results of these studies led to several conclusions as to the mobility at different areas of the dendrimer under different conditions. It was found that mobility increased from the interior of the dendrimer towards the periphery. However, mobility along the periphery decreased as generation increased. Studies conducted on the 300 MHz NMR suggest that the periphery becomes more rigid as the pD is increased. Data acquired on the 400 MHz in aqueous solutions was inconclusive at higher pD. Correct molecule behavior, small-molecule or large-molecule, was unable to be determined as there was no distinct trend in the relaxation values as a function of temperature. It is believed that this is due to the fact that the protons are located in several environments, some of which display small molecule behavior and some of which exhibit large molecule behavior.

While specific conclusions were not able to be drawn from some of the T_1 data, it was apparent that changing the pH had a significant effect on the dendrimer structure. Oligomerization of the pyrrole moieties also proved to be significantly dependent upon the solution pH. Using Zerbi's method it was shown that larger oligomers were formed at higher pH for pyrrole-termianted dendrimers. The current task at hand now is to answer the question as to whether these larger oligomers will be more efficient in retaining guests encapsulated by DAB-Py_{32}.

5.6 References

(1) Noble IV, C. O. *Pyrrole-Terminated Dendrimers for Use in Polymerizable Monolayers and Guest Encapsulation Systems, Louisiana State University, Baton Rouge,* 2001.

(2) Macura, S.; Ernst, R. R. *Elucidation of Cross Relaxation in Liquids by Two-Dimensional NMR Spectroscopy,* ***Molecular Physics*** **1980**, *41*, 95-117.

(3) Bothner-By, A. A.; Stephens, R. L.; Lee, J.; Warren, C. D.; Jeanloz, R. W. *Structure Determination of a Tetrasaccharide: Transient Nuclear Overhauser Effects in the Rotating Frame,* ***Journal of the American Chemical Society*** **1984**, *106*, 811-813.

(4) Solomon, I. *Relaxation Processes in a System of Two Spins,* ***Physical Review*** **1955**, *99*, 559-565.

(5) Balaram, P.; Bothner-By, A. A.; Breslow, E. *Localization of Tyrosine at the Binding Site of Neurophysin II by Negative Nuclear Overhouser Effects,* ***Journal of the American Chemical Society*** **1972**, *94*, 4017-4018.

(6) Balaram, P.; Bothner-By, A. A.; Dadok, J. *Negative Nuclear Overhuaser Effects as Probes of Macromolecular Structure,* ***Journal of the American Chemical Society*** **1972**, *94*, 4015-4017.

(7) Koper, G. J. M.; van Genderen, M. H. P.; Elissen-Roman, C.; Baars, M. W. P. L.; Meijer, E. W.; Borkovec, M. *Protonation Mechanism of Poly(propylene imine) Dendrimers and Some Associated Oligo Amines,* ***Journal of the American Chemical Society*** **1997**, *119*, 6512-6521.

(8) Welch, P.; Muthukumar, M. *Tuning the Density Profile of Dendritic Polyelectrolytes,* ***Macromolecules*** **1998**, *31*, 5892-5897.

(9) Maiti, P. K.; Cagin, T.; Lin, S.-T.; Goddard, W. A., III. *Effect of Solvent and pH on the Structure of PAMAM Dendrimers,* ***Macromolecules*** **2005**, *38*, 979-991.

(10) Lee, I.; Athey, B. D.; Wetzel, A. W.; Meixner, W.; Baker, J. R., Jr. *Structural Molecular Dynamics Studies on Polyamidoamine Dendrimers for a Therapeutic Application: Effects of pH and Generation,* ***Macromolecules*** **2002**, *35*, 4510-4520.

(11) Betley, T. A.; Banaszak Holl, M. M.; Orr, B. G.; Swanson, D. R.; Tomalia, D. A.; Baker, J. R., Jr. *Tapping Mode Atomic Force Microscopy Investigation of Poly(amidoamine) Dendrimers: Effects of Substrate and pH on Dendrimer Deformation,* ***Langmuir*** **2001**, *17*, 2768-2773.

(12) Jones, J. W.; Bryant, W. S.; Bosman, A. W.; Janssen, R. A. J.; Meijer, E. W.; Gibson, H. W. *Crowned Dendrimers: pH-Responsive Pseudorotaxane Formation,* ***Journal of Organic Chemistry*** **2003**, *68*, 2385-2389.

(13) Morara, A. D. *Characterization of a Modified Poly(Propylene Imine) Dendrimer Host System, Louisiana State University, Baton Rouge,* 2005.

(14) Zerbi, G.; Veronelli, M.; Martina, S.; Schlueter, A. D.; Wegner, G. *Delocalization Length and Structure of Oligopyrroles and of Polypyrrole from their Vibrational Spectra,* ***Journal of Chemical Physics*** **1994**, *100*, 978-984.

Chapter 6

Encapsulation of Nile Red by Pyrrole-Terminated Dendrimers

6.1 Introduction

Soon after dendrimers were introduced to the scientific community,[1] researchers pondered about their potential to act as a host for smaller molecular guests. However, seven years went by after their introduction before two independent researchers demonstrated their ability to act as a host to smaller molecular guests.[2,3] Their ability to encapsulate guest molecules leads to an infinite number of uses which is limited only by the imagination of the scientists working with these molecules.

The purpose of these studies is to demonstrate the ability to control the guest-encapsulation and guest-release properties of dendrimers, which may eventually find applications in drug delivery. The guest used in our approach is the hydrophobic dye Nile Red due to its high molar absorptivity and limited solubility in aqueous solutions.[4] The ability of both PAMAM[5] and PPI[6,7] dendrimers to host Nile Red, and the ability of PPI dendrimers to host phenol blue,[8] have previously been demonstrated. More specifically, pyrrole-terminated PPI dendrimers have been proven to be efficient host systems, in which the retention of the guests can be controlled by changing the oxidation state of the terminal pyrrole functionalities.[6,7]

Encapsulation of Nile Red by the pyrrole-terminated dendrimers was conducted with the pyrrole moieties in the monomeric state. Solution conditions were then altered in an effort to increase the retention of the dynamically entrapped guests. Previously encapsulation was conducted in pH 2 HCl in the absence of salt.[6,7,9] The effect of increasing the pH and the addition of sodium chloride were investigated to determine if the system could be converted from a dynamic trapping scheme to that of a static trapping scheme. Additionally, the pyrrole

functional groups were chemically oxidized, forming oligomers along the periphery of the dendrimer in an effort to further reduce guest leakage from the dendrimer core. The effect of pH on these oligomeric dendrimers was studied as well.

6.2 Nile Red

The ability of Nile Red to partition into different regions of dendrimers has already been demonstrated.[5-7] It has also been shown that Nile Red retains its absorption properties even after encapsulation by micelles.[4] Nile Red is an excellent guest for these studies because of its rather large molar absorptivity[4] and its ability to withstand a wide pH range.[10,11] The concentration of Nile Red encapsulated in these studies is limited by the low solubility of the pyrrole-terminated dendrimers in aqueous solutions. To enhance solvation of these dendrimers, the pH of the solution is lowered by adding HCl. Therefore it is essential that the chosen guest remains unaffected in acidic solution. As it turns out, the molar absorptivity of Nile Red remains constant in the presence of acids.[11] Furthermore, the limited solubility of Nile Red ($< 10^{-6}$ M) in aqueous solutions[4] suggests that any absorbance by the guest in solutions containing both Nile Red and dendrimer is the result of guest incarceration by the dendrimer as the guest will be forced to precipitate or partition into the dendritic core upon removal of acetone from the solution.

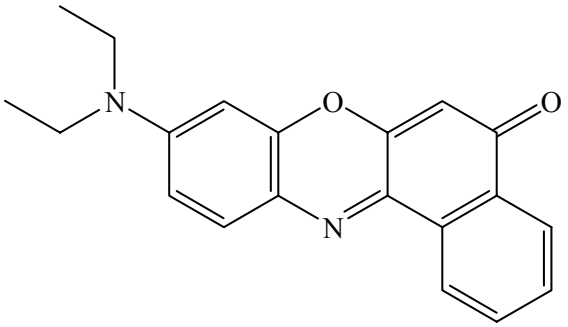

Figure 6.1 The structure of Nile Red used in these encapsulation studies.

Another characteristic of Nile Red that makes it a desirable guest is its absorption properties. The absorption maximum of Nile Red is strongly dependent on the polarity of the solvent used.[11-16] Two different excited states are possible depending on the orientation of the

diethylamine group relative to the ring structure. These excited states have been classified as internal charge transfer (ICT), planar configuration, and twisted-internal charge transfer (TICT), perpendicular configuration.[12] It has been shown that the planar configuration associated with the higher energy ICT is dominant in nonpolar solvents and results in an absorption maximum near 505 nm, while the perpendicular configuration of the TICT is more dominant in polar solvents and displays an absorption maximum near 690 nm.[11] For this reason, Nile Red is an attractive probe, as the absorption spectrum will allow one to determine the relative polarity of the dye's environment. Such information may allow one to conclude the exact location of the dye in the interior of larger molecular hosts.

Visible spectroscopy was used to measure the amount of Nile Red present in solution. Several standards were prepared of known concentration in acetone and the absorption spectra taken for each. The maximum absorption (λ_{max} = 532 nm) was plotted against concentration and the molar absorptivity was calculated to be 30,900 M^{-1} cm^{-1} which is 19% lower than the value reported in the literature. This value was used to determine the number of Nile Red molecules per dendrimer, as the concentration of dendrimer was always known.

6.3 Nile Red Encapsulation

The limited solubility of Nile Red in aqueous environments is exploited in these studies to facilitate guest uptake. Two different methods were used in previous investigations,[6,7] and it was found that a modified approach combining steps from both studies yielded the best results. In both methods, pH 2 HCl was added to solutions containing Nile Red and pyrrole-terminated dendrimers dissolved in acetone; however, the means of removing the acetone layer differed. In one study, in which a tri(ethylene oxide) group was attached to the pyrrole to enhance solubility, the sample was purged with Argon overnight to remove the organic layer and then stirred for

several days to allow the guests to partition inside the dendrimer.[7] It was reported that the intensity of the absorption band increased over time as the guests were slowly taken up into the dendritic cavities. The data from current studies suggested that purging was ineffective in removing all of the acetone. Even after purging for several days, there was still acetone present. A correlation between the stirring time and absorption intensity was never observed. The absorption band associated with Nile Red was quite large after purging the sample, but decreased substantially when the sample was placed under vacuum for a short period of time.

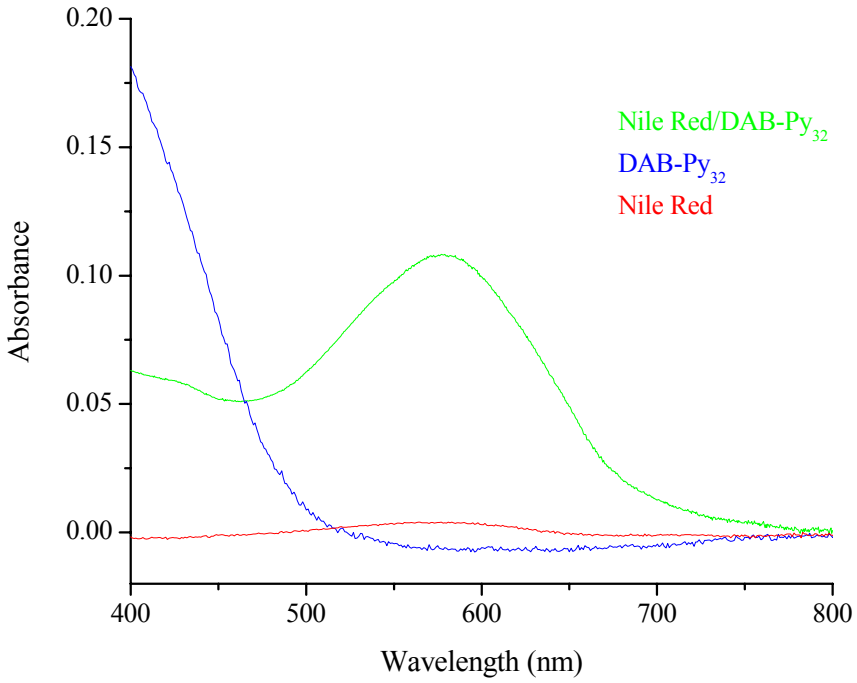

Figure 6.2 Visible absorbance data obtained from Nile Red, DAB-Py_{32}, and Nile Red/DAB-Py_{32} dissolved in pH 2 HCl. The solutions were 10 x 10^{-6} M in dendrimer.

Another approach considered was stirring the solution for an hour after adding the aqueous portion to the Nile Red/dendrimer solution and then removing the organic layer under vacuum.[6] This approach yielded a very low intensity for the Nile Red absorption band and suggested encapsulation was not occurring to a large extent. It was determined that allowing the

solutions to stir for 24 hours prior to removing the organic layers under vacuum provided the best results.

Solutions were prepared with 500 x 10^{-6} M Nile Red and 10 x 10^{-6} MDAB-Py_{32} in acetone. An equal portion of aqueous solution (pH 2, 4, or 7) in which the pH had been adjusted upon addition of HCl or NaOH was then added, and the samples were allowed to stir for 24 hours. The acetone was removed under vacuum, forcing the Nile Red to precipitate or to invade the internal cavities located in the core of the pyrrole-terminated dendrimers. The solutions were then filtered with #1 Whatman paper and diluted to yield an aqueous solution that was 5 x 10^{-6} M in DAB-Py_{32}. Experiments were performed in the presence and absence of dendrimer. As can be seen in Figure 6.2, the absorption band consistent with the solvation of Nile Red in aqueous environments is 28 times more intense in the presence of DAB-Py_{32} than in the absence of DAB-Py_{32}, suggesting that Nile Red is indeed incarcerated by the dendrimer. While the λ_{max} of Nile Red in the presence of DAB-Py_{32} is indicative of a polar environment comparable to that of water, the increase in absorbance when dendrimer is present, suggests encapsulation is occurring.

6.4 Salt and pH Effects

In previous studies, it was also found that Nile Red was not encapsulated by the dendrimers at higher pH. All of the encapsulation studies with these pyrrole-terminated dendrimers have taken place in pH 2 HCl.[6,7] Attempts to encapsulate at pH 7 were reported to be unsuccessful. It has been reported in the literature that the conformation of the dendritic branches of PPI dendrimers can be changed by altering solution conditions such as pH and ionic strength.[17-19]

Small-angle neutron scattering (SANS)[17] and diffusion-ordered spectroscopy (DOSY)[18] studies revealed a distinct change in dendritic structure as a function of solution pH. The results

of these investigations depicted dendrimer structures with a dense shell at lower pH and and a dense core at higher pH. Welch's Monte Carlo simulations predicted dendrimer conformations with a dense shell in the absence of salt and a dense core in the presence of salt.[19] The dense core conformation is the result of end groups backfolding into the interior of the dendrimer. It is believed that this backfolding may be the reason the guests are unable to penetrate the internal cavities of the pyrrole-terminated dendrimers. One would believe that these structural changes would alter the encapsulation/release properties of the dendritic hosts.

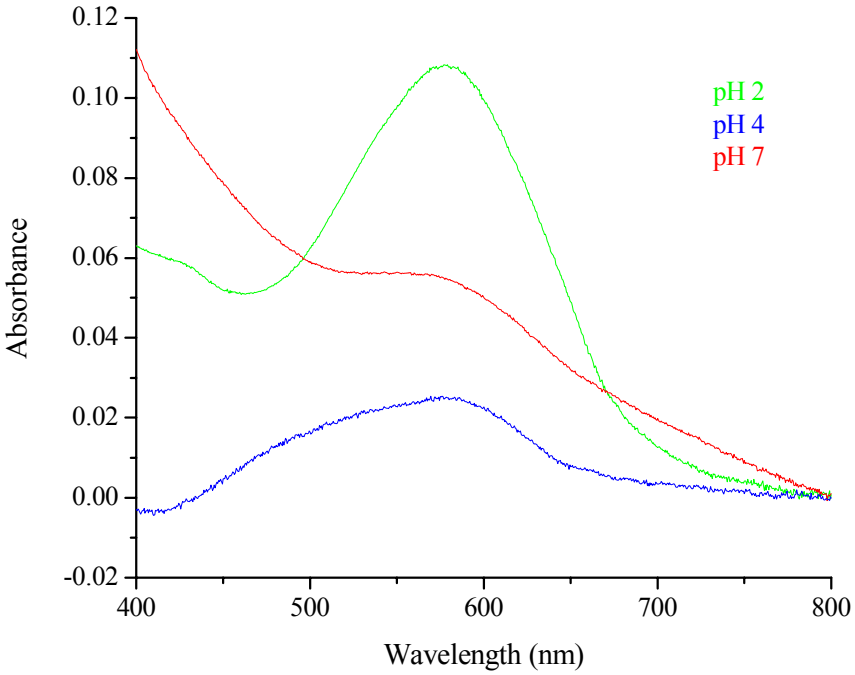

Figure 6.3 Encapsulation of Nile Red into DAB-Py_{32} at pH 2, 4, and 7. Acetone solutions were prepared with a DAB-Py_{32} concentration of 10 x 10^{-6} M and a Nile Red concentration of 500 x 10^{-6} M. An equal volume of pH 2, 4, and 7 aqueous solution was added and the acetone was removed yielding aqueous solutions with a concentration of 10 x 10^{-6} M in DAB-Py_{32}.

Attempts to encapsulate Nile Red into the core of DAB-Py_{32} at pH 4 and pH 7 have also been fruitless. While encapsulation does occur, the number of guests incarcerated by the dendrimer is only a fraction of the number that is encapsulated at pH 2. It is clear that increasing

the pH causes a significant change in the structure of the dendrimer, thereby blocking access to the interior cavities. The question then arose as to what effect these structural changes would have if the pH was altered after encapsulation is achieved at pH 2. If the branches are indeed backfolding into the interior of the dendrimer as predicted by the literature,[17-19] increasing the pH may force the guests out of the dendritic cavities. However, it is also possible that the branches are simply collapsing and remain along the outer regions of the dendrimer thereby blocking the entrance into the interior regions. If this is the scenario, increasing the pH may prove to be a useful means of trapping the guests inside and preventing premature leakage.

6.4.1 Encapsulation at pH 4, pH 7 and in the Presence of NaCl

Incarceration of Nile Red by DAB-Py_{32} was achieved in pH 2 HCl as described previously. Alter filtration was complete; four equal portions of the sample were transferred to separate flasks labeled pH 2, pH 4, pH 7 and NaCl. The sample transferred to the pH 2 flask was diluted with pH 2 HCl to yield a final concentration of 5 x 10^{-6} M DAB-Py_{32}. 1M NaOH was then added dropwise to flasks 2 and 3 until the pH was 4 and 7 respectively. The volume was increased with pH 4 HCl (flask 2) and pH 7 (flask 3) aqueous solutions to yield the desired dendrimer concentration (5 x 10^{-}6 M). An equal volume of 0.02 M NaCl was added to the fourth flask resulting in a solution that was 5 x 10^{-6} M in dendrimer and 0.01 M in NaCl. UV/Vis spectra were obtained for each sample using an aqueous sample with the same pH or ionic strength as the background.

As is seen in Figure 6.4, increasing the pH or adding salt did not cause the dendrimer to immediately expel the Nile Red guests. Initially the absorbance was not measured as a function of time. The purpose here was simply to demonstrate if an increase in pH or addition of salt would result in an immediate release of guests, as this was a possibility if the end groups are

backfolded into the dendrimer cavities. However, the absorption intensity was as large as and sometimes larger than that of the original pH 2 solution suggesting the pyrrole end groups were not displacing the trapped guests. Using the molar absorptivity value previously determined and the absorption intensity immediately after removing the acetone, it was found that there were 0.37, 0.39, and 0.38 Nile Red molecules for every dendrimer when the pH was 2, 4, and 7 respectfully. Immediately after the addition of salt there were 0.36 Nile Red molecules for every 1 dendrimer.

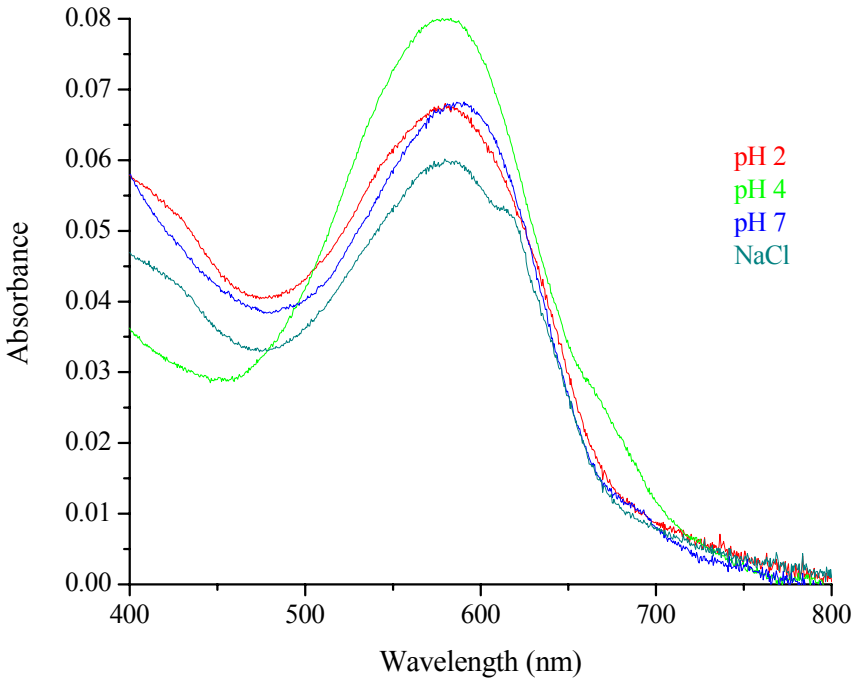

Figure 6.4 Visible absorption spectra before and after the pH was adjusted and upon addition of NaCl. The concentration of DAB-Py_{32} was 5 x 10^{-6} M in each case.

6.4.2 Release of Nile Red as a Function of pH and Ionic Strength

An important aspect of this research project is the ability to control the release of the guests from the dendrimer core. Therefore once encapsulation is achieved, it is necessary to monitor the retainment of the guests and quantify the number of guests remaining entrapped by

the dendrimer. In order to accomplish this task, dialysis was used to eliminate any released guest molecules from the bulk sample. The dendrimers and their encapsulated guests were transferred to dialysis membranes possessing a molecular weight cut off of 6,000-8,000 daltons. This relatively large pore size should facilitate the quick removal of any free guests in the solution, and concurrently prevent the dendrimers from diffusing into the dialysate. A 5 mL sample of the dendrimer solutions was taken prior to dialysis and a 5 mL sample was taken from the retentate every 2 hours after dialysis was initiated. The ratio of dialysate to retentate was held constant at 30:1 to help reduce any diffusion effects. Inconsistencies in the retentate/dialysate ratio would lead to varying concentration gradients. A greater concentration gradient would be present for samples analyzed after long dialysis periods and would favor a faster release rate of the Nile Red. Sustaining a constant dialysate/retentate ratio should eliminate any diffusion effects. Dialysis was also conducted in the absence of light to prevent photodegredation of Nile Red.

In Section 6.4 it was observed that Nile Red was unable to penetrate the dendrimer core at pH values above 2. The ability of the dendrimers to retain encapsulated guests after increasing the pH was not investigated and seemed promising. If the branches of the dendrimer would backfold inside the dendrimer and displace the Nile Red guests, one would expect to see the absorbance intensity decrease quickly. If the outer branches simply collapsed and remained along the periphery of the dendrimer, one may propose that the guests would be prevented from escaping. Due to previous 2D NMR studies discussed in Chapter 5, it was believed that the second scenario was more likely to occur.

As anticipated, it was observed that the dendrimers possessed greater retainment efficiency at higher pH. As can be seen in Figure 6.6, the percentage of guests remaining entrapped inside the dendrimer over time was always larger for higher pH values. After 8 hours,

only 38% of the guests remained encapsulated at pH 2 while 43% and 58% of the guests remainined at pH 4 and pH 7 respectively. Another interesting observation was that only 26% of the guests encapsulated in the presence of salt were present after 4 hours. After 6 hours, there was no detectable amount of Nile Red remaining in the dendrimer/salt solution. It was estimated that after 8 hours, there was 1 Nile Red molecule for every 7, 6, and 5 dendrimers at pH 2, 4, and 7 respectively. Interestingly after 4 hours, there was only 1 Nile Red molecule for every 12 dendrimers when salt was present.

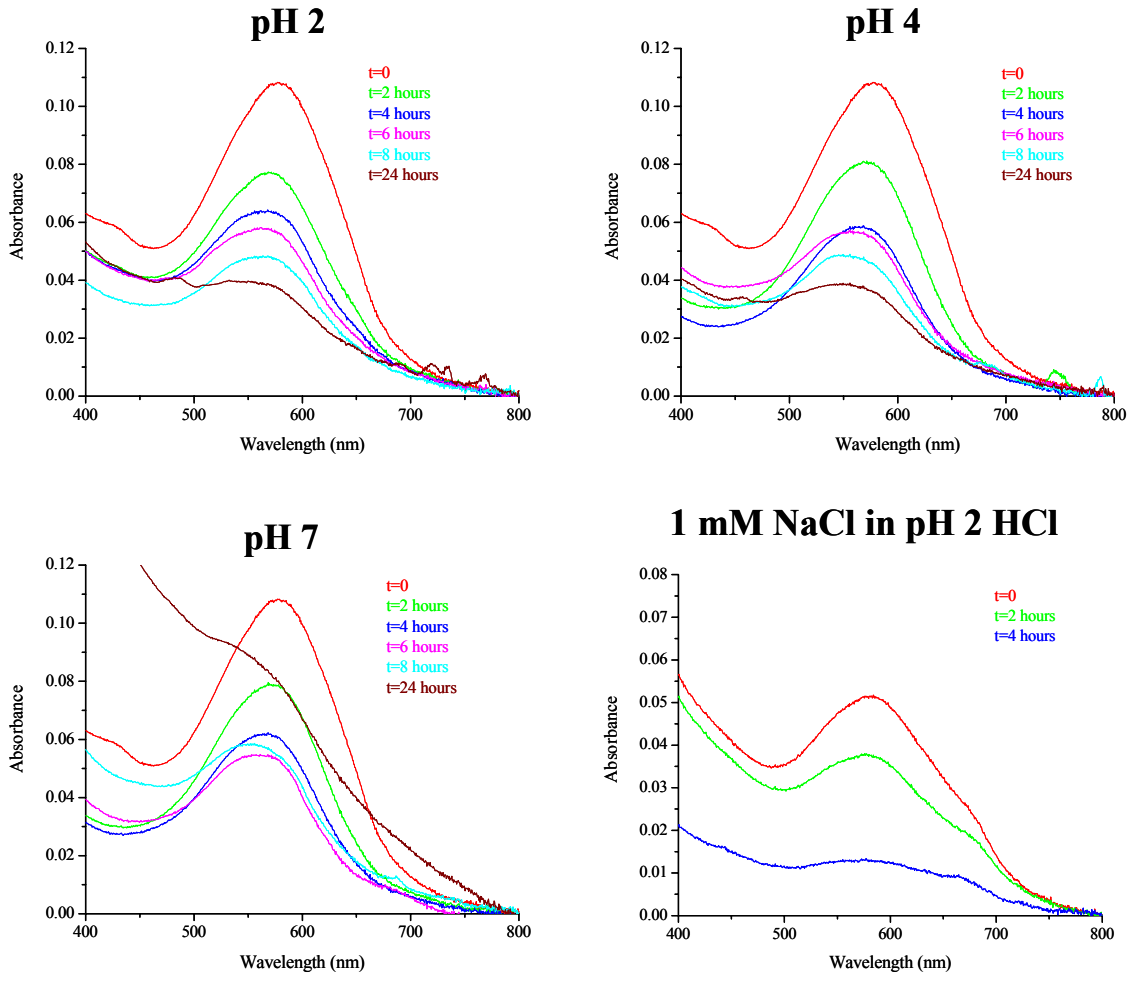

Figure 6.5 The absorbance spectra of encapsulated Nile Red as a function of dialysis time at pH 2, 4, and 7 and in 1 x 10^{-3} M NaCl with a DAB-Py_{32} concentration of 10 x 10^{-6} M for all solutions.

So while others have suggested an increase in pH and the addition of salt would have similar effects on the overall structure,[17-19] it is evident that the encapsulation properties are immensely different. The data shown here suggest the pyrrole moieties do not displace the encapsulated Nile Red guests at higher pH. Instead, the branches simply collapse about the periphery preventing guest uptake by the dendrimer and retarding the escape of guests located in the internal cavities. Adding salt to the system results in a much faster release rate of incarcerated guests. The data supports the dense core conformation predicted by Welch's Monte Carlo simulations[19] in which the dendrimer end groups backfold into the interior of the dendrimer in the presence of salt displacing any trapped guests.

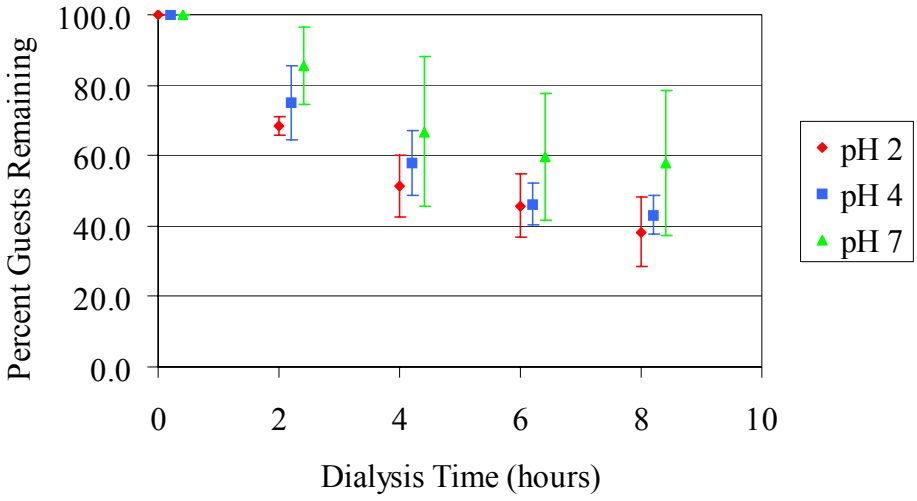

Figure 6.6 The percentage of guests remaining as a function of dialysis time at different pH.

6.4.3 Retention of Guests by Oligo-Pyrrole-Terminated Dendrimers

As discussed in Chapter 5, the length of the pyrrole oligomers formed upon chemical oxidation of pyrroles attached to the dendrimer periphery is dependent on the pH of the solution. It was observed that longer oligomers were formed when the pH was increased. It has also been

reported that the oligo-pyrrole-terminated dendrimers are better suited for retaining entrapped guests than dendrimers whose terminal groups were in the monomeric form.[6] Once the oxidized, oligomeric periphery was reduced, it was found that the guests were expelled from the core at a much higher rate. These studies were conducted at pH 2 and correlated well with modeling studies that predicted a larger internal cavity volume in the oxidized state and a smaller volume in the reduced state.[6] It was believed that the longer oligomers formed at higher pH would be even more efficient in retaining the trapped guests when the oligomers are in the oxidized state. At the same time, reducing the longer oligomers may have a much greater effect on the cavity volume expelling the guests at a higher rate.

Prior to oligomerizing the periphery of DAB-Py_{32}, Nile Red was once again encapsulated at pH 2. DAB-Py_{32} was dissolved in acetone and added to 100 mL of 500 x 10^{-6} M Nile Red solution in acetone. To this solution 50 mL of pH 2 HCl was added and allowed to stir on the benchtop overnight. The acetone and ~15 mL of water were removed under vacuum and the sample was filtered with #1 Whatman paper. The volume was increased to 50 mL by dilution with pH 2 HCl. A 20 mL portion was transferred to a flask labeled monomeric and then diluted with an equal portion of pH 2 HCl. $Fe(NO_3)_3 \cdot 9H_2O$ was then dissolved in 20 mL of pH 2 HCl and added to the remaining solution (10:1 Fe:Py). After 30 minutes the sample was divided into two 25 mL portions. One sample was transferred to a flask labeled oxidized to which 5 mL pH 2 HCl was added. The final portion was reduced with 95 mg of ascorbic acid (28:1 AA:Py), which was dissolved in 5 mL of pH 2 HCl. The resulting 3 solutions contained dendrimers with monomeric, oxidized, and reduced pyrrole peripheries, each of which had a dendrimer concentration of 5 x 10^{-6} M. The same procedure was repeated at each pH with the exception of a single step. After removing ~15 mL of water under vacuum the pH was increased by dropwise

addition of 1M NaOH until the desired pH was reached. The remaining steps were kept the same with the exceptions that iron nitrate and ascorbic acid were dissolved in solutions with the desired pH.

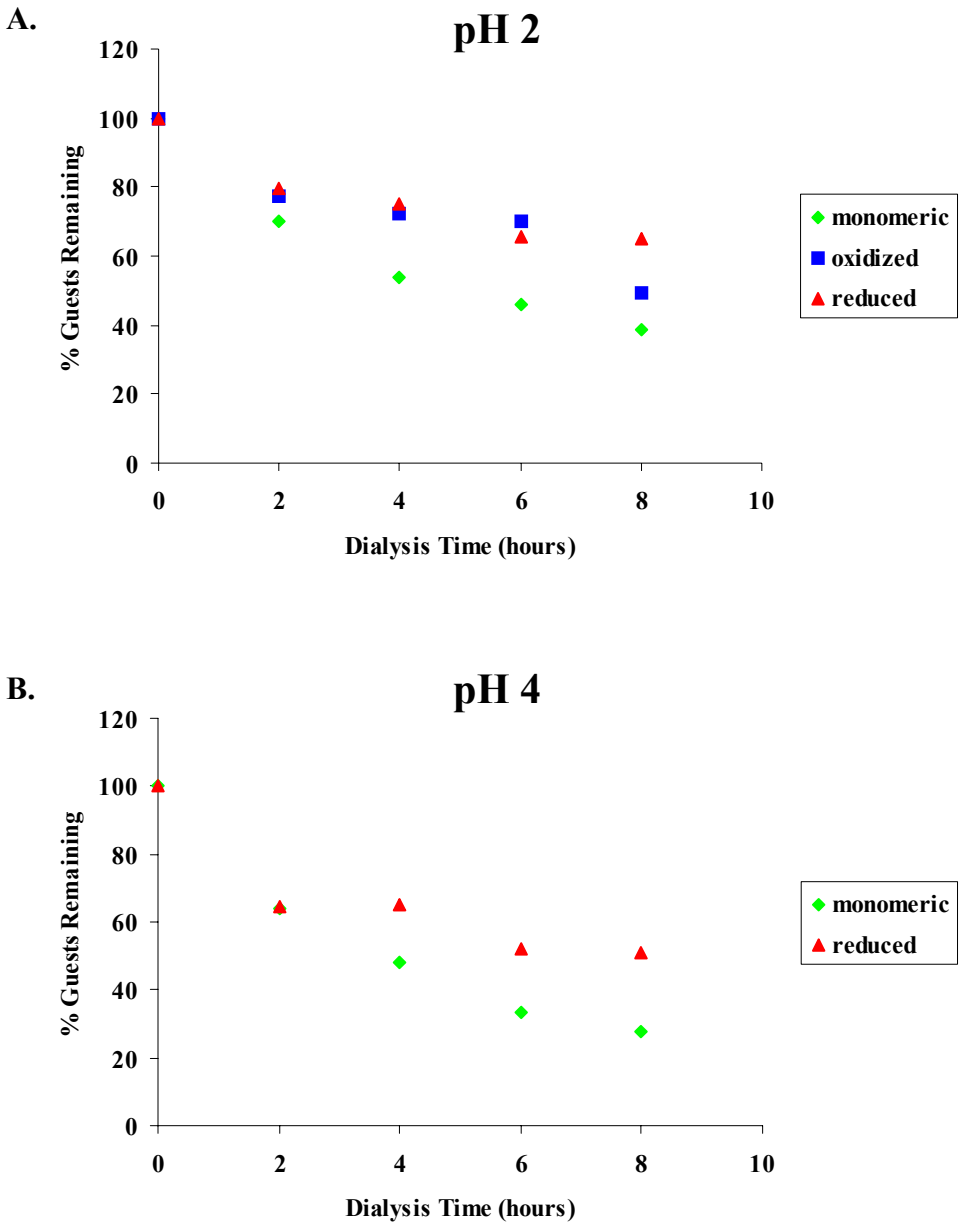

Figure 6.7 Monitoring the release of Nile Red in pH 2 (A) and pH 4 (B) HCl from DAB-Py_{32} with a monomeric, oxidized, and reduced periphery.

Previous encapsulation studies were repeated multiple times making it possible to calculate the average number of encapsulated Nile Red as a function of dialysis time and the average percentage of Nile Red remaining trapped by DAB-Py_{32}. The oligomerization studies were also repeated several times. However, great difficulty in obtaining clean spectra was had. In a large portion of the spectra a large increase in the baseline towards lower wavenumbers was present. It is believed that this is due to aggregation of the oligo(pyrrole)-terminated dendrimer or inter-dendrimer coupling as a result of the oligomerization. Because the dendrimer concentrations were extremely low, it is unlikely that inter-dendrimer coupling is the culprit. Instead, the increase in the baseline intensity is attributed to the scattering of UV light by aggregated dendrimers. Therefore, a single data set whose baseline was least affected by the UV scattering effect was chosen to represent the encapsulation properties at each pH. Therefore the uncertainty in the data presented in Figure 6.7 is unknown.

Previous encapsulation studies with this dendrimer revealed greater retention efficiency when the oligo-pyrroles were in the oxidized state and a faster release rate when the oligo-pyrroles were reduced.[6] However, these studies were only conducted at pH 2. One of the goals of this work was to determine the retainment efficiency for the different redox states at higer pH. For these studies, absorbance readings were only able to be acquired when oligomers were in the oxidized state at pH 2. At pH 4 and pH 7 an initial reading was made, but within 2 hours of the initial reading the solutions turned bright yellow and the absorbance measurements were too high to be measured. Further analysis of $Fe(NO_3)_3 \cdot 9H_2O$ solutions at pH 4 and 7 revealed a similar absorption after sitting on the bench top for 2 hours. Therefore this increase in intensity is attributed to the presence of $Fe(NO_3)_3$ rather than changes in the structure of the dendrimer. It has been observed that Fe^{3+} results in several absorption bands while Fe^{2+} possesses no

absorption characteristics.[20] In acidic solutions Fe^{2+} is the more dominant species which explains the ability to make absorbance measurements for Nile Red at pH 2. At higher pH however, the Fe^{3+} species is more dominant, often times resulting in absorption bands near 300 nm which have been assigned to $FeOH^{2+}$. This scenario is also supported by the results presented here. Data was obtained at higher pH when reducing agent was present, as any Fe^{3+} present will be reduced to Fe^{2+}.[20] Therefore the increase in absorbance observed in these studies at lower wavelengths is attributed to the hydrolysis of Fe^{3+}.

According to the data collected at pH 2, the presence of both oxidized and reduced pyrrole moieties along the periphery of the dendrimer hindered the release of Nile Red. However, interestingly there was no vast difference in the data between the oxidized and reduced states. The data for the reduced pyrrole oligomers was extremely similar to that of the pyrroles in the oxidized state. In these studies a rapid expelling of the guests was not observed when the pyrroles were reduced. In fact it was determined that the reduced periphery was more efficient in preventing the guests from escaping than the monomeric periphery. After dialysis was conducted for 8 hours the dendrimer was able to retain 65%, 49%, and 38% of the original encapsulated guests when the periphery was in the oxidized, reduced, and monomeric state respectively. This discrepancy with previous results may be due to the differences in reduction and dialysis. Previously the oxidized oligomers were reduced by conducting dialysis in methanol.[6] These results were compared to that of the oligo-pyrrole-terminated dendrimer remaining oxidized in which dialysis was conducted in pH 2 HCl. While the solubility of Nile Red in aqueous solutions is reported to be less than 0.12×10^{-6} M, the solubility of Nile Red in methanol is greater than 1×10^{-3} M.[21] Therefore, what appeared to be a quick release of Nile

Red by the reduced-dendrimer could simply be the result of the Nile Red partitioning to a more favorable environment rather than a change in the oligo-pyrrole redox state.

Oligomerization of the dendrimer periphery at pH 4 proved to be effective in retaining its encapsulated guests as well. While obtaining absorbance data of the oxidized pyrroles was unsuccessful, we were able to observe the retainment properties in the reduced state. Once again it was determined that the oligomeric periphery in the reduced state was more effective in retaining the guest molecules. After 8 hours of dialysis the oligomeric periphery retained over 51% of the original guests encapsulated while less than 28% remained trapped in the dendrimer possessing a monomeric periphery. While these numbers seem to be extremely different, it is important to mention that there was only 1 Nile Red molecule remaining for every 8 dendrimer molecules in the reduced state, and 1 guest for every 12 dendrimers with a monomeric periphery.

Analysis of the pH 7 data suggests oligomerization had very little effect on the retainment properties of the dendrimer host. When the percentages of guests remaining encapsulated are considered, it appears as though the reduced periphery is much more efficient in preventing leakage of the guests. When the actual numbers of guests are taken into account, there is very little difference between the monomeric and oligomeric periphery. Initially the monomeric dendrimer possessed slightly more guest molecules in its internal cavities than the oligomeric dendrimer. After only 4 hours of dialysis, the numbers of encapsulated guests were very similar. While the percentage of guests remaining entrapped by the dendrimer may be significantly different, there is little difference in the number of guest molecules remaining incarcerated.

6.5 Conclusions

After completing these studies, it is evident that the encapsulation properties of PPI dendrimers can be tuned by altering the solution conditions. It has been shown that the retention

efficiency of the dendrimer hosts can be increased by raising the pH. It was also observed that the guests were quickly expelled from the dendrimer core upon addition of NaCl to the solutions. Another route that can be taken to increase the holding efficiency of the dendrimers is to oligomerize the pyrrole end groups. The data suggests that at pH 2 and 4 the oligomeric periphery was better suited for trapping the guests and reducing leakage than the monomeric periphery. At pH 7 the encapsulation properties of both oligo(pyrrole)-terminated dendrimers and pyrrole-terminated dendrimers were essentially the same. Unlike previous studies, no difference was observed in the incarceration properties of dendrimers whose periphery are in the oxidized and reduced states. However, this is likely due to the differences in dialysis as discussed in Section 6.4.3 above. In the previous studies, dialysis was conducted in methanol in which the Nile Red guest is highly soluble in. It is likely that the guest molecules exited the dendrimer due to their preference of being solvated by methanol than the dendrimer host. Therefore, differences in the release rates were due to changes in solvent rather than changes in redox states. The results of these studies suggest there is little difference in the trapping effectiveness between both redox states at pH 2. We observed that guest retention was increased at each pH by oligomerizing the pyrrole periphery. Another surprising observation was that the shorter pyrrole oligomers formed at pH 2 were able to retain the Nile Red guests for a longer period of time than the longer oligomers formed at pH 4 and 7.

Interpretation of the data becomes more difficult when trying to compare all scenarios investigated. When completing the oligomerization studies, it was apparent that coupling the pyrrole monomers increased guest retention at each pH. However, when all of the studies are taken into consideration, the oligomerized dendrimer at pH 7 expelled the guests more quickly than the oligomers at lower pH and the dendrimers with a monomeric pyrrole periphery.

Another interesting observation was the monomeric dendrimer at pH 7 was the most efficient at retaining the encapsulated guests of all systems studied.

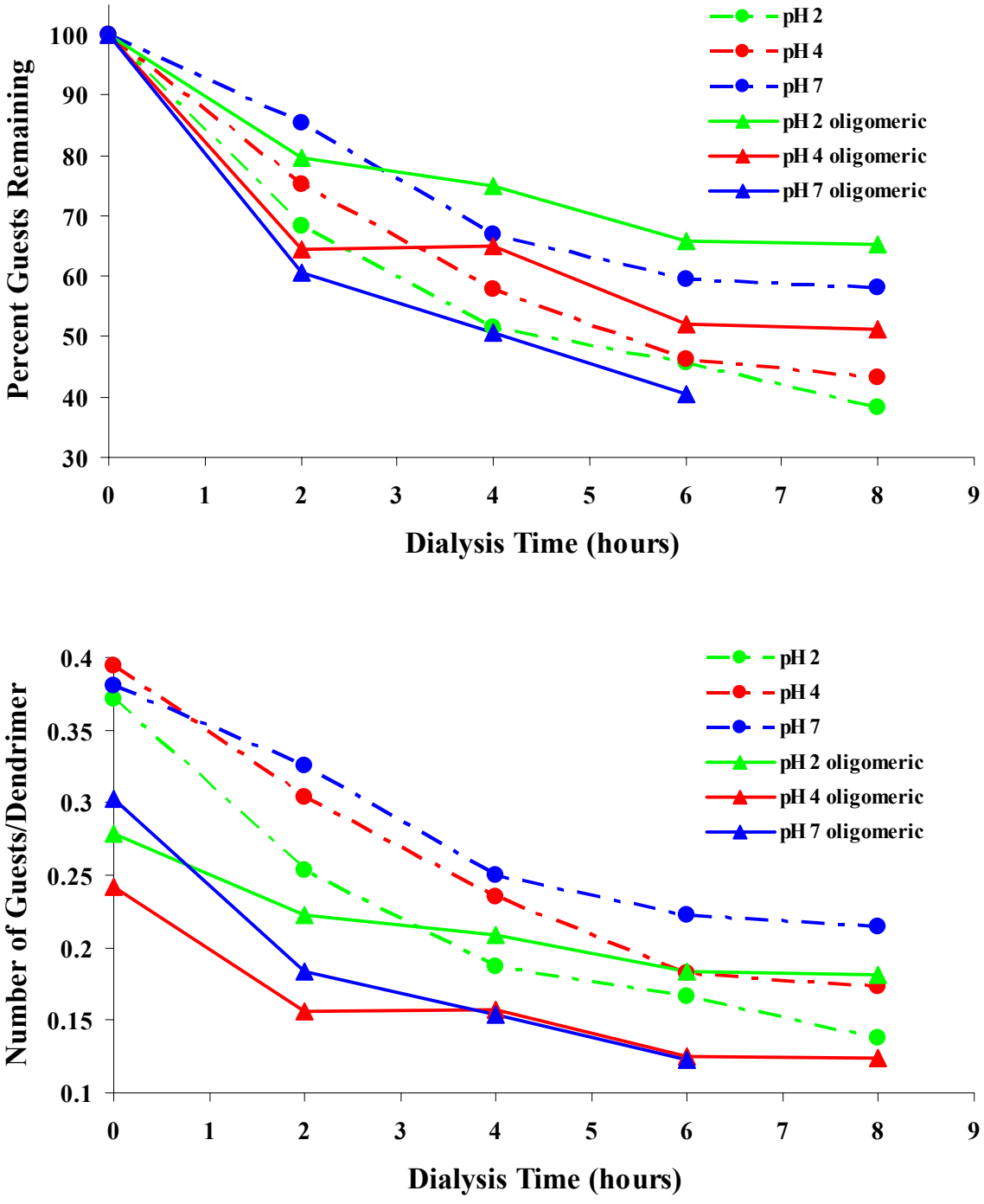

Figure 6.8 Graphic illustrating the encapsulation efficiency of DAB-Py_{32} with a periphery consisting of monomeric pyrrole at pH 2, 4, and 7 and oligo-pyrrole at pH 2, 4, and 7.

6.6 References

(1) Buhleier, E.; Wehner, W.; Vogtle, F. *"Cascade"- and "Nonskid-Chain-Like" Syntheses of Molecular Cavity Topologies,* ***Synthesis*** **1978**, 155-158.

(2) Tomalia, D. A.; Baker, H.; Dewald, J.; Hall, M.; Kallos, G.; Martin, S.; Roeck, J.; Ryder, J.; Smith, P. *A New Class of Polymers: Starburst-Dendritic Macromolecules,* ***Polymer Journal (Tokyo, Japan)*** **1985**, *17*, 117-132.

(3) Newkome, G. R.; Yao, Z.; Baker, G. R.; Gupta, V. K. *Micelles. Part 1. Cascade Molecules: A New Approach to Micelles. A [27]-Arborol,* ***Journal of Organic Chemistry*** **1985**, *50*, 2003-2004.

(4) Chen, G.; Guan, Z. *Transition Metal-Catalyzed One-Pot Synthesis of Water-Soluble Dendritic Molecular Nanocarriers,* ***Journal of the American Chemical Society*** **2004**, *126*, 2662-2663.

(5) Watkins, D. M.; Sayed-Sweet, Y.; Klimash, J. W.; Turro, N. J.; Tomalia, D. A. *Dendrimers with Hydrophobic Cores and the Formation of Supramolecular Dendrimer-Surfactant Assemblies,* ***Langmuir*** **1997**, *13*, 3136-3141.

(6) Noble IV, C. O. *Pyrrole-Terminated Dendrimers for Use in Polymerizable Monolayers and Guest Encapsulation Systems, Louisiana State University, Baton Rouge,* 2001.

(7) Morara, A. D. *Characterization of a Modified Poly(Propylene Imine) Dendrimer Host System, Louisiana State University, Baton Rouge,* 2005.

(8) Richter-Egger, D. L.; Tesfai, A.; Tucker, S. A. *Spectroscopic Investigations of Poly(Propyleneimine) Dendrimers Using the Solvatochromic Probe Phenol Blue and Comparisons to Poly(Amidoamine) Dendrimers,* ***Analytical Chemistry*** **2001**, *73*, 5743-5751.

(9) Morara, A. D.; McCarley, R. L. *Encapsulation of Neutral Guests by Tri(ethylene oxide)-pyrrole-Terminated Dendrimer Hosts in Water,* ***Organic Letters*** **2006**, *8*, 1999-2002.

(10) Davis, M. M.; Hetzer, H. B. *Titrimetric and Equilibrium Studies Using Indicators Related to Nile Blue A,* ***Anal. Chem.*** **1966**, *38*, 451-461.

(11) Deye, J. F.; Berger, T. A.; Anderson, A. G. *Nile Red as a Solvatochromic Dye for Measuring Solvent Strength in Normal Liquids and Mixtures of Normal Liquids with Supercritical and Near Critical Fluids,* ***Analytical Chemistry*** **1990**, *62*, 615-622.

(12) Rettig, W. *Charge Separation in Excited States of Decoupled Systems: Twisted Intramolecular Charge Transfer (TICT) Compounds and Implications for the Development of New Laser Dyes and for the Primary Process of Vision and Photosynthesis,* ***Angewandte Chemie*** **1986**, *98*, 969-986.

(13) Sarkar, N.; Das, K.; Nath, D. N.; Bhattacharyya, K. *Twisted Charge Transfer Processes of Nile Red in Homogeneous Solutions and in Faujasite Zeolite,* ***Langmuir*** **1994**, *10*, 326-329.

(14) Dutta, A. K.; Kamada, K.; Ohta, K. *Spectroscopic Studies of Nile Red in Organic Solvents and Polymers,* ***Journal of Photochemistry and Photobiology, A: Chemistry*** **1996**, *93*, 57-64.

(15) Golini, C. M.; Williams, B. W.; Foresman, J. B. *Further Solvatochromic, Thermochromic, and Theoretical Studies on Nile Red,* ***Journal of Fluorescence*** **1998**, *8*, 395-404.

(16) Hou, Y.; Bardo, A. M.; Martinez, C.; Higgins, D. A. *Characterization of Molecular Scale Environments in Polymer Films by Single Molecule Spectroscopy,* ***Journal of Physical Chemistry B*** **2000**, *104*, 212-219.

(17) Briber, R. M.; Bauer, B. J.; Hammouda, B.; Tomalia, D. A. *Small-Angle Neutron Scattering from Solutions of Dendrimer Molecules: Intermolecular Interactions,* ***Polymeric Materials Science and Engineering*** **1992**, *67*, 430-431.

(18) Young, J. K.; Baker, G. R.; Newkome, G. R.; Morris, K. F.; Johnson, C. S., Jr. *"Smart" Cascade Polymers. Modular Syntheses of Four-Directional Dendritic Macromolecules with Acidic, Neutral, or Basic Terminal Groups and the Effect of pH Changes on Their Hydrodynamic Radii,* ***Macromolecules*** **1994**, *27*, 3464-3471.

(19) Welch, P.; Muthukumar, M. *Tuning the Density Profile of Dendritic Polyelectrolytes,* ***Macromolecules*** **1998**, *31*, 5892-5897.

(20) Bongiovanni, R.; Pelizzetti, E.; Borgarello, E.; Meisel, D. *On the formation of iron (III) oxides via oxidation of iron (II),* ***Chimica e l'Industria (Milan)*** **1994**, *76*, 261-266.

(21) Koti, A. S. R.; Periasamy, N. *TRANES analysis of the fluorescence of nile red in organized molecular assemblies confirms emission from two species,* ***Proceedings - Indian Academy of Sciences, Chemical Sciences*** **2001**, *113*, 157-163.

Chapter 7

Conclusions and Future Studies

7.1 Introduction

Amine-terminated PPI dendrimers were modified with ferrocene, BOC, and pyrrole end-groups. H-bonding interactions were monitored with FTIR for BOC- and ferrocene-terminated dendrimers in an effort to gain an understanding as to the proximity of the end groups with respect to one another. The degree of intra-dendrimer H-bonding was strongly dependent upon dendrimer generation. Further, these dendrimers were used to study the binding mechanism to gold surfaces by adsorbing both fully functionalized dendrimers and amine-terminated dendrimers. Amine-terminated dendrimers were further modified with ferrocene after adsorption. The surface reaction was monitored using cyclic voltammetry and RAIRS.

Several studies suggest the end groups of PPI dendrimers are located along the periphery of the dendrimer. While these studies are not definitive, no data was acquired which suggests that backfolding is occurring. It has also been shown here that the structure of pyrrole-terminated PPI dendrimers can be altered by changing solution conditions. Determination of T_1 ^{1}H NMR relaxation data lead to the conclusion that the relative rigidity of the dendrimers, more specifically their end groups, could be manipulated by changing the pH of the solution in which they are dissolved. The length of the pyrrole oligomers formed through chemical oxidation of pyrrole-terminated dendrimers was also dependent upon the solution pH. This work demonstrates that while the chemical makeup of the dendrimers remains the same, the encapsulation properties of both pyrrole-terminated dendrimers and oligo-pyrrole-terminated dendrimers vary upon changing solution conditions.

7.2 Summary of Results

PPI dendrimers were modified with ferrocene and BOC terminal groups to study end-group location and the binding mechanism of dendrimers to gold surfaces. A common method used to measure H-bonding interactions in proteins[1] with FTIR spectroscopy was used to monitor the degree of H-bonding of dendrimers both in solution and adsorbed to surfaces. These studies revealed stronger H-bonding interactions for higher generation dendrimers. An increase in H-bonding was interpreted as a decrease in the proximity of the peripheral functional groups. Therefore, it was shown that the end groups of PPI dendrimers become forced in closer proximity as generation increases.

Both the ferrocene and BOC functionalities used in these studies do not independently adsorb to gold surfaces. However, completely modified BOC- and ferrocene-terminated dendrimers did adsorb quite well to gold substrates. Because the dendrimers were modified with end groups that do not independently adsorb to the surfaces, it was concluded that adsorption of these dendrimers occurred through the tertiary amines. Previous studies have included dendrimers possessing primary amines along the periphery[2] or functional groups that direct adsorption.[3-5] While it has been reported that the primary amines of PAMAM dendrimers direct adsorption,[6] this work demonstrates that a significant portion of the primary amines of PPI dendrimers are available for functionalization even after adsorption. Complete modification of DAB-Am_{16}/Au was not achieved which suggests it is possible for the primary amines of amine-terminated dendrimers to be involved in the adsorption process. Dendrimers whose periphery has been functionalized adsorb via the internal tertiary amines. Adsorption of dendrimers possessing amine functional groups may occur through the primary amines, the tertiary amines,

or a combination of both. However, it has been shown that some primary amines are readily available for functionalization.

The H-bonding studies also suggest the location of the terminal functional groups are along the periphery of the dendrimer. It is believed that the degree of H-bonding would be much less affected by dendrimer generation if these end groups were backfolded into the interior of the dendrimer. 2D NMR studies were conducted to further explore this scenario. After acquiring NOESY and ROESY data in both organic and aqueous solvents, there was no definitive evidence that the end groups are located in the interior regions of the dendrimer. If a portion of the functional groups are backfolded into the interior of the dendrimer, one would expect to observe cross-peaks in the NOESY and ROESY data between pyrrole protons and methylene protons located throughout the interior of the dendrimer. No such evidence was observed. The only crosspeaks observed in which the pyrrole protons were involved, were between the pyrrole protons and methylene protons located on the linker through which the pyrrole is attached to the dendrimer. So while there is no definitive evidence that the end groups are located solely along the periphery of the dendrimer, as a result of these findings it is believed that it is highly unlikely that a significant portion of functional groups are backfolded into the interior of the dendrimer.

Proton NMR T_1 relaxation experiments were conducted on all 5 generations of pyrrole-terminated dendrimers under a range of solution conditions. Data were collected in organic and aqueous solvents at several temperatures. As a result of the temperature studies, it was determined that protons located in the interior of the dendrimer (within the amide bond) demonstrated large molecule behavior, while protons located along the periphery of the dendrimer (beyond the amide linkage) exhibited small molecule behavior. It was then possible to deduce that the periphery of pyrrole-terminated PPI dendrimers becomes more rigid as the

generation increases, as shorter T_1 values were obtained for higher generations. Mobility also increases from the core of the dendrimer outward towards the periphery as relaxation times were much shorter for protons located in the interior regions of the dendrimer when compared to protons near the periphery.

After initial temperature studies on DAB-Py_{32} in aqueous solutions with a pD of 2, it was believed that the dendrimer periphery was more characteristic of a small molecule. However, after conducting temperature studies at higher pD, it became difficult to determine whether the molecules possessed small or large molecule behavior as there were no consistent trends in the T_1 times as a function of temperature. It is believed that this is attributed to the fact that the end groups are located in multiple environments. The 2D NMR studies revealed the pyrrole protons were in close proximity to several protons on the hexyl linker. Also at higher pD values, shoulders were observed for the peaks associated with pyrrole protons in the NMR spectra. Results from T_2 data acquired also supported the theory that the end groups were located in multiple environments. Initially with shorter *tau* values, single peaks were observed for pyrrole protons. However, at longer *tau* values after the transverse magnetization was allowed to dephase, it became apparent that there were multiple, different pyrrole protons. As the peak height decreased, the single broad peak gave rise to several more narrow peaks. Therefore, it is clear the pyrrole functional groups are located in multiple environments. It is believed that a significant number of the end groups are somewhat backfolded into the outer regions of the dendrimer.

Despite the fact that definitive conclusions were not drawn from some of the T_1 data, it was apparent that changing the pD had a significant effect on the dendrimer structure. Oligomerization of the pyrroles along the dendrimer periphery was then conducted at different

pH. RAIRS results showed that smaller oligomers were formed at lower pH, and longer oligomers were formed at higher pH. By comparing key bands in the spectra,[7] it was estimated that pyrrole trimers were formed at pH 2 and oligomers containing up to 7 pyrrole units were formed at pH 7. While it was extremely difficult to pinpoint the exact length of the oligomers, it was obvious that longer oligomers were formed as the pH was increased.

The relaxation time studies and oligomerization studies opened the door for numerous encapsulation scenarios. First, the effect of changing the pH was investigated for encapsulating Nile Red while the pyrroles were in the monomeric state. A higher percentage of guests were trapped at lower pH values. Therefore, encapsulation was always conducted at pH 2. The inability to encapsulate as many guests at pH 4 and pH 7 suggested either the end groups were backfolded into the interior of the dendrimer or the end groups are collapsed blocking access to the interior cavities. Therefore the effect of raising the pH after encapsulation was investigated. If the end groups backfold into the interior once the pH is increased, one would expect to see a quick release of the guests as the pyrrole functionalities displace the trapped guests. If the branches are simply collapsing along the outer regions of the dendrimer, one would expect to see an increase in retainment upon increasing the pH.

It was observed that a larger percentage of Nile Red remained incarcerated by the dendrimer when the pH was increased after encapsulation. This finding suggests the end groups are simply in a collapsed form rather than backfolded into the interior of the dendrimer. Despite the increased holding efficiency, the guests were still able to slowly be released from the dendrimer. A quick release of all guests was not observed at any pH. However, adding salt increased the migration rate of guests out of the dendrimer. It is believed that in the presence of salt the end-groups backfold into the interior of the dendrimer displacing the trapped guests.

After investigating the effect of pH on the encapsulation properties of the monomeric-pyrrole-terminated dendrimer, the effect of oligomerizing the periphery was investigated. At both pH 2 and pH 4, the retainment efficiency of the guests was somewhat higher for the oligo-pyrrole terminated dendrimer than that of the dendrimer possessing a monomeric periphery. In order to monitor this efficiency, the number guests encapsulated per dendrimer was calculated as well as the percentage of guests remaining as a function of dialysis time. The dendrimers containing the oligo-pyrrole periphery were able to retain a higher percentage of guests at pH 4 and pH 7. At first glance of the data, it seems as though these oligomers were significantly more efficient in retaining the guests than dendrimers whose periphery consisted of monomeric pyrroles. However, if the actual number of guests encapsulated is taken into consideration, the oligomeric periphery is only more efficient in preventing guest leakage at pH 2. After dialysis was conducted for 8 hours, the dendrimers whose periphery consisted of monomeric pyrrole possessed more Nile Red molecules than dendrimers whose periphery was made up of oligo-pyrrole when the solution pH was 4 and 7.

Upon completion of all studies it was found that the dendrimer with terminal monomeric pyrroles at pH 7 was able to retain more guests than all other scenarios investigated. The dendrimer at pH 7 with the oligo-pyrrole periphery was the least efficient at retaining encapsulated guests. Of all the oligo(pyrrole)-terminated dendrimers studied, the dendrimer with the shortest oligomers (pH 2) was the most efficient in preventing guest leakage.

7.3 Conclusions

Upon completing these studies it was found that the dendrimer functional groups are predominantly located along the periphery of the dendrimer allowing guests to occupy their internal cavities. It is evident however, that increasing the pH causes a significant change in the

dendrimer structure which greatly affects the dendrimers' encapsulation properties. It is believed that the dendrimer branches collapse amongst themselves at higher pH even though they are nott necessarily located in the interior regions of the dendrimer.

Collapsing of the dendrimer branches prevents the uptake of molecular guests by the dendrimer, but retards the release of guests already encapsulated. Therefore, in order for the dendrimer to accommodate more guests, encapsulation should occur at lower pH. Once the guests are located inside the periphery, the pH can be adjusted with no initial loss of guests. Once the pH is raised, the collapsed outer branches sterically inhibit the diffusion of guests from the interior cavities to the outside environment.

The results of these studies reveal several options to enhance encapsulation and release such that these dendrimers could be useful in host/guest systems. In order to encapsulate as many guests as possible, it is imperative that encapsulation occurs at pH 2. Once encapsulation is successful one may use a few options to retain and then trigger the release of the guests. One option is to simply raise the pH to 7. Once this occurs the outer branches will collapse about the periphery of the dendrimer and retard leakage of encapsulated guests. Once the pH is increased there are two options to increase the release rate of the guests. One route to speed up the release rate of the guests is to simply lower the pH. However, because the oligo-pyrrole-terminated dendrimers at pH 7 possessed the worst retainment efficiency, the pyrrole monomers could also be oxidized to yield oligomers which would increase the release rate of the guests.

Even with the interesting findings observed here, it is important to mention the small number of guests encapsulated by the dendrimers. Despite the large size of the dendrimer used for the encapsulation studies in this work, 8736.5 daltons, the maximum number of guests that may be incarcerated by each dendrimer is one. In fact, the overall average number of guests

encapsulated per dendrimer was always less than 1 in these studies and varied greatly. Even though every possible attempt was made to prevent variation in the experimental procedure, the number of guests encapsulated varied each time. The number of guests encapsulated per dendrimer ranged from 0.52 to 0.32 over the course of these studies. With these findings, it is pretty clear that this exact dendrimer would not be the ideal choice to use in encapsulation/release systems. However, perhaps other comparable dendrimers may be better suited.[8] A similar pyrrole-terminated dendrimer has been synthesized by this group that is more water soluble. A tri(ethylene oxide) group was added to the pyrrole to enhance water solubility. This makes it possible to use the 5th-generation dendrimer for encapsulation studies. Higher concentrations and the ability of the larger dendrimer to accommodate more guests would allow one to make a better assessment as to the encapsulation and release properties of the dendrimer as a function of solution conditions.

7. 4 Future Studies

It has been shown in this work that dendrimers whose periphery has been modified with groups that do not adsorb to gold substrates adsorb through their tertiary amines. Attempts to ascertain how amine-terminated dendrimers adsorb to gold surfaces were inconclusive. One of the techniques used was to adsorb amine-terminated dendrimers to a gold surface and then complete surface reactions to functionalize the adsorbed dendrimers with ferrocene. Once the surface reactions were complete, it was possible to determine the surface coverage of ferrocene. However, it was not possible to determine exactly how much dendrimer was adsorbed to the surface prior to modification. A solution to this problem would be to partially functionalize the dendrimers with ferrocene prior to adsorption and surface reactions. The extent of functionalization could be determined using MALDI-MS and NMR. Once the extent of

functionalization is known, the surface area of the dendrimers could be determined from the surface area of the partially functionalized dendrimers. Then after further modification of the adsorbed dendrimer, it would be possible to determine exactly how many primary amines, if any, remain unmodified.

It was also found that longer pyrrole oligomers were formed when the solution pH was raised. T_1 data also showed that the dendrimer's periphery was more rigid at higher solution pH. It is still unclear as to whether this decrease in mobility is the reason larger oligomers are able to form. Encapsulation studies reveal that it is highly likely that the end groups are in a collapsed form at higher solution pH. It may be possible that this collapsed state results in pyrrole units in closer proximity to one another enabling the coupling of more pyrrole monomers to make longer oligomers. H-bonding studies discussed in Chapter 4 could be completed on these pyrrole-terminated dendrimers at a range of solution pH in order to investigate the relative proximity of the end groups with respect to one another as a function of pH.

This work demonstrates that the encapsulation properties of pyrrole-terminated dendrimers can be altered by changing solution conditions such as pH. However, it is difficult to make specific conclusions as to the encapsulation efficiency due to the small amount of trapped guests (<1 guest per dendrimer). One way to overcome this problem is to use larger dendrimers. However, the 5th-generation pyrrole-terminated dendrimer used in these studies would not be an ideal choice because of its low solubility in water.

A solution to this dilemma would be to use a pyrrole-terminated dendrimer in which the pyrrole has been modified to increase solubility. Such a dendrimer has been synthesized in our labs.[8] The pyrrole end-groups were modified with tri(ethylene oxide), TEO, which makes it possible to use both higher concentrations of dendrimer and the larger 5th-generation dendrimer

in aqueous solutions. Increasing both the dendrimer concentration and the host's capacity for guests would significantly increase the absorbance for Nile Red. Completing studies with this system at a range of solution pH with overall higher concentrations of Nile Red would allow one to make a more accurate assessment as to the encapsulation properties of these dendrimers.

It would also be important to conduct relaxation studies on this TEO-Py-terminated dendrimer to determine if mobility about the periphery is affected by solution pH as were the pyrrole-terminated dendrimers in these studies. It would also be interesting to determine if altering the pH would result in different length oligomers and to further investigate the effect of oligomer length on guest retention. It is still not perfectly clear as to whether longer oligomers are more or less effective in trapping guests. The work presented here demonstrates that a smaller percentage of guests were retained by dendrimers with a oligo-pyrrole periphery containing longer oligomers. However, despite the fact that multiple studies were conducted on these oligo-pyrrole-terminated dendrimers, only a single data set was acquired that yielded acceptable data. UV scattering with most of the samples made it extremely difficult to assess the number of Nile Red guests harbored by each dendrimer. Using a smaller concentration of dendrimer, results in an equally smaller concentration of Nile Red. This lower concentration of Nile Red was found to be below the detection limit for visible spectroscopy.

7.5 References

(1) Manas, E. S.; Getahun, Z.; Wright, W. W.; DeGrado, W. F.; Vanderkooi, J. M. *Infrared Spectra of Amide Groups in Alpha-Helical Proteins: Evidence for Hydrogen Bonding between Helices and Water,* ***Journal of the American Chemical Society*** **2000**, *122*, 9883-9890.

(2) Tokuhisa, H.; Zhao, M.; Baker, L. A.; Phan, V. T.; Dermody, D. L.; Garcia, M. E.; Peez, R. F.; Crooks, R. M.; Mayer, T. M. *Preparation and Characterization of Dendrimer Monolayers and Dendrimer-Alkanethiol Mixed Monolayers Adsorbed to Gold,* ***Journal of the American Chemical Society*** **1998**, *120*, 4492-4501.

(3) Hong, M.-Y.; Yoon, H. C.; Kim, H.-S. *Protein-Ligand Interactions at Poly(amidoamine) Dendrimer Monolayers on Gold,* ***Langmuir*** **2003**, *19*, 416-421.

(4) Nijhuis, C. A.; Huskens, J.; Reinhoudt, D. N. *Binding Control and Stoichiometry of Ferrocenyl Dendrimers at a Molecular Printboard,* ***Journal of the American Chemical Society*** **2004**, *126*, 12266-12267.

(5) Rolandi, M.; Suez, I.; Dai, H.; Frechet, J. M. J. *Dendrimer Monolayers as Negative and Positive Tone Resists for Scanning Probe Lithography,* ***Nano Letters*** **2004**, *4*, 889-893.

(6) Rahman, K. M. A.; Durning, C. J.; Turro, N. J.; Tomalia, D. A. *Adsorption of Poly(amidoamine) Dendrimers on Gold,* ***Langmuir*** **2000**, *16*, 10154-10160.

(7) Zerbi, G.; Veronelli, M.; Martina, S.; Schlueter, A. D.; Wegner, G. *Delocalization Length and Structure of Oligopyrroles and of Polypyrrole from their Vibrational Spectra,* ***Journal of Chemical Physics*** **1994**, *100*, 978-984.

(8) Morara, A. D.; McCarley, R. L. *Encapsulation of Neutral Guests by Tri(ethylene oxide)-pyrrole-Terminated Dendrimer Hosts in Water,* ***Organic Letters*** **2006**, *8*, 1999-2002.

Appendix A: Supplemental NMR Data

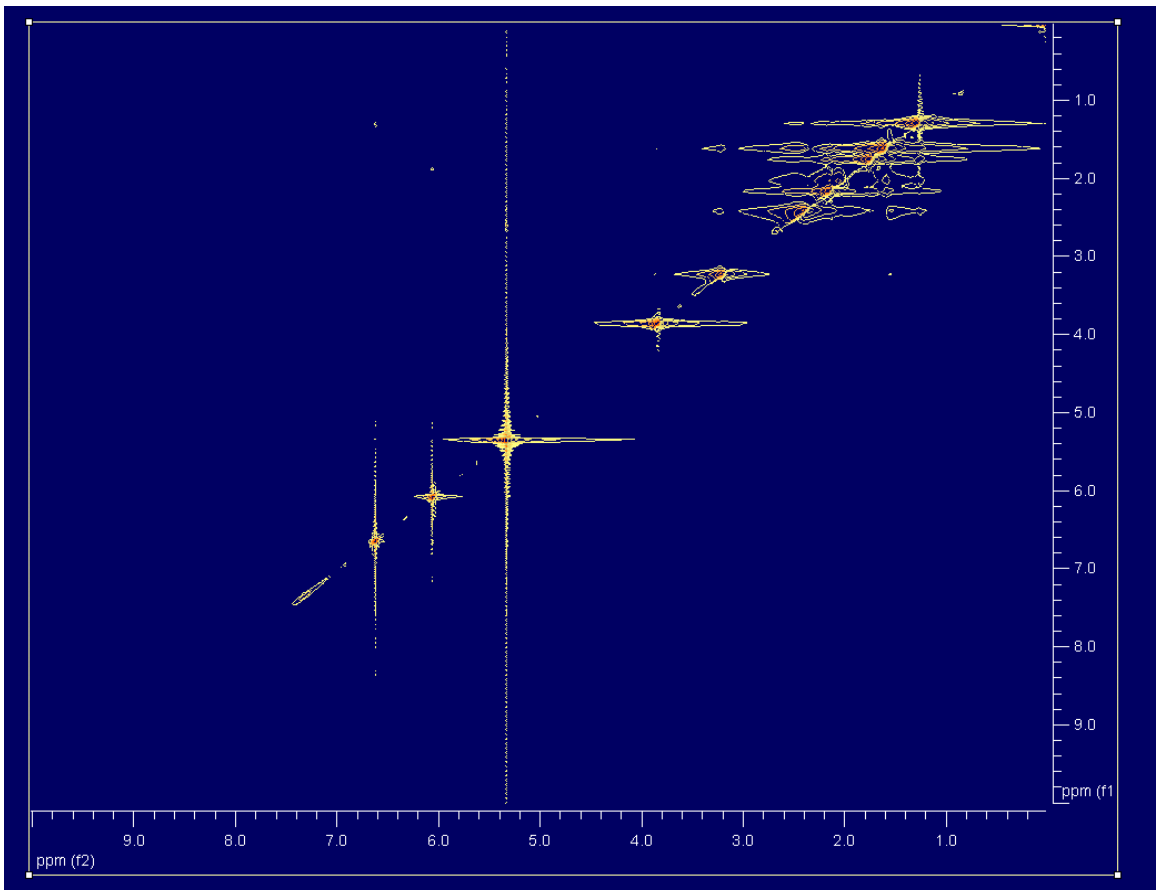

Figure A.1 NOESY data of DAB-Py_{32} in CD_2Cl_2 in which the end-group concentration was 0.01 M.

Table A.1 T_1 data in seconds for DAB-Py_{32} in CD_2Cl_2 obtained on a 300 MHz NMR at a variety of temperatures with an end-group concentration of 0.01 M.

Proton	Temperature (K)					
	305	**298**	**285**	**275**	**265**	**245**
-N*H*-C=0-	0.288	0.223	0.210	0.201	0.168	0.357
Py-2,5-*H*	3.065	2.778	2.533	2.131	1.901	1.375
Py-3,4-*H*	4.521	3.731	3.520	3.216	3.077	1.867
-CH_2-Py	0.935	0.751	0.765	0.651	0.586	0.451
-CH_2-NH-C=O	0.348	0.336	0.346	0.361	0.372	0.477
N(CH_2)$_3$	0.377	0.298	0.392	0.438	0.458	0.430
-CO-CH_2-(CH$_2$)$_4$-Py	0.543	0.498	0.517	0.502	0.461	0.443
-CO-CH$_2$-CH_2-(CH$_2$)$_3$-Py	0.716	0.621	0.603	0.540	0.487	0.424
-CO-(CH$_2$)$_3$-CH_2-CH$_2$-Py **-N-CH$_2$-CH_2-CH$_2$-N-**	0.456	0.420	0.424	0.415	0.412	0.419
-CO-(CH$_2$)$_2$-CH_2-(CH$_2$)$_2$-Py **-N-CH$_2$-(CH_2)$_2$-CH$_2$-N-**	0.923	0.656	0.819	0.708	0.606	0.458

Table A.2 T_1 data in seconds for DAB-Py_x (x = 4, 8, 16, 32, and 64) in CD_2Cl_2 obtained on a 300 MHz NMR at 298 K with an end-group concentration of 0.01M.

Proton	DAB-Py_4	DAB-Py_8	DAB-Py_{16}	DAB-Py_{32}	DAB-Py_{64}
Py-2,5-*H*	4.181	3.630	3.120	2.778	2.237
Py-3,4-*H*	5.307	4.569	4.120	3.731	2.939
-CH_2-Py	1.174	0.955	0.853	0.751	0.670
-CH_2-NH-C=O	0.302	0.257	0.282	0.336	0.367
N(CH_2)$_3$	0.319	0.202	0.232	0.298	0.362
-CO-CH_2-(CH$_2$)$_4$-Py	0.594	0.718	0.486	0.498	0.491
-CO-CH$_2$-CH_2-(CH$_2$)$_3$-Py	0.871	0.768	0.681	0.621	-
-CO-(CH$_2$)$_3$-CH_2-CH$_2$-Py **-N-CH$_2$-CH_2-CH$_2$-N-**	0.503	0.377	0.328	0.420	0.419
-(CH$_2$)$_2$-CH_2-(CH$_2$)$_2$-Py **-N-CH$_2$-(CH_2)$_2$-CH$_2$-N-**	0.836	0.691	0.667	0.656	0.615

Table A.3 T_1 data in seconds for DAB-Py_{32} in 1:1 *d*6-Acetone pD 2 DCl obtained on a 300 MHz NMR at a variety of temperatures with an end-group concentration of 0.01M.

Proton	Temperature (K)			
	305	**298**	**285**	**275**
Py-2,5-*H*	2.273	1.831	1.737	1.403
Py-3,4-*H*	2.992	2.458	2.335	1.933
-C*H*$_2$-Py	0.626	0.510	0.483	0.400
-C*H*$_2$-NH-C=O	0.320	0.344	0.346	0.380
N(C*H*$_2$)$_3$	0.282	0.327	0.327	0.377
-CO-C*H*$_2$-(CH$_2$)$_4$-Py	0.453	0.322	0.416	0.412
-CO-CH$_2$-C*H*$_2$-(CH$_2$)$_3$-Py	0.531	0.446	0.418	0.362
-CO-(CH$_2$)$_3$-C*H*$_2$-CH$_2$-Py **-N-CH$_2$-C*H*$_2$-CH$_2$-N-**	0.460	0.373	0.376	0.341
-CO-(CH$_2$)$_2$-C*H*$_2$-(CH$_2$)$_2$-Py **-N-CH$_2$-(C*H*$_2$)$_2$-CH$_2$-N-**	0.495	0.409	0.392	0.337

Table A.4 T_1 data in seconds for DAB-Py_x (x = 4, 8, 16, 32, and 64) in 1:1 *d*6-Acetone pD 2 DCl obtained on a 300 MHz NMR at 298 K with an end-group concentration of 0.01M.

Proton	DAB-Py_4	DAB-Py_8	DAB-Py_{16}	DAB-Py_{32}	DAB-Py_{64}
Py-2,5-*H*	2.723	2.435	1.974	1.831	1.464
Py-3,4-*H*	3.512	3.251	2.705	2.458	1.949
-C*H*$_2$-Py	0.678	0.623	0.533	0.510	0.466
-C*H*$_2$-NH-C=O	0.277	0.271	0.317	0.344	0.384
N(C*H*$_2$)$_3$	-	0.252	0.270	0.327	0.380
-CO-C*H*$_2$-(CH$_2$)$_4$-Py	0.229	0.256	0.282	0.322	0.354
-CO-CH$_2$-C*H*$_2$-(CH$_2$)$_3$-Py	0.568	0.508	0.448	0.446	0.421
-CO-(CH$_2$)$_3$-C*H*$_2$-CH$_2$-Py **-N-CH$_2$-C*H*$_2$-CH$_2$-N-**	0.459	0.426	0.393	0.373	0.398
-CO-(CH$_2$)$_2$-C*H*$_2$-(CH$_2$)$_2$-Py **-N-CH$_2$-(C*H*$_2$)$_2$-CH$_2$-N-**	0.515	0.462	0.415	0.409	0.398

Table A.5 T_1 data in seconds for DAB-Py_{32} in 1:1 *d*6-Acetone D_2O obtained on a 300 MHz NMR at a variety of solution pD with an end-group concentration of 0.01M.

Proton	pD					
	1.24	**1.70**	**2.00**	**2.60**	**3.70**	**6.00**
Py-2,5-*H*	1.927	1.946	1.831	1.451	1.275	1.050
Py-3,4-*H*	2.667	2.709	2.458	1.865	1.569	1.520
-C*H*$_2$-Py	0.529	0.528	0.510	0.452	0.454	0.305
-C*H*$_2$-NH-C=O	0.308	0.343	0.327	0.333	0.345	0.215
N(C*H*$_2$)$_3$	0.336	-	-	0.335	0.337	0.217
-CO-CH$_2$-C*H*$_2$-(CH$_2$)$_3$-Py	0.466	-	0.446	0.373	0.378	0.284
-CO-(CH$_2$)$_3$-C*H*$_2$-CH$_2$-Py **-N-CH$_2$-C*H*$_2$-CH$_2$-N-**	0.414	0.432	0.373	0.372	0.381	0.236
-CO-(CH$_2$)$_2$-C*H*$_2$-(CH$_2$)$_2$-Py **-N-CH$_2$-(C*H*$_2$)$_2$-CH$_2$-N-**	0.433	0.418	0.409	0.385	0.379	0.242

Table A.6 T_1 data in seconds for DAB-Py_4 in CD_2Cl_2 obtained on a 400 MHz NMR at a variety of temperatures with an end-group concentration of 0.01 M.

Proton	Temperature (K)		
	303	**288**	**273**
Py-2,5-*H*	5.514	3.047	3.270
Py-3,4-*H*	7.649	5.082	4.446
-C*H*$_2$-Py	1.487	1.062	0.827
-C*H*$_2$-NH-C=O	0.420	0.371	0.349
N(C*H*$_2$)$_3$	0.321	0.301	0.251
-CO-C*H*$_2$-(CH$_2$)$_4$-Py	0.692	0.592	0.513
-CO-CH$_2$-C*H*$_2$-(CH$_2$)$_3$-Py	1.166	0.848	0.657
-CO-(CH$_2$)$_3$-C*H*$_2$-CH$_2$-Py **-N-CH$_2$-C*H*$_2$-CH$_2$-N-**	0.727	0.613	0.524
-CO-(CH$_2$)$_2$-C*H*$_2$-(CH$_2$)$_2$-Py **-N-CH$_2$-(C*H*$_2$)$_2$-CH$_2$-N-**	0.985	0.769	0.610

Table A.7 T_1 data in seconds for DAB-Py_8 in CD_2Cl_2 obtained on a 400 MHz NMR at a variety of temperatures with an end-group concentration of 0.01 M.

Proton	Temperature (K)		
	303	288	273
Py-2,5-*H*	4.266	3.405	2.787
Py-3,4-*H*	5.764	4.526	3.747
-C*H*$_2$-Py	1.198	0.915	0.715
-C*H*$_2$-NH-C=O	0.366	0.356	0.362
N(C*H*$_2$)$_3$	0.282	0.294	0.323
-CO-C*H*$_2$-(CH$_2$)$_4$-Py	0.692	0.789	0.840
-CO-CH$_2$-C*H*$_2$-(CH$_2$)$_3$-Py	1.033	0.730	0.590
-CO-(CH$_2$)$_3$-C*H*$_2$-CH$_2$-Py **-N-CH$_2$-C*H*$_2$-CH$_2$-N-**	0.401	0.427	0.483
-CO-(CH$_2$)$_2$-C*H*$_2$-(CH$_2$)$_2$-Py **-N-CH$_2$-(C*H*$_2$)$_2$-CH$_2$-N-**	0.558	0.696	0.854

Table A.8 T_1 data in seconds for DAB-Py_{16} in CD_2Cl_2 obtained on a 400 MHz NMR at a variety of temperatures with an end-group concentration of 0.01 M.

Proton	Temperature (K)		
	303	288	273
Py-2,5-*H*	3.431	2.742	2.383
Py-3,4-*H*	4.408	3.607	3.231
-C*H*$_2$-Py	1.004	0.793	0.654
-C*H*$_2$-NH-C=O	0.395	0.415	0.456
N(C*H*$_2$)$_3$	0.321	0.371	0.440
-CO-C*H*$_2$-(CH$_2$)$_4$-Py	0.603	0.614	0.705
-CO-CH$_2$-C*H*$_2$-(CH$_2$)$_3$-Py	0.908	0.672	0.550
-CO-(CH$_2$)$_3$-C*H*$_2$-CH$_2$-Py **-N-CH$_2$-C*H*$_2$-CH$_2$-N-**	0.455	0.453	0.487
-CO-(CH$_2$)$_2$-C*H*$_2$-(CH$_2$)$_2$-Py **-N-CH$_2$-(C*H*$_2$)$_2$-CH$_2$-N-**	0.539	0.633	0.785

Table A.9 T_1 data in seconds for DAB-Py_{32} in CD_2Cl_2 obtained on a 400 MHz NMR at a variety of temperatures with an end-group concentration of 0.01 M.

Proton	Temperature (K)		
	303	288	273
Py-2,5-*H*	3.667	2.606	2.076
Py-3,4-*H*	4.482	3.434	2.788
-C*H*$_2$-Py	0.979	0.754	0.601
-C*H*$_2$-NH-C=O	0.461	0.500	0.562
N(C*H*$_2$)$_3$	0.404	0.473	0.587
-CO-C*H*$_2$-(CH$_2$)$_4$-Py	0.616	0.594	0.739
-CO-CH$_2$-C*H*$_2$-(CH$_2$)$_3$-Py	1.182	0.704	0.537
-CO-(CH$_2$)$_3$-C*H*$_2$-CH$_2$-Py -N-CH$_2$-C*H*$_2$-CH$_2$-N-	0.559	0.515	0.523
-CO-(CH$_2$)$_2$-C*H*$_2$-(CH$_2$)$_2$-Py -N-CH$_2$-(C*H*$_2$)$_2$-CH$_2$-N-	0.750	0.616	0.488

Table A.10 T_1 data in seconds for DAB-Py_{64} in CD_2Cl_2 obtained on a 400 MHz NMR at a variety of temperatures with an end-group concentration of 0.01 M.

Proton	Temperature (K)		
	303	288	273
Py-2,5-*H*	3.108	2.515	2.062
Py-3,4-*H*	4.324	3.532	3.009
-C*H*$_2$-Py	0.863	0.708	0.616
-C*H*$_2$-NH-C=O	0.524	0.609	0.725
N(C*H*$_2$)$_3$	0.529	0.673	0.869
-CO-C*H*$_2$-(CH$_2$)$_4$-Py	0.765	0.880	0.716
-CO-CH$_2$-C*H*$_2$-(CH$_2$)$_3$-Py	0.718	0.625	0.580
-CO-(CH$_2$)$_3$-C*H*$_2$-CH$_2$-Py -N-CH$_2$-C*H*$_2$-CH$_2$-N-	0.629	0.583	0.568
-CO-(CH$_2$)$_2$-C*H*$_2$-(CH$_2$)$_2$-Py -N-CH$_2$-(C*H*$_2$)$_2$-CH$_2$-N-	0.567	0.645	0.760

Table A.11 T_1 data in seconds for DAB-Py_{32} in 1:1 *d*6-Acetone pD 2 DCl obtained on a 400 MHz NMR at a variety of temperatures with an end-group concentration of 0.01M.

Proton	Temperature (K)		
	305	290	275
Py-2,5-*H*	2.413	1.815	1.186
Py-3,4-*H*	3.120	2.474	1.480
-C*H*$_2$-Py	0.687	0.528	0.471
-C*H*$_2$-NH-C=O	0.462	0.526	0.655
N(C*H*$_2$)$_3$	0.462	0.570	0.730
-CO-CH$_2$-C*H*$_2$-(CH$_2$)$_3$-Py	0.528	0.504	0.491
-CO-(CH$_2$)$_3$-C*H*$_2$-CH$_2$-Py **-N-CH$_2$-C*H*$_2$-CH$_2$-N-**	0.531	0.470	0.490
-CO-(CH$_2$)$_2$-C*H*$_2$-(CH$_2$)$_2$-Py **-N-CH$_2$-(C*H*$_2$)$_2$-CH$_2$-N-**	0.553	0.461	0.446

Table A.12 T_1 data in seconds for DAB-Py_{32} in 1:1 *d*6-Acetone pD 4 DCl obtained on a 400 MHz NMR at a variety of temperatures with an end-group concentration of 0.01M.

Proton	Temperature (K)		
	305	290	275
Py-2,5-*H*	1.539	1.102	1.120
Py-3,4-*H*	1.053	0.847	1.064
-C*H*$_2$-Py	0.699	0.579	0.434
-C*H*$_2$-NH-C=O	0.543	0.592	0.539
N(C*H*$_2$)$_3$	0.587	0.599	0.673
-CO-CH$_2$-C*H*$_2$-(CH$_2$)$_3$-Py	0.535	0.604	0.604
-CO-(CH$_2$)$_3$-C*H*$_2$-CH$_2$-Py **-N-CH$_2$-C*H*$_2$-CH$_2$-N-**	0.549	0.591	0.627
-CO-(CH$_2$)$_2$-C*H*$_2$-(CH$_2$)$_2$-Py **-N-CH$_2$-(C*H*$_2$)$_2$-CH$_2$-N-**	0.541	0.564	0.593

Table A.13 T_1 data in seconds for DAB-Py_{64} in 1:1 *d*6-Acetone pD 7 D_2O obtained on a 400 MHz NMR at a variety of temperatures with an end-group concentration of 0.01M.

Proton	Temperature (K)		
	305	290	275
Py-2,5-*H*	1.830	1.166	1.063
Py-3,4-*H*	1.127	1.000	1.250
-C*H*$_2$-Py	0.712	0.598	0.548
-C*H*$_2$-NH-C=O	0.532	0.599	0.655
N(C*H*$_2$)$_3$	0.500	0.582	0.786
-CO-CH$_2$-C*H*$_2$-(CH$_2$)$_3$-Py	0.528	0.601	0.598
-CO-(CH$_2$)$_3$-C*H*$_2$-CH$_2$-Py **-N-CH$_2$-C*H*$_2$-CH$_2$-N-**	0.554	0.593	0.619
-CO-(CH$_2$)$_2$-C*H*$_2$-(CH$_2$)$_2$-Py **-N-CH$_2$-(C*H*$_2$)$_2$-CH$_2$-N-**	0.541	0.564	0.587

Vita

Henry Paul Wiggins was born in Morgan City, Louisiana, on September 27, 1979, to Carol and Donald Wiggins. He lived in Patterson, Louisiana, throughout his childhood. After graduating from Patterson High School in May of 1997, he attended Nicholls State University where he received his Bachelor of Science Degree in chemistry in May of 2001. It was here that he met his future wife, Sarah Ann Leonards. In order to further his education he and Sarah moved to Baton Rouge, Louisiana, and he entered graduate school in the Department of Chemistry at Louisiana State University. During this time he and his wife had their first child, Lance Michael Wiggins. He chose to work under the direction of Dr. Robin L. McCarley and is currently finishing his requirements for the Doctor of Philosophy degree in chemistry. He has accepted a position with Halliburton in Duncan, Oklahoma.